pubs.acs.org/Biomac

Review

Polysaccharide-Based Double-Network Hydrogels: Polysaccharide Effect, Strengthening Mechanisms, and Applications

Pengguang Wang, Qingyu Liao, and Hongbin Zhang*

Cite This: https://doi.org/10.1021/acs.biomac.3c00765

Read Online

ACCESS | Metrics & More | Article Recommendations | Supporting Information

ABSTRACT: Polysaccharides are carbohydrate polymers that are major components of plants, animals, and microorganisms, with unique properties. Biological hydrogels are polymeric networks that imbibe and retain large amounts of water and are the major components of living organisms. The mechanical properties of hydrogels are critical for their functionality and applications. Since synthetic polymeric double-network (DN) hydrogels possess unique network structures with high and tunable mechanical properties, many natural functional polysaccharides have attracted increased attention due to their rich and convenient sources, unique chemical structure and chain conformation, inherently desirable cytocompatibility, biodegradability and environmental friendliness, diverse bioactivities, and rheological properties, which rationally make them prominent constituents in designing various strong and tough polysaccharide-based DN hydrogels over the past ten years. This review focuses on the latest developments of polysaccharide-based DN hydrogels to comprehend the relationship among the polysaccharide properties, inner strengthening mechanisms, and applications. The aim of this review is to provide an insightful mechanical interpretation of the design strategy of novel polysaccharide-based DN hydrogels and their applications by introducing the correlation between performance and composition. The mechanical behavior of DN hydrogels and the roles of varieties of marine, microbial, plant, and animal polysaccharides are emphatically explained.

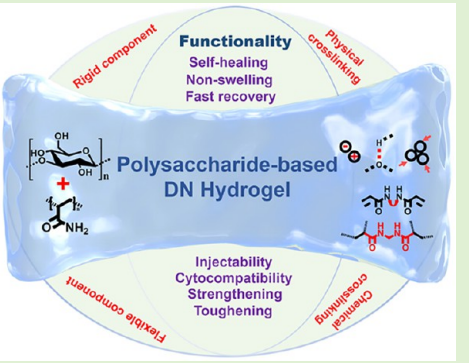

1. INTRODUCTION

As cross-linked polymer networks are infiltrated with water, hydrogels form the major parts of animals that possess extreme mechanical properties.[1] These properties include fracture toughness (tendon of 20−30 kJ/m^2, skeletal muscle of ∼2490 J/m^2, articular cartilage of 800−1800 J/m^2, and heart valve of ∼1000 J/m^2) and tensile strength (tendon of 10−100 MPa and aorta of 0.2−3.7 MPa).[1] Hydrogels require high mechanical properties to be applied in many fields, such as biomaterials and smart machines.[2] Strategies have been proposed to fabricate hydrogels with high fracture toughness, strength, resilience, and interfacial toughness as well as fatigue and interfacial fatigue thresholds. Such hydrogels include DN hydrogels, nanocomposite gels, topological slide-ring gels, and dual-cross-link gels. DN hydrogels are considered some of the toughest hydrogels,[2] and a series of polysaccharide-based DN hydrogels with notable mechanical properties, features, and applications have been fabricated. For example, a sodium alginate (SA)/polyacrylamide (PAAm) DN hydrogel with a fracture toughness of ∼9000 J/m^2 and a notch insensitivity (Figure 1A) has been prepared.[3] Moreover, in 1991, binary polysaccharide hydrogel networks were summarized (Figure 1B).[4] The synergistic interaction and gelation of two kinds of polysaccharides in water, xanthan gum (XG) and konjac glucomannan (KGM), were investigated in 1995 (Figure 1C,D).[5−7] Besides the synergistic enhancement between two polysaccharides, the polysaccharide-based DN structures in nature confers the dactyl club shell of *Odontodactylus scyllarus* with extreme mechanical properties (Figure 1E), enabling it to bear a force of 1500 kg·m/s^2 and an acceleration of 98 000 m/s^2 at a speed of 23 m/s.[8] The shell comprises ∼88 vol% hydroxyapatite (HAP) phase and 17 wt% organic phase (probably chitin and protein), where the breakage of the HAP phase dissipates energy and provides damping. DN hydrogel has grown into a large family. Many components form DN hydrogels, such as DNA,[9] protein, polysaccharides and their derivatives, synthetic polymers (e.g., poly(2-acrylamido-2-methylpropanesulfonic acid) (PAMPS), PAAm, poly(acrylic acid) (PAAc), polyvinyl alcohol (PVA), and polyethylene glycol (PEG)), and inorganic materials (e.g., graphene oxide (GO),[10] reduced GO,[11] carbon nanotube,[12] carbon nanofibre,[13] Mxene,[14] polysilicic network,[15] silver nanoparticle,[16] and HAP[17]). Furthermore, the two networks of DN hydrogels are cross-linked by different cross-linking types,[18] including covalent bonds, dynamic covalent bonds, ionic bonds, hydrogen bonds, hydrophobic interaction, and host−guest

Received: July 29, 2023
Revised: August 31, 2023

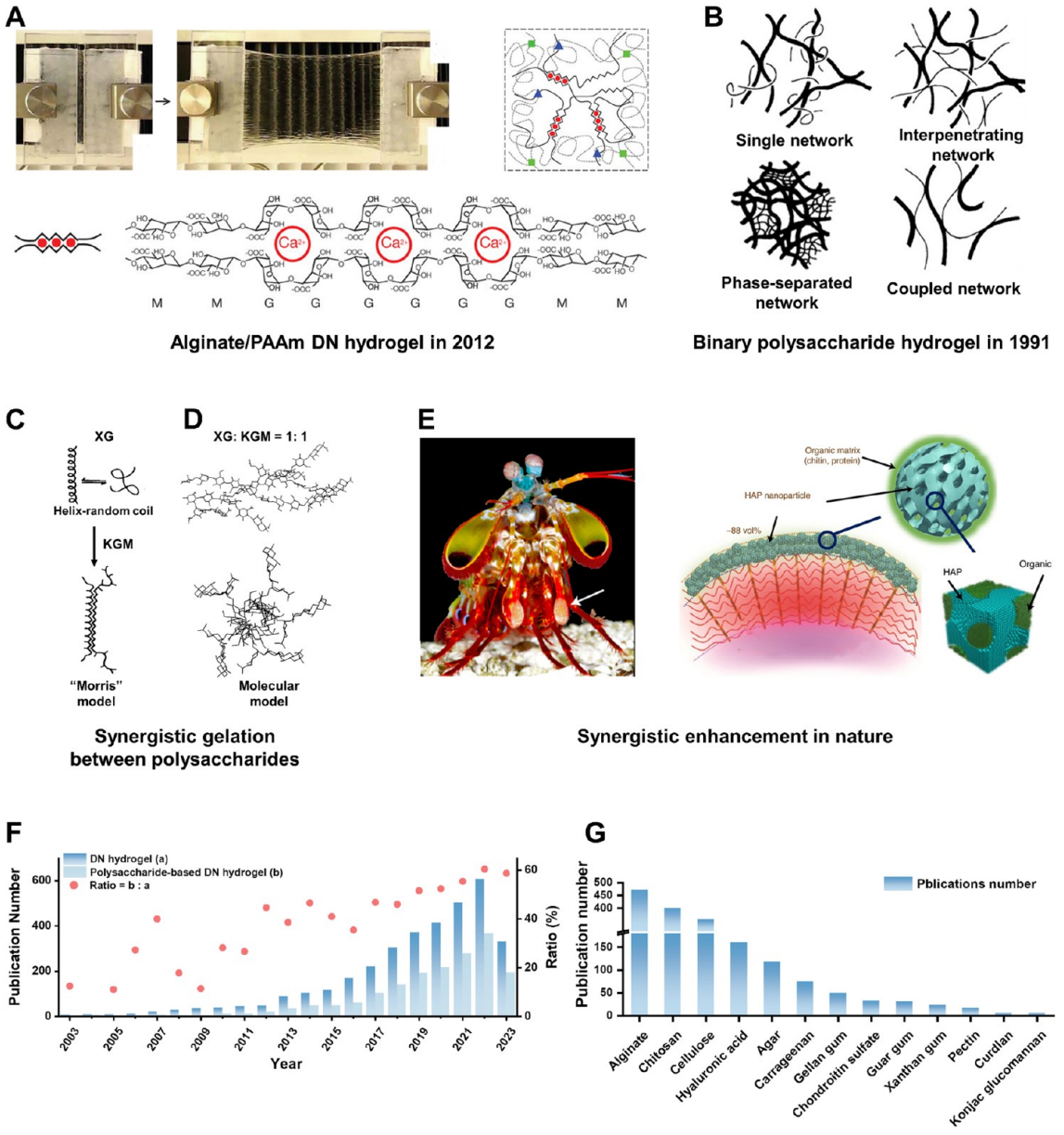

Figure 1. (A) Schematics for four types of binary hydrogel networks. (B) SA/PAAm DN hydrogel. (C) Synergistic interaction and gelation of the XG/KGM solution. (D) Molecular model of an XG/KGM solution. (E) Natural polysaccharide-based structure containing the DN strategy in the dactyl club shell of *Odontodactylus scyllarus*. (F) Publication number per year, by searching the topics of "double network hydrogel**" between 2003 and 2023 (data based on Web of Science). Paper number of polysaccharide-based DN hydrogel is gathered statistically by searching "double network hydrogel**" with the following topics separately: "alginate**", "chitosan**", "cellulose**", "hyaluronic acid **", "agar**", "carrageenan**", "gellan gum**", "chondroitin sulfate**", "guar gum**", "xanthan**", "pectin**", "curdlan**", and "konjac glucomannan**". (G) The publication numbers are for some polysaccharides. Panel A is adapted with permission from ref 3. Copyright 2012 Springer Nature. Panel B is reproduced with permission from ref 4. Copyright 1991 Elsevier. Panel C is adapted with permission from ref 5. Copyright 1995 ACS Publications. Panel D is reproduced with permission from ref 6. Copyright 2002 ACS Publications. Panel E is adapted with permission from ref 8. Copyright 2020 Springer Nature.

interaction. Thus, DN hydrogels are divided into chemically/chemically cross-linked networks, physically/chemically cross-linked networks, and physically/physically cross-linked networks.[19]

Polysaccharides are carbohydrate polymers and some of the major components of plants, animals, and microorganisms with inherent abundance, renewability, cytocompatibility, generally low toxicity, and bioactivity.[20] As far as the biocompatibility of polysaccharides is concerned, it should be noted that the biocompatibility represents various mechanisms of interaction between materials and tissues or tissue components, which is considered a property of a system and not of a material.[21] To alleviate the climate crisis, polysaccharides with outstanding physicochemical properties have been extensively applied as renewable resources, such as in food chemistry, biomaterials, cosmetics, and drugs. Meanwhile, polysaccharides can present various bioactivities such as immune regulatory, anticoagulant, anti-inflammatory, antitumor, antioxidative, anti-HIV, and antimutagenic activities.[22] Furthermore, the chemical groups of polysaccharides contribute to functionalization and post-modification, which provides great perspectives for the applications of polysaccharides in different fields. Polysacchar-

https://doi.org/10.1021/acs.biomac.3c00765
Biomacromolecules XXXX, XXX, XXX−XXX

Scheme 1. Illustration of Fabrication, Strengthening Mechanism, Property, and Application of Polysaccharide-Based DN Hydrogels

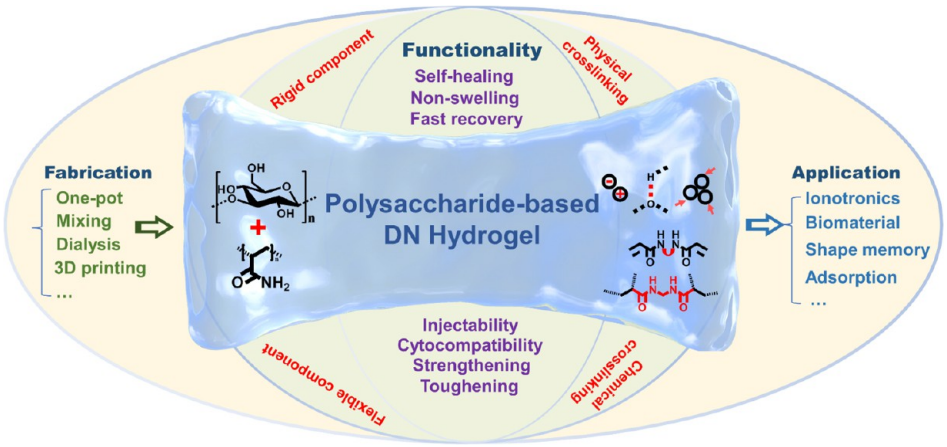

ides have been applied as rigid networks for DN hydrogels. Since Suo et al.[3] used the SA to prepare highly stretchable and tough DN hydrogels in 2012, a large amount of polysaccharide-based DN hydrogels have been fabricated and shown to have attractive properties endowed by the polysaccharides, such as fast self-recovery, self-healing, biodegradability, and cytocompatibility. Polysaccharide-based DN hydrogels are one of the most important topics of DN hydrogels between 2003 and 2023 (Figure 1F, the publication situation of the dual polysaccharide network). The ratio of the number of papers on polysaccharide DN hydrogels to that on DN hydrogels increased from 51% during 2003−2023 to 58% during 2021−2023. The last year, this ratio exceeds 60%. The question of why polysaccharides are selected arises. Here, intrinsic reasons and inherent abilities explain why polysaccharides stand out as one of the most important parts of the DN hydrogel. The union of polysaccharides and hydrogels benefitting from the DN strategy greatly expand the application of polysaccharides.

Some notable reviews have discussed the progress of DN hydrogels. However, a systematic review of understanding the association between polysaccharides and DN hydrogels from the aspect of inner strengthening mechanisms remains lacking. At the beginning of DN hydrogel research, Gong et al.[23,24] summarized the fundamental concepts, classic strengthening mechanisms, and applications of the DN strategy. In 2015, Chen et al.[25] introduced the preparation methods, cross-linking types, detailed strengthening mechanisms, and applications of DN hydrogels. Meanwhile, the potential applications of DN hydrogels as biomaterials are noticed.[26−28] Recently, DN hydrogel reviews have added bioinspired concepts, properties, classifications, 3D bioprinting, as well as sensor, energy, and environmental applications of DN hydrogels.[18−20,29] DN hydrogels based on polysaccharides have been further concluded.[20,30] For elucidating the important role of polysaccharides in DN hydrogels, basic information on the DN concept (the principles, fabrication approaches, and strengthening mechanisms) must be involved. Thus, following on an overview of the DN strategy and the polysaccharides involved (including the marine polysaccharides of sodium alginate, chitin, chitosan (CHT), agar, agarose and κ-carrageenan (κ-CG), microbial polysaccharides of gellan gum (GG), XG and Curdlan, plant polysaccharides of cellulose, pectin, guar gum, KGM and locust bean gum; and animal polysaccharides of hyaluronic acid (HA) and chondroitin sulfate), we comprehensively supplement some experimental and simulated evidence of the detailed strengthening mechanisms, several theoretical models about the behavior of DN hydrogels, the fundamental properties of applied polysaccharides, and the properties of polysaccharide-based DN hydrogels (component, cross-linking type, mechanical character, feature, and application) (Scheme 1), thereby providing a holistic perspective on the development of polysaccharide-based DN hydrogels. Above all, the advantages and reasons why polysaccharides are selected for the preparation of DN hydrogels are critically described and discussed with illustrations of a variety of examples from recent literature.

To explain the significant role of polysaccharides in the DN concept (section 5), this review introduces relevant theories and experimental evidence about the strengthening mechanisms of DN hydrogels and gathers the latest developments in polysaccharide-based DN hydrogels. This review demonstrates (1) the basic fabrication principles of the DN hydrogel (section 2). Then, we introduce (2) the classic and detailed strengthening mechanisms and their experimental evidence (section 3), and (3) the basic information and gelling properties of the applied polysaccharides (section 4) to discuss (4) the reasons why polysaccharide-based DN hydrogels are used (section 5). (5) Several theories describing the behavior of hydrogels and DN hydrogels (section 3) are also shown for further in-depth research. (6) Unique features endowed by polysaccharides and other components (section 6), and (7) applications (section 7) are discussed to help the future application of polysaccharides in DN hydrogels. Most importantly, considering these previous reviews about DN hydrogels, the current review may help the selection of polysaccharides (sections 4 and 6), as well as enrich the introduction of polysaccharides (section 5) and the discussion of mechanical properties (section 3) for further research on polysaccharide-based DN hydrogels.

2. FABRICATION

Since some review papers on DN hydrogel have summarized the preparation procedures,[18−20,23−25,29] here, only a brief introduction is given. Different preparation strategies are used to deal with different kinds of polysaccharides and monomers (Figure 2), including one-pot, mixture, dialysis, and 3D

https://doi.org/10.1021/acs.biomac.3c00765
Biomacromolecules XXXX, XXX, XXX−XXX

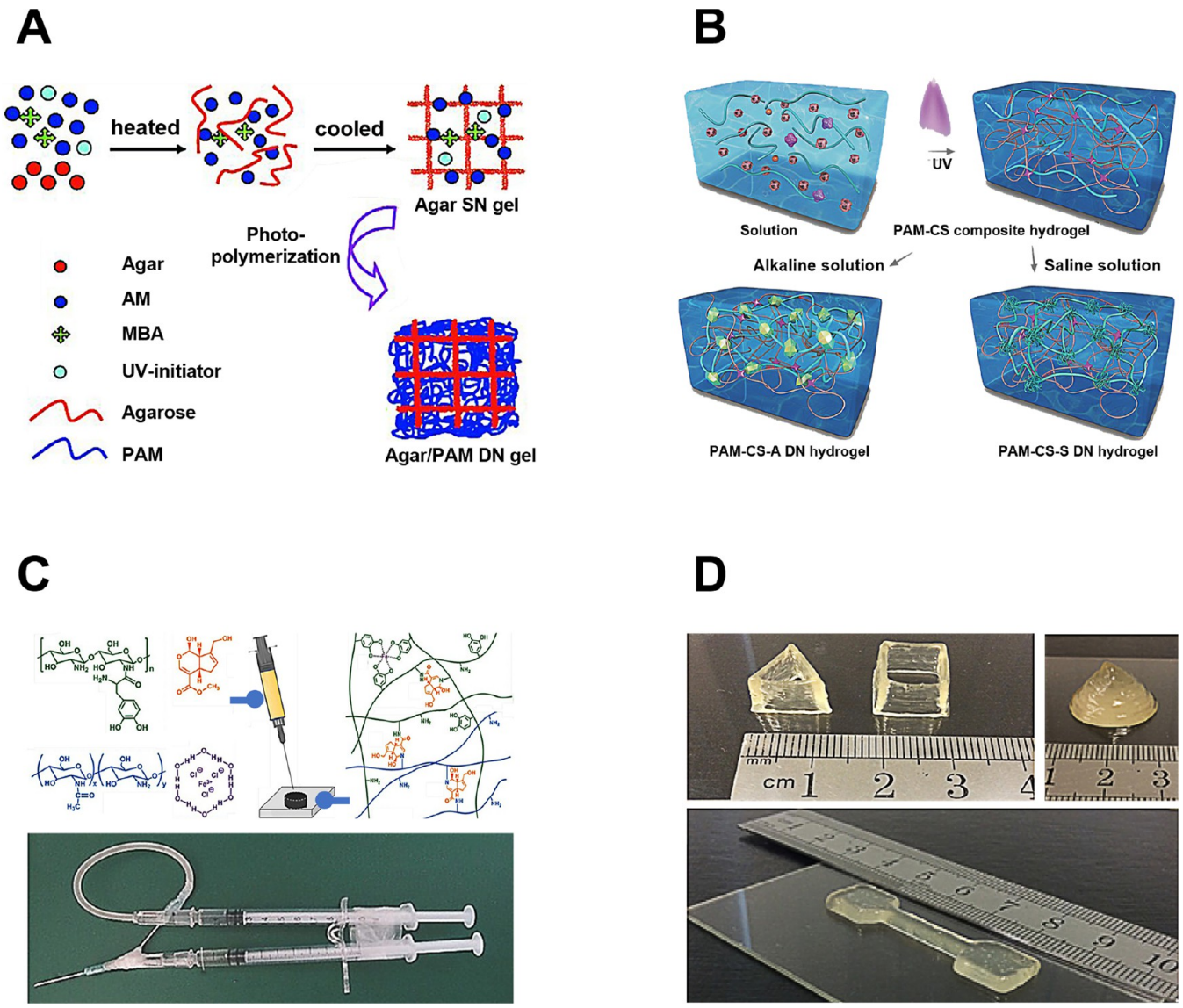

Figure 2. Fabrication methods of DN hydrogels: (A) the agar/PAAm DN hydrogel through the one-pot method; (B) the CHT/PAAm DN hydrogels dialyzed in NaOH and NaCl solutions; (C) an injectable CHT-based DN hydrogel fabricated by mixture; (D) 3D printing to fabricate the κ-CG/PAAm DN hydrogels. Panel A is adapted with permission from ref 31. Copyright 2013 Wiley-VCH. Panel B is adapted with permission from ref 32. Copyright 2016 Wiley-VCH. Panel C is adapted with permission from ref 33. Copyright 2017 Wiley-VCH. Panel D is adapted with permission from ref 34. Copyright 2017 ACS Publications.

printing. Detailed design principles of DN hydrogels and fabrication methods of polysaccharide-based DN hydrogels have been provided in Supporting Discussion 1 in the Supporting Information. In addition, the classification of DN hydrogels depending on chemistries has been briefly discussed in Supporting discussion 2 in the Supporting Information while highlightable review papers[18−20,25,29,30] are suggested for more information on the classifications and cross-linking types of DN hydrogels.

3. STRENGTHENING MECHANISM

The strengthening mechanisms of DN hydrogels are gathered in this section and shown schematically in Figure 3, involving several subsections regarding the sacrifice bond (section 3.1), crack resistance (section 3.1), rigid network (section 3.2.1), inhomogeneity (section 3.2.2), mechanical balance (section 3.2.3), entanglement (section 3.2.4), yield behavior (section 3.2.5), necking (section 3.2.6), and "chain-pulling-out" mechanism (section 3.2.7), respectively. The synthetic and polysaccharide-based rigid networks have been shown to have no essential difference in the strengthening mechanism.[31,35−41] These mechanisms enable researchers to have a deeper insight into the mechanical responses and greatly enrich the mechanical interpretation, which is significant for developing new polysaccharide-based DN hydrogels with desirable properties.

3.1. Classic Strengthening Mechanism. For all DN hydrogels, the enhanced mechanical properties are interpreted by two mechanisms.[23,24] (1) The rigid network breaks into fragments with an ∼100 μm width during deformation to dissipate energy, whereas the flexible network maintains the integrity (Figure 4A). Observations are made by phase-contrast microscopy (Figure 4B),[42] SANS (Figure 4C),[43] polarized optical microscopy (Figure 4D),[42] and SAXS (Figure 4E).[44] (2) Once a crack forms, the fracture of the rigid network delocalizes the stress at the crack tip and dissipates the

https://doi.org/10.1021/acs.biomac.3c00765
Biomacromolecules XXXX, XXX, XXX−XXX

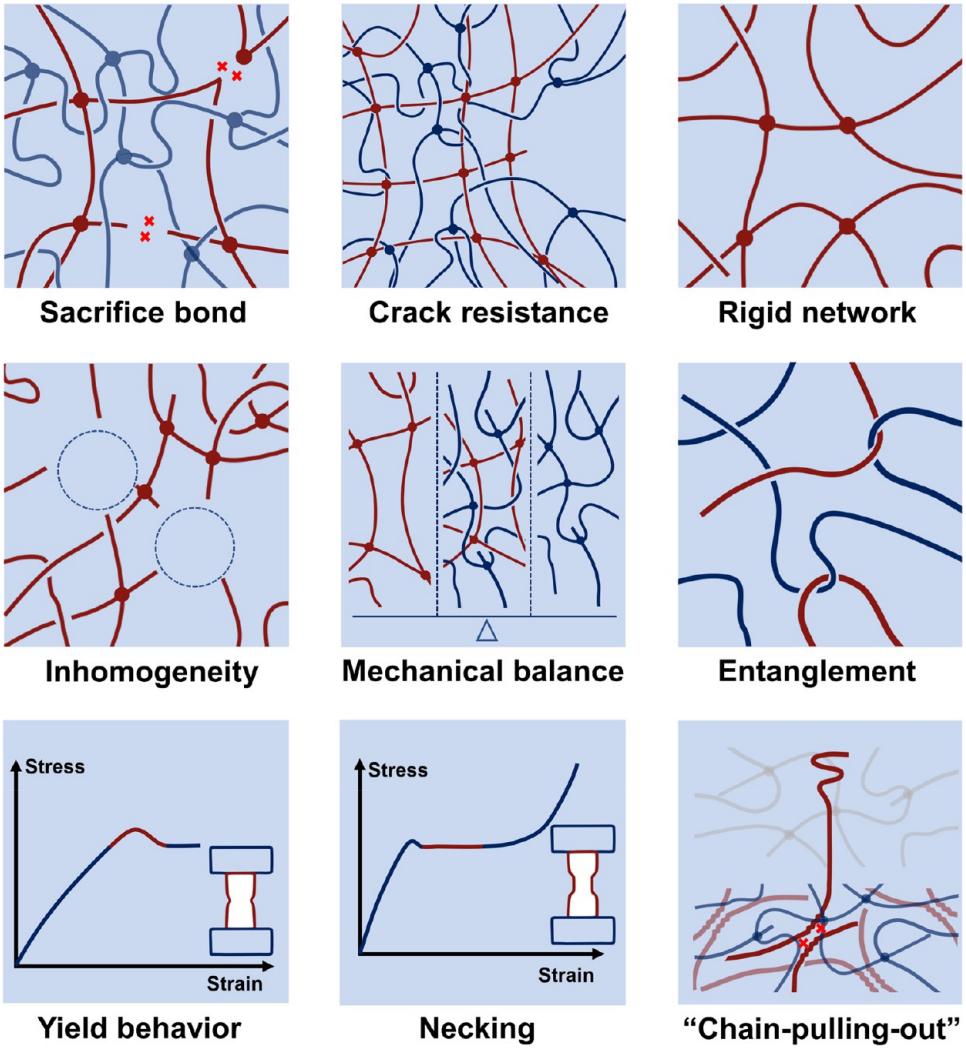

Figure 3. Schematics of classic and detailed strengthening mechanisms, including the sacrifice bond, crack resistance, rigid network, inhomogeneity, mechanical balance, entanglement, yield behavior, necking, and "chain-pulling-out" mechanism.

energy to retard the crack propagation (Figure 4F),[23,24,45] as verified by phase-contrast microscopy (Figure 4G),[42] AFM (Figure 4H),[46] and color 3D violet laser scanning microscopy (Figure 4I).[47] The strengthening mechanisms are important to design a DN hydrogel with high mechanical properties.[3]

3.2. Detailed Strengthening Mechanism. The main strengthening mechanisms have been discussed in the above description. Many other factors also influence the mechanical properties of the DN hydrogels. Therefore, this section further details the strengthening mechanisms.

3.2.1. Rigid Network. The rigid network greatly influences the mechanical properties of the DN hydrogel.[48] First, in the prenecking region, the rigid network dominates the initial mechanical response and the yield stress,[49,50] where the stress contribution from the highly cross-linked network is estimated to be ~10 times larger than that of the flexible network at small strain.[51] Meanwhile, the outstanding toughness of the DN hydrogel primarily originates from the fracture of the rigid network upon deformation because the formation of broken zones of the rigid network allows overlay damages before macroscopic rupture.[25] In addition, the rigid network is important for the Young's modulus because a tense network is hardly deformable at a low strain.[52] Furthermore, the toughness of the DN hydrogel, quantified by the Lake–Thomas theory, is proportional to the rigid network toughness within the experiment scope because most dissipated energy is attributed to the broken rigid network.[53] More excellent toughness of the rigid network leads to more dissipated energy of the DN hydrogel.[53]

The fracture of the DN hydrogel can be calculated. The fracture strength of hydrogels and elastomers can be represented by threshold tearing energy (T_0) that is the energy needed to break molecular chains per unit area at the fracture cross-section.[55] T_0 is measured experimentally using cut-growth tests, and the typical values are 10−100 J/m^2 for elastomers and 0.1−1 J/m^2 for hydrogels. An equation is proposed to estimate T_0 for elastomers:

$$T_0 = \frac{1}{2}\nu_0 \bar{L} NE \tag{1}$$

where ν_0 is the overall chain density, $\bar{L}$ is the average displacement length related to the end-to-end distance of the chains, N is the number of segments between two cross-link points, and E is the energy stored in each segment. Therefore, $\frac{1}{2}\nu_0\bar{L}$ is the number density of the chains at the fracture cross-section, and NE is the total elastic potential energy stored

https://doi.org/10.1021/acs.biomac.3c00765
Biomacromolecules XXXX, XXX, XXX−XXX

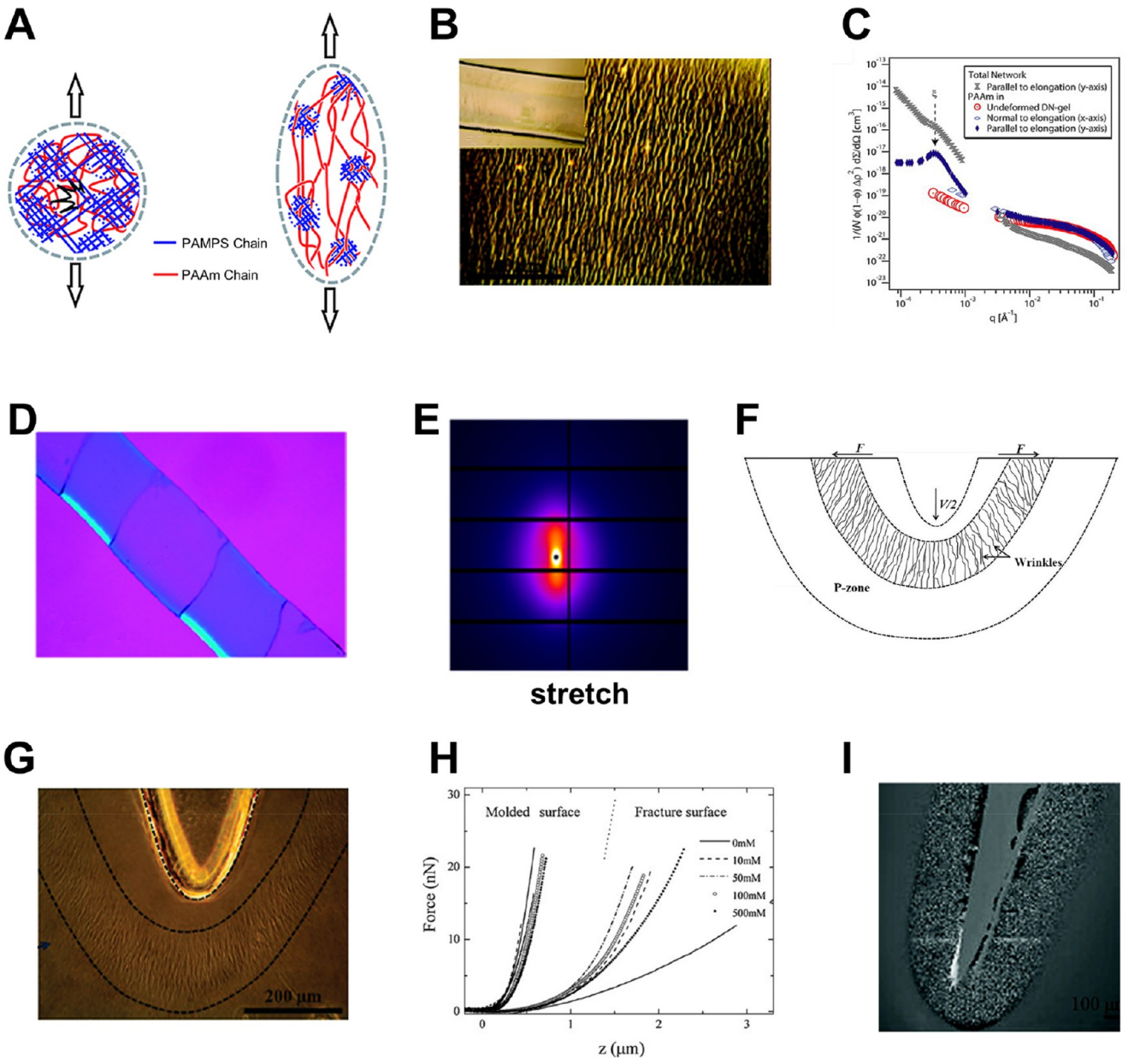

Figure 4. (A) Schematic illustration demonstrates the structure of DN hydrogel under stress observed by (B) phase contrast microscopy, (C) small angle neutron scattering (SANS), (D) polarized optical microscopy, and (E) small-angle X-ray scattering (SAXS). (F) Sketch showing the DN structure around the crack tip studied by (G) phase contrast microscopy, (H) atomic force microscopy (AFM), and (I) color 3D violet laser scanning microscopy. Panel A is adapted with permission from ref 24. Copyright 2010 Royal Society of Chemistry. Panels B, D, F, and G are adapted with permission from ref 42. Copyright 2011 ACS Publications. Panel C is adapted with permission from ref 43. Copyright 2007 Elsevier. Panel E is reproduced with permission from ref 44. Copyright 2020 ACS Publications. Panel H is reproduced with permission from ref 46. Copyright 2008 Wiley-VCH. Panel I is adapted with permission from ref 47. Copyright 2009 ACS Publications.

during the stretch as an indirect evaluation of the energy required for chain scission.

Lake−Thomas theory is successful due to its simplicity, while limits are introduced. Recently, research has focused on the effect of network topological defects on the fracture properties of the polymer networks (Figure 5) and has expanded the Lake−Thomas theory as follows:[54]

$$T_0 = \frac{\nu_0}{2}[(1 - Ax_{\text{loop}} - Bx_{\text{dangling}})L_{\text{linear}}E_{\text{linear}}(\lambda^{\max}) + (x_{\text{loop}} + Cx_{\text{dangling}})L_{\alpha\text{-chain}}E_{\alpha\text{-chain}}(\lambda^{\max})] \quad (2)$$

where x_{loop} and x_{dangling} are the fractions of primary loop strands and dangling-end strands, respectively; ν_0, $\overline{L}$, and $E(\lambda^{\max})$ are the corresponding chain density, displacement length, and total bond energy stored within the strand at the strain ($\lambda^{\max}$) where fracture initiates. Furthermore, the chain that directly attaches onto the effectively dangling strands is called the α-chain.

Compared with the Lake−Thomas theory, some modifications on the theoretical basis are considered as follows:

(1) Different types of defective strands of the network are considered, such as loops, bridges, and dangling ends (Figure 5), meaning that

https://doi.org/10.1021/acs.biomac.3c00765
Biomacromolecules XXXX, XXX, XXX−XXX

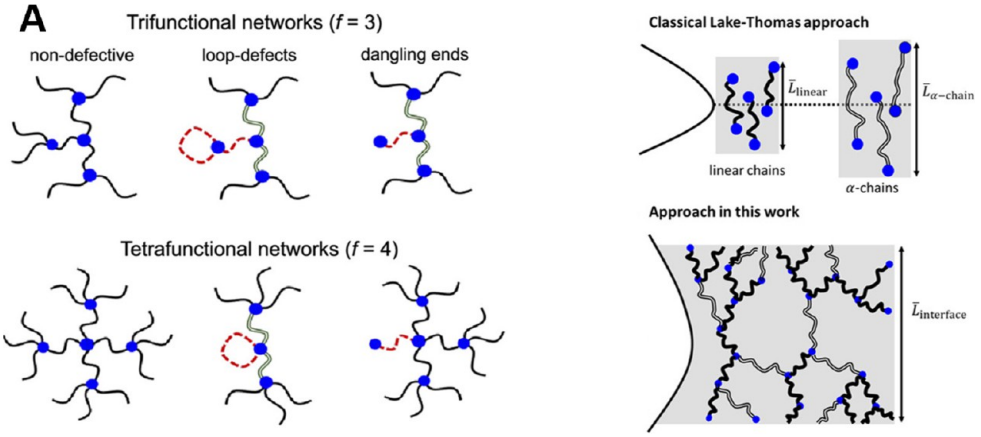

Figure 5. Expanded Lake-Thomas theory involving network topological defects. Adapted with permission from ref 54. Copyright 2020 ACS Publications.

$$(A, B, C) = (4,3,1)$$

for the trifunctional networks

$$(A, B, C) = (3,1,0)$$

for the tetrafunctional networks

(2) Instead of using a predetermined bond-dissociation energy per segment parameter, a force−extension model is involved to determine E_{chain} to estimate the total dissipated energy:

$$\frac{E_{chain}}{k_B T} = N\left[\frac{\lambda}{\sqrt{N}\lambda_b} + \ln\left(\frac{\beta}{\sinh\beta}\right) + \frac{1}{2}E_b(\ln\lambda_b)^2\right] \quad (3)$$

where β is the inverse Langevin function, λ_b is the extension of each Kuhn segment and assumed to be $\lambda_b = 1.4$, E_b is segment stiffness calculated from density functional theory, and a value $E_b = 1200k_BT$ for several flexible polymers is used. Energy stored per segment and per bond can be further calculated.

(3) The stretched network strand around the crack stores the total energy instead of simply the superposition of bond-dissociation energy per segment:

$$\bar{L}_{linear} = \bar{L}_{\alpha\text{-chain}} = \bar{L}_{interface} \quad (4)$$

$\bar{L}_{interface}$ is expected to scale with $N^{1/2}$ for two idealized networks with a very low and a very high x_{loop}, respectively.

(4) As shown in Figure 5, the Flory−Stockmayer theory of gelation is introduced as a criterion to determine the occurrence of fracture instead of assuming that the macroscopical rupture occurs when all chains at the crack cross-section have been broken:

$$q^* = \frac{x_{\alpha\text{-chain}}}{x_{linear} + x_{\alpha\text{-chain}}+} = q \le \frac{1}{f-1} \quad (5)$$

where q is the fraction of load-bearing strands that has not been ruptured, and q^* is the fraction of the α-chain strands. This finding means that when $q < 1/(f-1)$, the network ruptures. The requirement of the fracture criteria is relaxed using the Flory−Stockmayer gel point to provide a zeroth-order estimate. Given that the α-chain is two times longer than the linear chain, two situations are deduced: (1) if q^* is smaller than the Flory−Stockmayer gel point, the rupture of linear strands dominates the crack propagation; and (2) if q^* is larger, fracture occurs after all strands have ruptured.

3.2.2. Inhomogeneity. Inhomogeneity is important for the specific toughening mechanism of DN hydrogels (Figure 6A).[56] First, submicrometer-scale voids of the PAMPS networks in DN hydrogels have been observed by DLS[57] and SAXS[44] (Figure 6B,C). Meanwhile, inhomogeneity is one of the intrinsic properties of hydrogels synthesized from radical polymerization.[57] Voids form and become much larger than the mesh size of the microgel if the growth rate of the polymer cluster is much higher than the relaxation rate.[58−60] The arisen inhomogeneity of the synthetic networks is also supported by the MD simulation results (Figure 6D).[52] Furthermore, the polysaccharide-based rigid network has inhomogeneity. Recently, the MD simulation on a κ-CG-based DN hydrogel also revealed the inhomogeneity of the rigid κ-CG network (Figure 6E).[35] As shown in Figure 6F, the simulation on an agarose/PAAm DN hydrogel shows an inhomogeneous agarose network, where the PAAm network has close and dominant contacts with agarose molecules via hydrogen bonds.[61]

The mechanical properties of the PAMPS/PAAm DN hydrogel could be brittle, ductile (necking), and paste-like at different inhomogeneity levels of the PAMPS network.[62] At an appropriate inhomogeneity, the DN hydrogel performs necking and exhibits high mechanical properties. Spherical voids are further introduced into the PAMPS network to promote the degree of inhomogeneity (Figure 6G).[63] Stress concentration occurs around defects (holes) during deformation, leading to an increased amount of fracture in the rigid network and enhanced toughness. To further explore the role of inhomogeneity in the strengthening mechanism, a kind of DN hydrogel with a nearly homogeneous and well-defined rigid network is designed.[56] As shown in Figure 6H, the TPEG network is established as a homogeneous rigid network. Inhomogeneity is found to be not essential but important for the strengthening mechanism. Inhomogeneity decreases the critical stress for the hierarchical-structure failure.

3.2.3. Mechanical Balance. The DN hydrogel becomes tougher when the strand density of the flexible network is much more than that of the rigid network.[64] As shown in Figure 7A, the model indicates that the effective polymer chain density ratio of the two networks, $\nu_{e,2}/\nu_{e,1} = \kappa$, should be larger than 3.8−9.5 (equivalently expressed as the fracture stress ratio, $\sigma_{f,2}/\sigma_{f,1} = \kappa^{2/3}$, of 2.5−4.5).[25,64] These physical quantities are expressed as the following equations:

https://doi.org/10.1021/acs.biomac.3c00765
Biomacromolecules XXXX, XXX, XXX−XXX

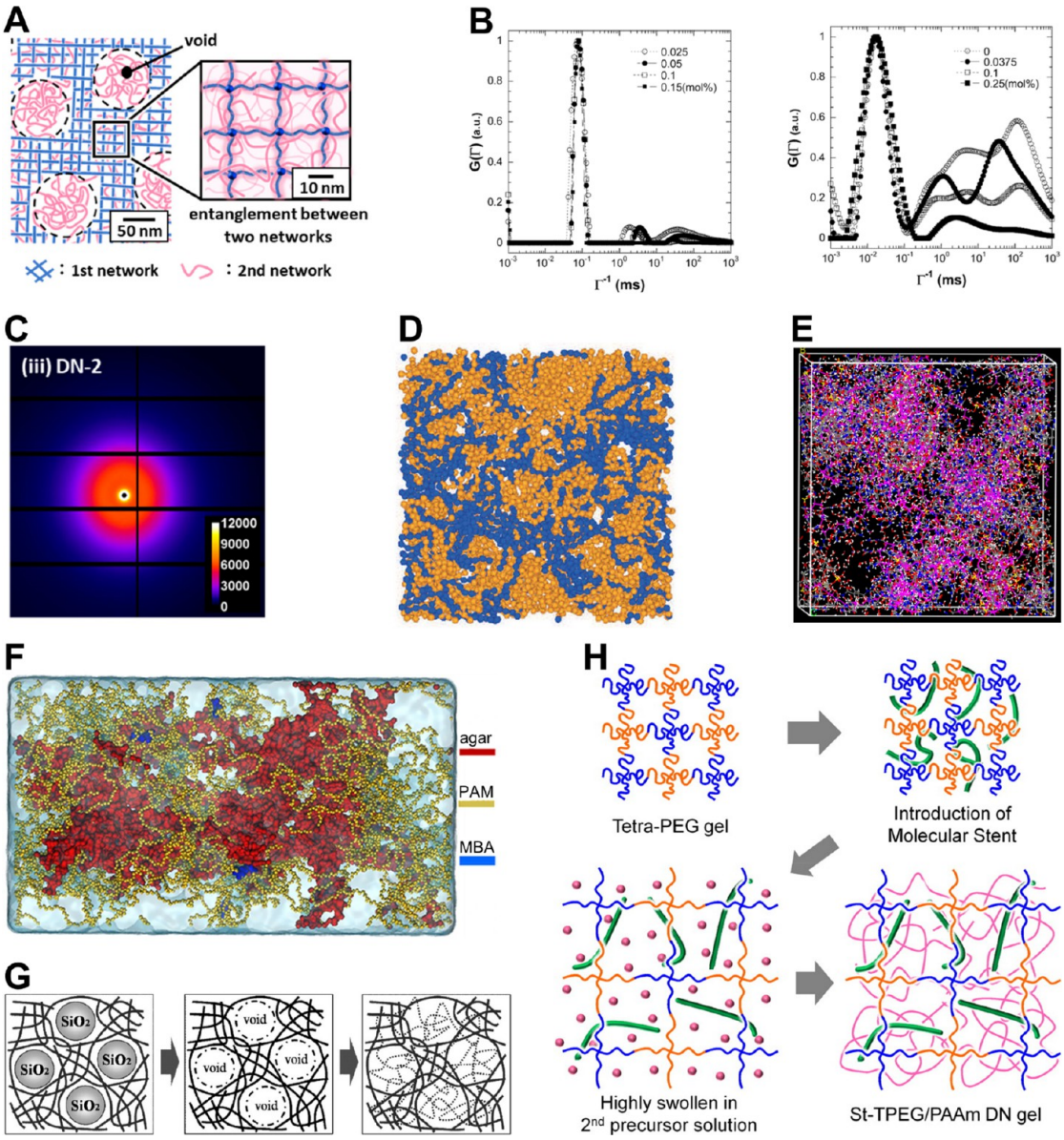

Figure 6. (A) Inhomogeneity of the rigid network was observed by (B) dynamic light scattering (DLS) and (C) SAXS. The inhomogeneity was simulated by (D, E) the MD simulations and (F) a multiscale simulation platform. The introduction of (G) spherical defects and (H) a well-defined tetra-PEG (TPEG) rigid network for the investigation of inhomogeneity. Panel A is reproduced with permission from ref 44. Copyright 2020 ACS Publications. Panel B is adapted with permission from ref 57. Copyright 2004 ACS Publications. Panel C is reproduced with permission from ref 44. Copyright 2020 ACS Publications. Panel D is reproduced with permission from ref 52. Copyright 2018 ACS Publications. Panel E is adapted with permission from ref 35. Copyright 2023 ACS Publications. Panel F is reproduced with permission under a Creative Commons Attribution 4.0 International License from ref 61. Copyright 2021 Springer Nature. Panel G is reproduced with permission from ref 63. Copyright 2011 ACS Publications. Panel H is reproduced with permission from ref 56. Copyright 2013 ACS Publications.

$$\nu_{e,1} = \nu_{e,1}^{s} = \frac{E_0}{3RT}\left(\frac{V_0}{V}\right) \tag{6}$$

$$\nu_{e,2} = \nu_{e,2}^{s} + 3\nu_{e,1}^{s\,1/3}\nu_{e,2}^{s\,1/3}(\nu_{e,1}^{s\,1/3} + \nu_{e,2}^{s\,1/3}) \tag{7}$$

$$\frac{\sigma_{f,2}}{\sigma_{f,1}} = \frac{(\nu_{e,2}N_A)^{2/3}f_2}{(\nu_{e,1}N_A)^{2/3}f_1} = \frac{(\nu_{e,2})^{2/3}}{(\nu_{e,1})^{2/3}} \tag{8}$$

where $\nu_{e,1}^{s}$ and $\nu_{e,2}^{s}$ are the polymer strands number density of the isolated first and second networks, respectively; $\nu_{e,1}$ and $\nu_{e,2}$ are those of the hybrid network, respectively; V_0 and V are the volume of the as-prepared and equilibrium swollen gels, respectively; σ_f and f are the fracture stress of the corresponding network and the fracture force of the single polymer strand, respectively; E_0 is the Young's modulus of the as-prepared gel, R is the gas constant, and T is the temperature.

Simulation results also offer the following insights:[49,52] (1) DN hydrogel suffers from early fracture if the concentration of the flexible network is lower than that of the rigid network. The DN hydrogel gradually exhibits tough mechanical properties when the concentrations of the first and second networks decrease and increase, respectively. (2) When M_c is small, the bond rupture of the flexible network prematurely occurs at a low strain, leading to the macroscopic fracture. The flexible network with increased M_c leads to a higher fracture strength of the DN hydrogel because the flexible network

https://doi.org/10.1021/acs.biomac.3c00765
Biomacromolecules XXXX, XXX, XXX−XXX

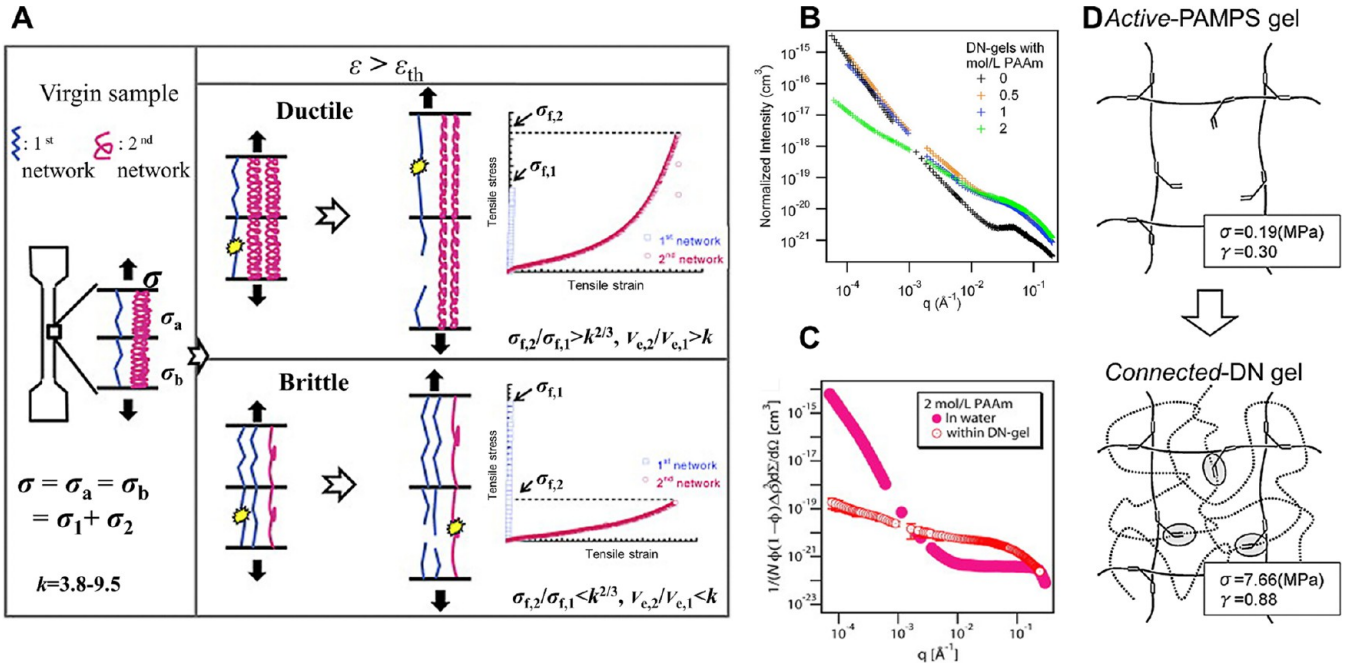

Figure 7. (A) Mechanical balance between the two networks was interpreted by a two-springs model. (B−D) Entanglement in the DN hydrogel: (B) the thermodynamic interaction and (C) molecular association between the two networks revealed by SANS; and (D) the synthetic rigid network grafted by the flexible network. Panel A is reproduced with permission from ref 64. Copyright 2014 Elsevier. Panel B is reproduced with permission from ref 65. Copyright 2008 ACS Publications. Panel C is reproduced with permission from ref 43. Copyright 2007 Elsevier. Panel D is reproduced with permission from ref 66. Copyright 2009 ACS Publications.

remains at a high strain. (3) Desirable mechanical performance could be adjusted by controlling the M_c of the SN network.

3.2.4. Entanglement. The molecular entanglement between the two networks is important in the design of tough DN hydrogels. The entanglement between PAMPS and PAAm is strong only at a high PAAm concentration; thus, the mechanical strength is enhanced.[67] SANS is further applied to reveal the contributions of thermodynamic interaction and the molecular association between the constituents of the DN hydrogel (Figure 7B,C).[43,65] This finding confirms that favorable interactions exist between the two networks and further offer an energy-dissipation mechanism. Moreover, weight-average molecular weight (M_w) affects the entanglement. A study on a DN hydrogel comprising a covalently cross-linked PAMPS network and linear PAAm chains without a cross-linker[68] has shown that the M_w of PAAm is one of the most dominant parameters to significantly the enhancement of a DN hydrogel with a critical value of $M_w = 10^6$.

Entanglement can be enhanced by covalent cross-linking and physical interaction. First, the residual vinyls of the synthetic rigid network are grafted by the monomers of the flexible network (Figure 7D).[66] Accordingly, the research has explored the effect of grafting between the two networks and found that the DN hydrogel with the grafting effect has a higher mechanical strength than the DN hydrogel formed by two isolated networks.[69] Meanwhile, MD simulation shows that the covalent internetwork cross-linking helps the delocalization of stress, resulting in enhancement.[52] During deformation, entanglement enhances elongation of the rigid network, leading to bond breaking. Additionally, a simulation on the polysaccharide-based agarose/PAAm DN hydrogel indicates that the PAAm chains have close and dominant contacts via hydrogen bonds with the agarose bundles.[61] The external stress is transferred gradually from the agarose network to the PAAm network due to the extensive entanglements with increased strain. Therefore, by introducing the covalent and physical interactions between the two networks, the improved entanglement enhances polysaccharides-based DN hydrogels (e.g., covalent bond,[3] ionic bond,[70] and hydrogen bond[71]).

3.2.5. Mechanism of Yield Behavior. The yield point of the DN hydrogel shows an obvious transformation of the mechanical character, which is regarded as the rigid network's internal vast fracture point. By using the TPEG hydrogel as a well-defined and homogeneous rigid network, the yielding behavior of the TPEG/PAAm gel is exposed as follows:[48] (1) the yield point is dominated only by the strain along the stretch direction, irrelevant to other directions; (2) the yield point appears when TPEG chains are stretched to the theoretical maximum molecular-chain length, involving the bond angle/length change most probably (Figure 8A); (3) the yield stress depends on the area density of the TPEG chains; and (4) the flexible network has negligible influence on the yield point.

A hypothesis is further proposed that the rigid network splinters into fragments at the yield point.[48] As shown in Figure 8B, research on a PAMPS/PAAm DN hydrogel[72] exposes the inner fracture process of the rigid network during deformation: (1) the PAMPS network comprises microgels to form a hierarchical and inhomogeneous structure bonded by elastically effective chains that bear the external stress under slight deformation; (2) the elastically effective chains along the stretch direction have started to break at 40% strain in order of length far before the yield point at 200% strain while the PAMPS network remains; (3) around the yield point, most elastically effective chains (90% ratio) have fractured and the network still maintains a certain degree of integrity; (4) after the yield point, the bulk continuous PAMPS network starts to break into discontinuous and anisotropic fragments; and (5) in

https://doi.org/10.1021/acs.biomac.3c00765
Biomacromolecules XXXX, XXX, XXX−XXX

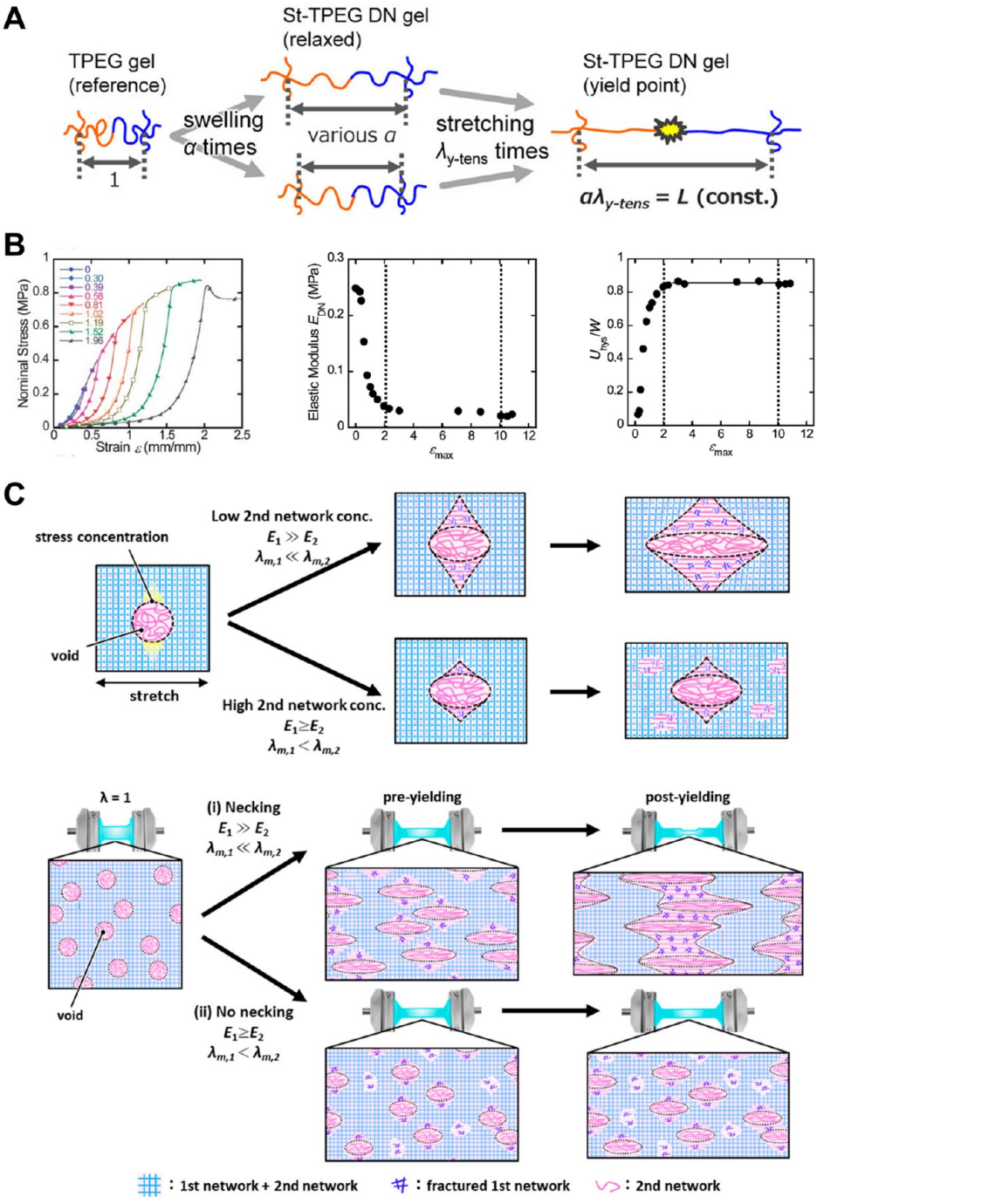

Figure 8. (A) Schematic illustrations for the fracture process of the TPEG chains during deformation. (B) Fracture process of the PAMPS network at the prenecking region of a PAMPS/PAAm DN hydrogel was observed by observing the tensile hysteresis loops, elastic moduli, and dissipated energies. (C) Schematic illustration of the fracturing process governed by the relative strength of the rigid and flexible networks, reflecting the yield behavior and necking. Panel A is reproduced with permission from ref 48. Copyright 2016 ACS Publications. Panel B is adapted with permission from ref 72. Copyright 2013 Royal Society of Chemistry. Panel C is reproduced with permission from ref 44. Copyright 2020 ACS Publications.

the hardening region, the anisotropic fragments further splinter into smaller isotropic clusters.

The investigation on a PAMPS/PAAm DN hydrogel reveals the contributions of both networks to the tensile stress−strain curves (Figure 8B).[50] Before the yield point, the mechanical characters are primarily governed by the rigid PAMPS network and depend weakly on the flexible PAAm network. After the yield point, the mechanical properties are determined by both networks. Furthermore, an empirical guiding principle is proposed for highly tough DN hydrogels:

$$T \propto U_{\mathrm{hys,f}} \propto \varepsilon_{\mathrm{f}} C_{1\mathrm{st}} \tag{9}$$

where T is the tearing energy, $U_{\mathrm{hys,f}}$ is the dissipated energy density at the fracture point, ε_{f} is the fracture strain, and $C_{1\mathrm{st}}$ is the concentration of the rigid network. This is also supported by a MD simulation.[49]

3.2.6. Principle of Necking. Necking appears visually when the rigid network fractures as a yielding phenomenon.[48] Necking represents the stacked damage of the rigid network.[73] A DN hydrogel with necking dissipates a large amount of

https://doi.org/10.1021/acs.biomac.3c00765
Biomacromolecules XXXX, XXX, XXX−XXX

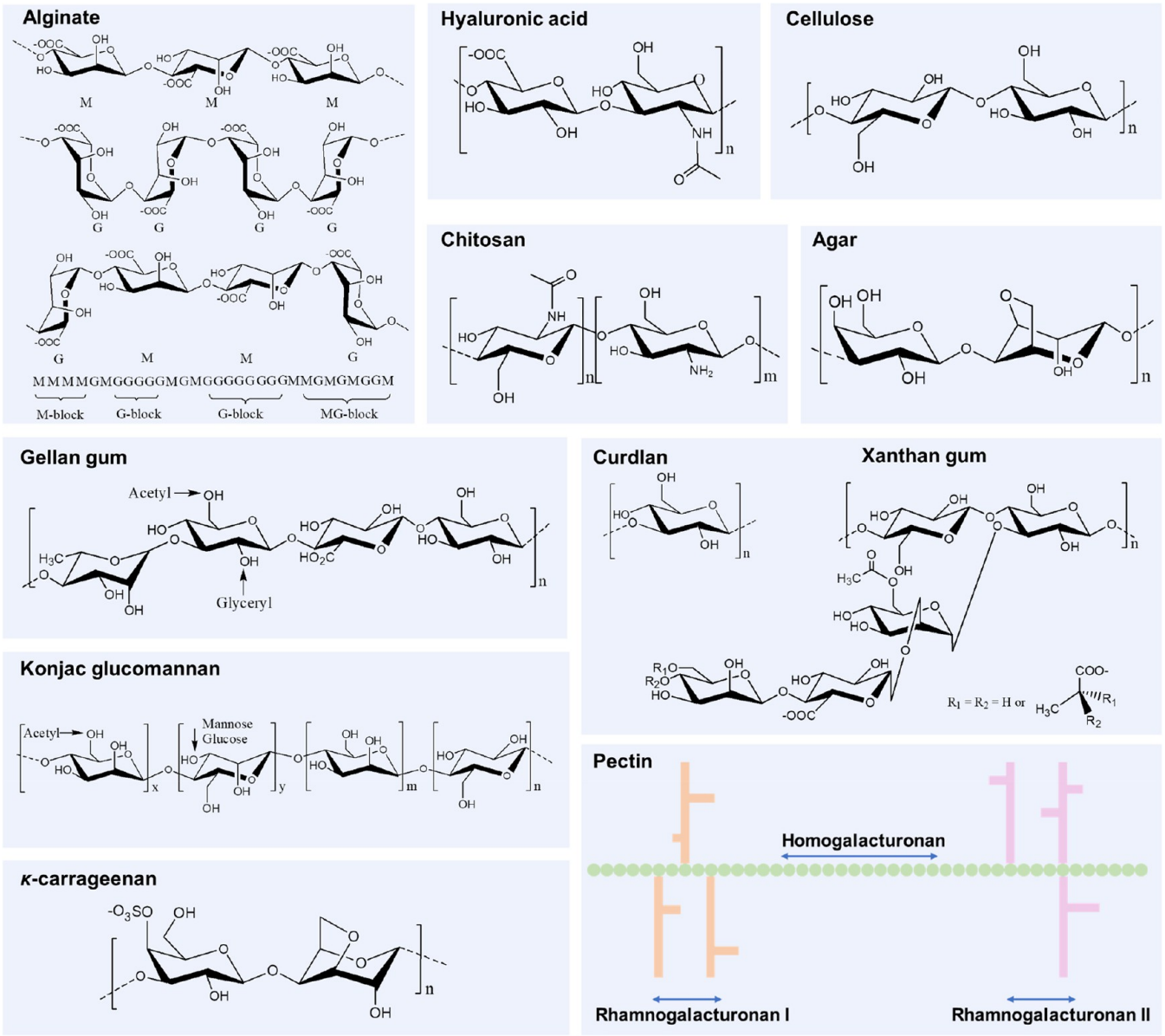

Figure 9. Structural formulas of some polysaccharides, including alginate, hyaluronic acid, cellulose, chitosan (m > n), agarose, κ-carrageenan, gellan gum, Curdlan, xanthan gum, konjac glucomannan, and pectin.

energy, leading to enhanced toughness. Necking is determined by the rigidity and inhomogeneity of the sacrifice network as well as the molecular entanglement and mechanical balance between the two networks.

A study showed that necking requires a brittle rigid network. The extent of molecular entanglement between the two networks is also an important factor for neck propagation.[74] Moreover, necking is related to the inhomogeneity of the rigid network. Distinct necking phenomena are exhibited on PAMPS/PAAm DN hydrogels, where the inhomogeneity of the PAMPS network is adjusted by adding a poor solvent during synthesis.[62] Furthermore, the fracturing process of necking can be determined by the mechanical balance between the two networks (Figure 8C).[44] The initiation and percolation of the fracture near the voids along the direction vertical to the stretching is described as necking, derived from a significant mechanical difference between the two networks. Moreover, the fracture is dispersedly distributed rather than necked if the two networks possess relatively fewer mechanical differences.

A mathematical model is proposed to analyze the necking behavior and energy dissipation, in other words, the pseudoelasticity and damage evolution of the DN hydrogel.[75] Constitutive relations are established by incorporating two internal variables η and J_m in the free-energy function to describe the damage process. η is the stiffness ratio between the damaged phase and the virgin phase. J_m is the tensile threshold of the damaged phase. The free-energy function (Eqn. 10) and the damage evolution (Eqns. 11 and 12) form a complete model for the nonlinear behavior of the DN hydrogel. They are as follows:

$$W(\lambda_1, \lambda_2, \lambda_3, \eta, J_m) = -\frac{\mu}{2}\eta J_m \ln\left(1 - \frac{J_1}{J_m}\right) \quad (10)$$

https://doi.org/10.1021/acs.biomac.3c00765
Biomacromolecules XXXX, XXX, XXX−XXX

Table 1. Component, Cross-Linking Type, Mechanical Property, Feature, and Application of Some Representative Polysaccharide-Based DN Hydrogels

Polysaccharide	Synthetic network	Mechanical properties				
Polysaccharide	Synthetic network	Tensile stress /(Compression stress) (MPa)	Elongation at break /(Compression strain)	Features	Applications	Ref.
$SA^{Ca^{2+}}$	$PAAm^{MBAA}$	0.156	2300%			3
$SA^{Na^{+},Ca^{2+},Ba^{2+},Sr^{2+},Al^{3+},Fe^{3+}}$	$PAAm^{MBAA}$	0.9391	~1400%			37
$SA^{Eu^{3+},Tb^{3+}}$	$PAAm^{MBAA}$	1.02	~1900%	Cytocompatibility, photoluminescent		82
$SA^{Na^{+}}$	$PAAm^{MBAA}$	~0.66	~1980%	Self-healing	Strain sensor	83
$SA^{Ca^{2+},A\text{-}aGO}$	$PAAm^{MBAA}$	0.8627/(33.2)	3324%/(~95%)		3D-printing	84
$SA^{Zn^{2+}}$	$PAAm^{MBAA}$	~0.014	~600%		Zn-air/iodide battery	85
$SA^{Ca^{2+}}$,CNT	$PAAm^{MBAA,\ CNT}$	0.27168/(0.15118)	4200%/(80%)	Self-healing, photoresponse	Strain sensor	86
$SA^{Fe^{3+}}$	Poly(AAm-*co*-AAc)$^{Fe3+}$	3.24	1228%	Self-healing, non-swelling	3D-printing, shapeability, shape memory	87
$SA^{Ca^{2+}}$	$PAAm^{MBAA}$ Glass fabric	2.40 MPa	~57%	Impact-resistant	Protective material	88
(SA and CHT)$^{Ca^{2+}}$		(~0.19)	(43%)		Adsorption	89
$SA^{Ca^{2+}}$ κ-$CG^{Ca^{2+}}$		(1.07)	(90%)		Adsorption	90
$SA^{Fe^{3+},glutaraldehyde}$ Guar $gum^{glutaraldehyde}$		4.02	127%	Self-healing, fast recovery	Strain sensor	91
$SA^{Ca^{2+}}$ $Gelatin^{microbial\ transglutaminase}$		~1.3 MPa	~245%	Cytocompatibility	Bioprinting	92
Oxidized $HA^{ELP\text{-}HYD}$	$ELP\text{-}HYD^{HA}$			Injectability	Cell encapsulation	93
Glycidyl methacrylate HA	$PAAm^{MBAA}$	(5.2)	(70%)	Cytocompatibility		94
BC	PVA	51/(98)	~14%/(~47%)	Wear resistance, Adhesion		95
BC Gelatin		(3.7)	(37%)	Anisotropy		96
CNC	$PAAm^{MBAA}$	~0.06	~800%	Anisotropy by deformation		97
CNC	$PAAm^{PEGDA}$	0.151/(1)	1388%/(90%)			98
$CMC^{Zn^{2+}}$	Poly(AAc-*co*-NVP)$^{Zn^{2+}}$	0.86	1019%	Self-healing	3D-printing, strain sensor	99
$CMC^{Fe^{3+}}$	PNAGA	2.9	639%	Self-healing, cytocompatibility, non-swelling		71
$CEQC^{ZnSO_4}$	$PAAm^{MBAA}$	0.2/(0.525)	990%/(80%)	Conductivity	Aqueous zinc battery	100
QCE	$PVAPAAc^{Fe^{3+}}$	1.13	465%	Self-healing	Antibacteria	101
$Chitin^{PEGDE}$	$PAAm^{MBAA}PEGDE$	0.449	1400%	Cytocompatibility	Antibacteria	102
$CHT^{NaOH,\ NaCl}$	$PAAm^{MBAA}$	2.12	470%	Fast recovery		32
$CHT^{Na_2SO_4,Na_3cit}$	$PAAm^{MBAA}$	5.6	390%	Fast recovery		103
CHT^{NaCl}	Poly(AAm-*co*-AAc-*co*-DOPA-AAm)^{Fe_3O_4}	0.421	~150%	Self-healing, cytocompatibility	3D-printing NMR-imaging	104
$HACC^{PAAc}$	$PAAc^{HACC}$	3.31	870%	Self-healing, fast recovery, nonswelling	Supercapacitor	70
CHT^{NaCl} Tannic acid coated CNC	$PAAm^{MBAA}$	1	800%	Adhesion	Strain sensor	105
DOPA-$CHT^{Fe^{3+},genipin}$ $CHT^{genipin}$		(2.5)	(90%)	Self-healing, fast recovery, injectability, cytocompatibility		33
(Methacryloyl CHT and catechol methacryloyl CHT)$^{Fe^{3+},C-Cbond}$		(0.6966)	(90%)	Adhesion, injectability, cytocompatibility	Wound healing, antibacteria	106
(CCHT and Odex)$^{imine\ bond}$				Self-healing, injectability, cytocompatibility	Wound healing	107
(Thiolated CHT and Odex)$^{imine\ and\ disulfide\ bonds}$				Injectability, cytocompatibility		108
Agar	$PAAm^{MBAA}$	1/(38)	2000%/(98%)			31
Agar	$PAAm^{MBAA}$				Strain sensor	13
Agar	$PAAm^{SMA}$	0.267	5260%	Self-healing, fast recovery		109

https://doi.org/10.1021/acs.biomac.3c00765
Biomacromolecules XXXX, XXX, XXX−XXX

Table 1. continued

Polysaccharide	Synthetic network	Mechanical properties				
Polysaccharide	Synthetic network	Tensile stress /(Compression stress) (MPa)	Elongation at break /(Compression strain)	Features	Applications	Ref.
Agarose	(4-arm-PEG-NHS) and (4-arm-PEG-NH_2)	(28.8)	(∼98%)	Injectability, cytocompatibility		110
Agar	Poly(AAm-*co*-AAc)$^{Fe^{3+}}$	8.8	300%	Fast recovery		76
Agar	$PAAc^{Fe^{3+}}$	0.321	1130%	Self-healingFast recovery		111
Agar	$PAAm^{SMA}$	∼0.75	3400%		Electrocircuit, supercapacitor	112
$GG^{Ca^{2+}}$	$PAAm^{MBAA}$	(0.216)	(77%)			113
$GG^{Na^+,K^+,Ca^{2+}}$	$PAAm^{MBAA}$	∼0.54	∼2360%	Self-healing	Strain sensor	114
GG^{Na^+}	$PAAm^{SMA}$	0.400/(∼3.8)	1640%/(90%)	Self-healing, antifatigue, cytocompatibility	Cartilage repair	115
GGLocust bean $gum^{B(OH)_4^-}$		0.0282	216%	Self-healing	Recurrent shapeability, shape memory	116
(Methacrylate GG and methacrylamide gelatin)$^{C-C\ bond}$		(6.9)	(81%)	Cytocompatibility		117
κ-CG^{K+}	$PAAm^{MBAA}$	0.558/(15.4)	2100%/(95%)	Self-healing, fast recovery		39
κ-CG^{K+}	$PAAm^{MBAA}$	∼0.69	∼1150%	Self-healing, fast recovery	3D-printing, strain sensor	34
κ-CG^{K+}	$PAAm^{SMA}$	1.35	1400%	Self-healing, cytocompatibility		118
κ-$CG^{K^+,Ca^{2+}}$	$PAAm^{MBAA}$	∼0.67	∼2000%	Self-healing		40
κ-CG^{K+}	PNV	0.274/(1.55)	1042%/(99%)	Injectability, thermoplasticity, controllable adhesion, cytocompatibility, fast recovery	Hydrogel coating, touch strip, touch panel	35
XG^{Ca2+}	$PAAm^{SMA}$	3.64	1575%	Self-healing		119
Curdlan	$PAAm^{SMA}$	0.805/(62.5)	2530%/(99%)	Self-healing, fast recovery		120
$CMCD^{Ca^{2+}}$	$PAAm^{MBAA}$	0.69	2185%	Cytocompatibility	Cartilage repair	36
$Pectin^{Fe^{3+}}$	$PAAm^{MBAA}$	0.9	1300%			41
$Pectin^{Fe^{3+}}$	$PAAm^{SMA}$	∼1.6	∼1300%	Cytocompatibility		121
CS^{PDA}	$PAAm^{MBAA}PDA^{CS}$	(0.15)	(80%)	Cytocompatibility, adhesion	Cartilage repair	122
Guar $gum^{B(OH)_4^-}$	$PAAm^{MBAA}$	0.843	1400%	pH responsion		123

https://doi.org/10.1021/acs.biomac.3c00765
Biomacromolecules XXXX, XXX, XXX−XXX

$$\eta(\lambda_{max}) = 1 - \frac{\eta_0}{2}\left[\mathrm{erf}\left(\frac{1}{\sqrt{2}\,d}\ln\frac{\lambda_{max}-1}{\lambda_0-1}\right)+1\right] \quad (11)$$

$$J_m = J_0 + \alpha J_{1max} \quad (12)$$

where λ_1, λ_2, and λ_3 are the strain and $\lambda_1\lambda_2\lambda_3 = 1$; $J_1 = \lambda_1^2 + \lambda_2^2 + \lambda_3^2 - 3$ is the deformation gradient; $W(\lambda_1,\lambda_2,\lambda_3,\eta,J_m)$ is Helmholtz free energy per unit volume of a DN hydrogel; μ is the modulus of the virgin phase; λ_0 is approximately the most probably fracture stretch; d is a parameter controlling the width of the probability distribution; and η_0 is a dimensionless parameter for normalization. This model is used for the homogeneous uniaxial and biaxial tensions of a DN hydrogel. The energy dissipations of the homogeneous and neck deformations are further calculated. This model also shows that energy dissipation is the key to the high toughness of the DN hydrogel, which is ready for further association with field theories to describe the DN hydrogel under complex deformations.

3.2.7. "Chain-Pulling-Out" Fracture Mechanism. Research indicates that shorter polysaccharide chains of polysaccharide-based DN hydrogels are first pulled out from junction zones during deformation, which is the "chain-pulling-out" fracture mechanism.[38,76,77] A simulation supports this mechanism.[61] At a certain strain, fracture occurs in the agarose network through the chain pulling-out mechanism, where agarose bundles are separated by unzipping interfacial interactions with the partial disruption of helical conformations, resulting in energy dissipation. Rigid agarose molecules are pulled out, leading to the rupture of hydrogen bonds, chain entanglement, and water association. Meanwhile, the conformations of PAAm chains range from entangled coils to stretched chains.

The classic DN strategy needs the destruction of the chemically cross-linked rigid network, which results in a decrease in the mechanical characteristics of the DN hydrogel after the first deformation. However, for the physically cross-linked polysaccharide network, shorter polysaccharide chains pull apart junction zones. Meanwhile, the polysaccharide network is preserved and has a decreased cross-linking strand density, which allows the stack of the network damages to show a velocity-dependent fracture behavior and toughness.[76,77] As the strain increases, polysaccharide chains maintain integrity along with the sacrifice of hydrogen bonds, water associations, and chain entanglements.[61] Benefitted from the "chain-pulling-out" fracture mechanism, the chains of physically cross-linked polysaccharide networks can maintain integrity during the deformation to offer reparable rigid networks and repeatable energy dissipations compared with the synthetic networks.[31,32,34] As a result, the DN hydrogels with such polysaccharide networks will present a self-recovery ability.

3.2.8. Challenges and Outlook. The field of strengthening mechanisms has witnessed important progress in explaining the mechanical properties of DN hydrogels. However, challenges need to still be overcome to guide the design of polysaccharide-based DN hydrogels. The yield point of a polysaccharide-based DN hydrogel is generally explained by the "chain-pulling-out" fracture mechanism. However, many polysaccharide-based DN hydrogels exhibit unsharp yield points, low-yielding stress and strain, and no flat necking platform,[76] which is hard to be interpreted through existing strengthening mechanisms[39] and requires further investigation. Meanwhile, the mechanical behavior of fully physical cross-linked DN hydrogels needs further research to guide the fabrication of next-generation DN hydrogels. Additionally, mathematic and simulated models for understanding the associations among various factors (e.g., mechanical property, composition, network structure, and cross-linking type) are still lacking. Finally, the reason why a concentration as low as 1% of some polysaccharides significantly enhances the mechanical strength of the DN hydrogel remains unclear. The deformation process of the polysaccharide-based DN hydrogel is still in its infancy, such as the structural transformation of the rigid polysaccharide network, dissociation of physical interactions, and dissipated energy.

4. PROPERTIES OF POLYSACCHARIDES USED IN DN HYDROGEL

To answer the question of why we chose polysaccharides to prepare DN hydrogels, the basic properties of commonly used polysaccharides for DN hydrogels are essential. Polysaccharides including SA, HA, cellulose, CHT, agar, GG, κ-CG, XG, Curdlan, pectin, CS, guar gum, KGM, and locust bean gum, are used, whose chemical structures are shown in Figure 9.

Polysaccharides from plants and algae show very large differences in physical and chemical properties from batch to batch, which vary with the botanic source, growth condition, maturity at harvest, and extraction method.[78,79] Exopolysaccharides (e.g., XG, GG, and Curdlan) are produced from the fermentation of a well-defined medium by a pure bacterial culture that is strict in the process parameters, such as pH, temperature, aeration, and agitation. Meanwhile, the products are extracted from fluid broths, rather than tissues. Thus, exopolysaccharides are expected to show far less variability of physical and chemical properties.[80,81]

Highlightable polysaccharide-based DN hydrogels are selected and displayed in Table 1, including the kinds and cross-linking ways of the applied polysaccharides and synthetic polymers, the representative mechanical properties selected by the author, the unique features, and the applications. If two polysaccharide networks exist in interaction with each other, they are mentioned as X and Y. The superscripts of polysaccharides and synthetic polymers are the cross-linking approaches. Compared with self-recovery, only fast recovery is considered because all DN hydrogels possess a certain extent of self-recovery. Cytocompatibility means that in vitro experiments are performed and show no obvious cytotoxicity. When explicit and precise mechanical properties are not given in the corresponding research, data are obtained from the reported stress−strain curves and prefixed with symbol "∼". The number of significant digits is consistent with that in the corresponding research.

4.1. Alginate. Alginate (SA), existing in brown seaweed, is a linear anionic block copolymer of β-1,4-linked D-mannuronic acid (M) and α-1,4-linked L-guluronic acid (G) residues.[124,125] The gelling of SA is determined by the coordination number of cations and is weakly influenced by the temperature, pH, and hydrophobic interaction.[126] The formation of a SA hydrogel exposed to cations originates from the electrostatic shielding and ionic bond, which is explained by the "egg-box" model.[124] Meanwhile, the mechanical properties of ion-induced SA hydrogel are proportional to M_w and the amount of guluronic acid.[127] The type of multivalent cation also influences the mechanical properties of the SA hydrogel. The binding mechanism differs with the type of cation. For example, Ca^{2+} can bind only to the G- and MG-blocks, Ba to G- and M-

https://doi.org/10.1021/acs.biomac.3c00765
Biomacromolecules XXXX, XXX, XXX−XXX

blocks, and Sr to G-blocks only.[124] By contrast, the binding of trivalent cations is tougher than divalent cations, where trivalent cations interact with three carboxyl groups to form a more compact network.[37] Some trivalent cations show more effective improvement in the strengths of SA-based DN hydrogels than divalent cations, such as Al^{3+}, Eu^{3+}, and Tb^{3+}.[37,82] In addition, SA hydrogels can be formed through external gelation (dialysis to introduce cations) and internal gelation (e.g., using $CaCO_3$ and $CaSO_4$). SA hydrogels can also be obtained via hydrogen bonds by decreasing the pH to a value below the disassociation constant (pK_a, 3.38 and 3.65 for M and G residues, respectively).[124] Moreover, the affinity between divalent ions and SA follows the order $Pb^{2+} > Cu^{2+} > Cd^{2+} > Ba^{2+} > Sr^{2+} > Ca^{2+} > Co^{2+}$, Ni^{2+}, $Zn^{2+} > Mn^{2+} > Mg^{2+}$, Hg^{2+}. The hydrogel stability decreases in the following order: $Ba^{2+} > Cd^{2+} > Cu^{2+} > Sr^{2+} > Ni^{2+} > Ca^{2+} > Zn^{2+} > Co^{2+} > Mn^{2+} > Mg^{2+}$.

In addition, alginate is considered nonimmunogenic, and biodegradable, which has been widely applied in different fields, such as biomaterials, ionic absorbents, and food applications.[80,128] Alginate possesses abundant free hydroxyl and carboxyl groups on the backbone, which can be chemically functionalized (e.g., oxidation, sulfation, esterification, amidation, or grafting methods) to modify its physical, chemical, and biological properties.[128,129]

4.2. Hyaluronic Acid. HA, also called hyaluronan, comprises a linear anionic backbone of repeating disaccharide units of D-glucuronic acid and *N*-acetyl-D-glucosamine linked through β-(1,4) and β-(1,3) glycosidic junctions.[130] Up to now, HA hydrogels are mainly formed by chemical cross-links. Besides, it is proved that HA hydrogels can be formed through physical interactions during the freeze/thaw process.[130] Furthermore, HA is the major component of the extracellular matrix (ECM) of skin, cartilage, and vitreous humor expressed in almost all bodily tissues and fluids with different concentrations and molecular weights, reflecting its biological importance and potential for clinical use.[131] This biopolymer has unique properties, such as biodegradability, nonimmunogenicity, noninflammatory, and viscoelastic characteristics.[80] It offers abundant mechanical and biological signals to surroundings via cell surface receptors, which will affect cell adhesion, migration, and downstream cell signaling.[131] Moreover, HA is accessible to chemical modifications via hydroxyl, carboxyl, and amide groups, which greatly expands its application in many fields.

4.3. Cellulose. Cellulose is a linear homopolymer of β-1,4-linked D-glucose with degrees of polymerization from 100 to 20 000.[132] Cellulose cannot dissolve in water and common organic solvents because the molecular chains (usually 36) are arranged closely and orderly via hydrogen bonds, which is called cellulose microfibril with high crystallinity.[126] Therefore, ionic liquids are developed to dissolve cellulose, such as 1-butyl-3-methylimidazolium chloride and 1-*N*-butyl-3-methylimidazolium chloride.[132] Meanwhile, a mixture of *N*-methylmorpholine-*N*-oxide and water can dissolve cellulose. Cellulose dissolved in ionic liquids or *N*-methylmorpholine-*N*-oxide/water can be used for the fabrication of cellulose hydrogels by exposure of the precursor solutions to water. Cellulose can also be dissolved in customized aqueous solutions, such as NaOH/urea and NaOH/thiourea solutions, where cellulose hydrogels have been prepared by changing the temperature of these solutions.[132] Furthermore, some cellulose derivatives present the gelling property, e.g., methyl cellulose, hydroxypropyl cellulose, and hydroxypropylmethyl cellulose, whose gelation is mainly attributed to the hydrophobic interaction.

Cellulose is the most abundant structural polysaccharide of plants and a renewable polymeric raw material existing extensively on earth.[80] Crystalline cellulose is divided into different types, such as I, II, III, and IV. Cellulose I is the natural cellulose with two polymorphs (triclinic and monoclinic structures) from plants, tunicates, algae, and bacteria. Cellulose has outstanding mechanical properties, such as a high elastic modulus (130−150 GPa), a high specific surface area (up to several hundreds of m^2/g), and low density (1.6 g/cm^3).[133] Moreover, the increasing requirements for environmental friendliness and biodegradability have led to numerous studies on cellulose-based materials and applications. Cellulose with abundant hydroxyl groups is suitable for modification to obtain the desired structures and properties.[132] Cellulose generates important commercial products, such as cellulose ethers/esters and micro/nanosized cellulose products. In addition, cellulose particles attract considerable attention, such as wood and plant fibers, nanofibrilated cellulose, cellulose nanocrystal, algae cellulose particle, and bacterial cellulose (BC) particle.[133]

Compared with cellulose, BC is a kind of cellulose synthesized by bacteria, such as *Rhizobium*, *Agrobacterium*, *Pseudomonas*, and *Salmonella*.[134] The structure and property of BC vary with cultivation techniques, such as static culture and agitated culture. The typical degree of polymerization for BC ranges between 2000 and 6000.[134] BC contains twisted ribbon-shaped fibrils with a width of 50−100 nm and a thickness of 3−8 nm. Meanwhile, the BC sheet can possess a high Young's modulus (15 GPa) and form a hydrogel simply treated with water because of the high porosity and water-holding capacity. In addition, BC presents the anisotropic layered structure originating from the static culture formed by the stacking of fibrils at the liquid−gas interface.[134] Therefore, BC hydrogels can be fabricated in situ during production.[132] The as-biosynthesised BC hydrogel contains only about 10% free water of the total 99 wt% water, whereas the other water molecules are tightly bound to the cellulose.[132]

4.4. Chitin and Chitosan. Chitin contains a linear backbone comprising β-1,4-linked *N*-acetylglucosamine.[135,136] Chitin is structurally similar to cellulose, which is the major component of the cytoderm of fungi and the cuticula of insects, crustaceans, and radulae of mollusks. Chitin is classified into α-type (a structure of antiparallel chains), β-type (parallel chains and intrasheet hydrogen bond), and γ-type (the combination of α-type and β-type). Moreover, except for hexafluoroisopropanol, hexafluoroacetone sesquihydrate, some chloroalcohols, and concentrated acids, chitin is insoluble in most solvents because of the high crystallinity and strong hydrogen bond.[135] In addition, chitin hydrogels can be formed by increasing the concentration in specific solutions (e.g., solvents of *N*,*N*-dimethylacetamide/LiCl, NaOH/urea, $CaCl_2$/methanol, and ionic liquid) and dialysing the solutions in poor solvents (e.g., water, ethanol, and H_2SO_4/Na_2SO_4).[137] For more information on the solvents for chitin, refer to Shamshina et al.[135] Chitin-based hydrogels are promising as biomaterials due to their inherent properties of cytocompatibility, biodegradability, safety, and nontoxicity.[80]

CHT is a polycationic copolymer formed by the *N*-deacetylation of chitin and comprises glucosamine and *N*-acetylglucosamine units.[138] It is widely exploited on account of its cytocompatibility, antibacterial and hemostatic activities,

https://doi.org/10.1021/acs.biomac.3c00765
Biomacromolecules XXXX, XXX, XXX−XXX

biodegradability, and muco-adhesiveness.[80,138,139] Furthermore, CHT dissolves in an acidic solution (such as acetic acid) and is insoluble under neutral and alkaline conditions. CHT is soluble at a pH lower than ~6.3 and in ferric solutions through coordination interaction among ferric ions, hydroxyl groups, and amino groups.[138] CHT hydrogels can be fabricated by treating the CHT solution with the aqueous solutions of NaOH, NaOH/Na_2CO_3, sodium citrate, tripolyphosphate, and β-glycerophosphate.[137] In addition, CHT hydrogels can also be prepared by the ionotropic gelation of an aqueous solution containing CHT/EDTA/urea or CHT/citric acid/urea under heating. Furthermore, the addition of yeast cells to the CS network can enhance the CS/yeast hybrid hydrogels.[140]

4.5. Agarose. Agarose is a linear polysaccharide comprising β-1,3-linked D-galactose and α-1,4-linked 3,6-anhydro-αL-galactose residues.[141] Agar, usually extracted from marine red algae, comprises agaropectin and agarose that is the major part of agar.[126] Agarose and its derivatives are widely used as biomaterials for different applications such as neurogenesis, angiogenesis, cartilage and bone regeneration, and wound healing. Agarose can be dissolved in water, dimethyl sulphoxide, dimethylformamide, formamide, *N*-methylformamide, and 1-butyl-3-methylimidazolium chloride. In addition, agarose forms an aqueous solution above 80 ~ 90 °C and undergoes a thermoreversible sol−gel transition cooled below 30 ~ 40 °C, where the temperature is determined by the molecular weight, concentration, and number of side groups.[141] Agarose molecules are primarily random coils in the sol state above the melting point. The gelation is primarily attributed to the transition of coil-helix conformation and the aggregation of single helices induced by hydrogen bonds and electrostatic interaction.[141] Besides the thermal gelling property, agarose presents the pH-response property and electro-responsive activity.[80] Meanwhile, agarose hydrogel with a low concentration has been used for simulating the brain with poroelasticity and soft tissue mechanics.[141]

4.6. Xanthan Gum. XG is an anionic exopolysaccharide with a high M_w (1×10^6 to 20×10^6 g/mol) and is primarily derived from the fermentation process of the Gram-negative bacterium *Xanthomonas campestris*.[142] The backbone of XG has 1,4-linked β-D-glucose as a repeating unit with side chains.[126] Furthermore, the trisaccharide side chain comprises a glucuronic acid residue between two mannose units linked to every alternate glucose residue by β-1,3.[142] The glucuronic acid is linked to the α- and β-D mannoses via α-1,2 and β-1,4, respectively. For about two β-D mannoses, a pyruvic acid residue is bonded by the keto group to the 4 and 6 positions. The acetate group is attached onto the α-D mannose at the 6 positions. Moreover, the composition and molecular weight of XG vary with the type of *Xanthomonas pathovar* and procedure condition. The contents of the acetate group and pyruvic acid residue are 60%−70% and 30%−40%, respectively.

The conformation of the XG chain in water changes between the helix and coil structure, which depends on the pH, ionic strength, and acetyl and pyruvyl contents. XG forms physical networks exposed to bivalent cations by involving two disaccharide units in the backbone and O-acetyl and pyruvyl residues in side chains. Generally, higher pyruvate content and lower acetyl content benefit the gelation.[143] The transition from coil to double-helix is a prerequisite for stronger gelation. XG ionic liquid solutions have been soaked in water to generate high performance hydrogels by involving ionic cross-links from Na^+, Ca^{2+}, and Fe^{3+}.[144] In addition, XG has extensively been applied in different fields, such as the food industry, water treatments, and biomedicine, because of its thickening ability, high viscosity even at a very low concentration, high stability at broad temperatures, pH, ionic strength, stability under shear, nontoxicity, cytocompatibility, and immunological response.[80]

4.7. Gellan Gum. GG has a linear chain with a repeating sequence of a structure (D-glucose-(β-1,4)-D-glucuronic acid-(β-1,4)-D-glucose-(β-1,4)-L-rhamnose-(α-1,3)).[145] GG is an anionic exopolysaccharide obtained by the fermentation of *Sphingomonas elodea*.[80,126] In addition, GG is commercially available in two forms (high acyl GG and acylated GG). High acyl GG has two substituents on the 3-linked glucose with one L-glyceryl group on O(2) per repeat unit and one acetyl group on O(6) per every two repeat units.[145] By contrast, the acylated GG, known as "gellan gum", is obtained through a deacetylation process of high acyl GG by alkali treatment.

High acyl GG forms a soft and flexible hydrogel under cooling below 65 °C, whereas low acyl GG hydrogel is rigid and brittle below 40 °C. Furthermore, GG has native cations (primarily Na^+, K^+, Mg^{2+}, and Ca^{2+}) that are introduced from the nutrient salts during fermentation and postfermentation. The gelling mechanism of GG without external ions is attributed to the following:[145] (1) the conformational transition between random coil and double helix; (2) the spontaneous aggregation of the double helices as the junction zone; and (3) the intra- and intermolecular hydrogen bonds between the hydroxymethyl groups of the 4-linked glucose in one chain and carboxylate groups in the other. Moreover, the gelation of GG exposed to Group I cations is attributed to the electrostatic shielding and the coordination between cations and oxygen atoms. Five oxygen atoms interact with the monovalent cation in the helix, namely, the two atoms from the carboxylate group, O(2) of the adjacent glucose, O(2) of glucuronic acid from the other strand, and O(6) of the adjacent glucose from the other strand. The effect of monovalent and divalent cations on the gel strength increases in the following order: $Li^+ < Na^+ < K^+ < Cs^+ < Mg^{2+} \leq Ca^{2+}$, Sr^{2+}, $Ba^{2+} < Zn^{2+} < Cu^{2+} < Pb^{2+} < H^+$, where H^+ is called "the most potent gel-former". The affinity between divalent ions and GG follows the order $Ba^{2+} < Zn^{2+} < Cu^{2+} < Pb^{2+}$.[78]

GG has been extensively developed for tissue engineering and regenerative medicine applications since GG presents cytocompatibility, bioactivity, noncytotoxicity, low induction of inflammation, mild processing conditions, structural similarity with nature glycosaminoglycans, and mechanical similarity to the tissue moduli.[80,145]

4.8. κ-Carrageenan. Carrageenan is extracted from certain species of red seaweeds.[146] Carrageenan contains different types, such as λ, κ, ι, ε, and μ.[147] κ-CG exists in the tropical seaweed *Kappaphycus alvarezii*.[126] It has a linear backbone of alternating α-1,3-linked D-galactose-4-sulfate and β-1,4-linked 3,6-anhydro-D-galactose) containing ~ 25 w/w% sulfate and ~ 34 w/w% 3,6-anhydro-D-galactose.[147] Furthermore, κ-CG forms a thermal-reversible hydrogel that comprises double helices, aggregated monohelices, and aggregated helical dimers meanwhile.[148] Meanwhile, cations will enhance the mechanical strength of the κ-CG hydrogel.[149] The order of cation enhancement ability follows: Li^+, $Na^+ < Ca^{2+}$, Cu^{2+}, $NH_4^+ < K^+$, $Cs^+ < Rb^+$. For divalent cations, it increases as follows: $Co^{2+} < Zn^{2+} < Mg^{2+} < Sr^{2+} < Ca^{2+} < Ba^{2+}$. For anions, the inhibitory effect is as follows: $Cl^- < NO_3^- < Br^- < SCN^- < I^-$.[148] Moreover, the κ-CG hydrogel cross-linked by K^+ forms

https://doi.org/10.1021/acs.biomac.3c00765
Biomacromolecules XXXX, XXX, XXX−XXX

through the electrostatic interaction to form the bridge of (the sulfate group of D-galactose)-K^+-(the anhydro-O-3,6 ring of another D-galactose).[35] κ-CG possesses outstanding properties, such as low cost, nontoxicity, cytocompatibility, biodegradability, low immunogenicity, which is widely applied in pharmaceutical formulation, the food industry, and drug delivery induced in USP35-NF30 S1.[35,80]

4.9. Curdlan. Curdlan, a straight-chain polymer, is made up of β-1,3-linked D-glucose produced by *Agrobacterium biobar*.[150,151] Curdlan is insoluble in cold water due to the intra/intermolecular hydrogen bond and dissolves in an alkaline solution and dimethylsulfoxide. Moreover, Curdlan has unique gelation properties.[126] When the Curdlan suspension at 55 °C is cooled to room temperature or heated to 80−100 °C, thermally reversible and irreversible Curdlan hydrogels will be formed, called low-set gel and high-set gel, respectively. The low-set and high-set gels are primarily cross-linked by triple helices and single helices. The intrachain hydrogen bond between the O(2) hydroxyls on glucopyranose residues results in single helices, while the triple helices originate from the hydrogen bond between O(4) and O(6).[152] Furthermore, Curdlan has antitumor, anti-infective, anti-inflammatory, immunomodulating, and anti-HIV properties. The triple helical structure of Curdlan is crucial for anticancer and antitumor activity.[153] Curdlan hydrogel presents high thermal stability. Meanwhile, the molecular chains of Curdlan show high stability during the freezing and thawing process to guarantee its use in frozen foods.[80,153]

4.10. Konjac Glucomannan. KGM, extracted from the root tuber of *Amorphophallus konjac*, contains β-1,4-linked D-mannose and D-glucose with a ratio range of 1.4−3 that varies with konjac breeds.[154,155] The M_w of KGM generally ranges within 500 000−2 000 000 g/mol, depending on the production condition.[81,126] Acetyl groups (∼1 per 19 mannose residues) and β-1,3-linked hexose residues (primarily mannose, 1 per 50−60 hexose residues) exist randomly on the main chain, which needs further study.[154] What is more, the solubility of KGM increases with the increase in acetyl-group content because the acetyl groups weaken the intramolecular hydrogen bonds. Furthermore, konjac flour is obtained from the grind of tuber and contains 51%−72% KGM, and thus, extra processing is needed to purify KGM.

KGM can form stable and thermoirreversible hydrogels through a deacetylation-induced gelation process in an alkaline environment. The elastic modulus of the deacetylated KGM hydrogel is proportional to the degree of deacetylation. Deacetylation induces the conformation transition from semicrimping to self-crimping and the aggregation of KGM chains, which is related to the intermolecular hydrogen bond and hydrophobic interaction. Moreover, several factors affect gelation, including the acetylation degree, temperature, KGM concentration, M_w of KGM, and alkali concentration. NaOH, KOH, $Ca(OH)_2$, Na_2CO_3, and K_2CO_3 are used to trigger the gelation, and KOH has a higher deacetylation effect.[156] KGM hydrogels can be further strengthened by treating the deacetylated KGM solution with freeze−thawing as well as freeze-drying and rehydration.[156] Furthermore, additives such as GO, sodium montmorillonite, and carbon nanotube can improve the mechanical properties of KGM hydrogel.[156] Nishinari et al.[157] have suggested that weak KGM gels can form by the addition of several salts. He then summarized the praising ability of some salts related to the Hofmeister effect. KGM has been applied in the food industry and medical biology because of its effective thickening property, gelation, and cytocompatibility.[80]

4.11. Pectin. Pectin has a smooth region and a hairy region on the molecule chain extracted from plant cell walls.[127] The smooth region (homogalacturonan, HGA) comprises α-1,4-linked D-galacturonic acid.[126] By contrast, the hairy region (Rhamnogalacturonan I and Rhamnogalacturonan II) contains monosugars, such as D-xylose, D-glucose, L-rhamnose, L-arabinose, and D-galactose (Figure 9).[127] Moreover, according to the degree of methoxylation (DM) on galacturonic acid, pectin can be divided into high methoxy pectin (HMP; DM > 50%) and low methoxy pectin (LMP; DM < 50%). The HMP hydrogel can be formed at pH ≤ 3 or with a high-concentration cosolute (e.g., sucrose ≥ 65 wt %) through cross-linking the methyl groups via hydrogen bond and hydrophobic interaction.[127] LMP will form stronger hydrogels than HMP. Furthermore, Ca^{2+}-induced gelation occurs only for LMP, where the gelation mechanism is also described by the egg-box model. The gelation mechanism of LMP is almost identical to that of SA because SA and LMP present mirror symmetric spatial conformations.[127] In addition, the mechanical properties of Ca^{2+}-induced pectin hydrogel are proportional to M_w and the amount of galacturonic acid.[127] Several factors will influence the gelation of LMP: the concentrations of LMP and Ca^{2+}, the addition method of Ca^{2+}, pH, ion strength, temperature, and cosolutes.[112]

Pectin is widely used in food chemistry due to its gelation, thickening property, and emulsification. Meanwhile, pectin hydrogels present soft nature, cytocompatibility, unique structure, and resemblance to natural materials, which are applied for food ingredients/additives, food packaging, bioactive delivery, and health management applications.[80,158,159] Additionally, pectin has hypoglycemic activity by raising insulin production and presents the hypocholesterolemic effect.[158]

5. SPECIFIC ADVANTAGES OF POLYSACCHARIDES IN DN CONCEPT

Based on section 2 (the design principle and fabrication of DN hydrogels), section 3 (strengthening mechanism for DN hydrogels), and section 4 (properties of the applied polysaccharides), the reasons why we widely use polysaccharides for the fabrication of DN hydrogels can be further summarized. The reasons are stated from two aspects, namely, the strengthening mechanism aspect and the application aspect.

The reasons from the perspective of the strengthening mechanism can be stated as follows. For more information, please refer to sections 3 and 4.

(1) Some polysaccharides such as agarose, κ-CG, GG, and Curdlan inherently form brittle and rigid hydrogels, which constitutionally meet the requirement of the rigid network in the DN concept without extra postprocessing. However, for the synthetic rigid networks, the swelling process to transform the as-prepared flexible network to a rigid network is usually needed. Therefore, polysaccharides with gelling properties are inherently and highly suitable for rigid network fabrications.

(2) Through strong and extensive inter/intramolecular interactions, many polysaccharides can spontaneously self-assemble into elaborate structures: (i) egg-box structure (e.g., SA and pectin); (ii) coil-helix transition and helix aggregation (e.g., agarose, GG, κ-CG, and Curdlan); (iii) single-triple helix transition (e.g., Curdlan); and (iv) nanocrystal (e.g., cellulose

https://doi.org/10.1021/acs.biomac.3c00765
Biomacromolecules XXXX, XXX, XXX−XXX

and CHT). Benefitting from the self-assembled structure, involving a polysaccharide-based network with a very low concentration can exhibit a significant enhancement. Thus, polysaccharides can endow DN hydrogels with unique network structures, which is difficult for many synthetic polymers.

(3) Many polysaccharide-based networks can be cross-linked by diverse ions and different physical interactions accompanied by complex junction zones. The polysaccharide-based DN hydrogels thus can present tunable and multiple mechanical properties, which greatly help the design of such hydrogels with desirable properties. By contrast, this is challenging for synthetic polymers.

(4) Many polysaccharide-based networks spontaneously form extensive inhomogeneity relying on gelling mechanisms. Hence, the intrinsic inhomogeneity allows the rigid polysaccharide network to rupture stepwise and hierarchically. Shorter polysaccharide chains are first pulled out so that soft and loosely bound micro areas fracture before hard and tightly bound regions, thereby permitting the stack of damages, the prevention of premature fracture, the development of large strain, and high toughness. Inhomogeneity can be observed optically by the decrease in visible-light transmittance during gelation from clear and transparent to semitransparent (e.g., CHT, agarose, GG, and Curdlan), which can be explained by the equation of Rayleigh−Gans scattering:[160]

$$I = \frac{1 + \cos^2\theta}{2}\frac{4\pi^2V^2}{\lambda^4 r^2}(n-1)^2|R(\theta,\psi)|^2 I_0 \tag{13}$$

When the observing direction is opposite to the light, $\theta = 0$ and $R(\theta,\psi) = 1$, that is:

$$I = \frac{4\pi^2V^2}{\lambda^4 r^2}(n-1)^2 I_0 \tag{14}$$

where I_0 is the colored light intensity, r is the observing distance, V is the volume of a single particle, λ is the wavelength of light, and n is the refractive index. Moreover, Eqn. 13 applies in the case of $|n-1| \ll 1$ and $r \ll \lambda/|n-1|$, where r is the radius of the particle. Thus, if the hydrogel becomes semitransparent, the size of the microstructure approaches or even exceeds the wavelength of visible light. When the size is much larger than the wavelength of visible light, Mie scattering, reflection, refraction, and Fraunhofer diffraction replace Rayleigh−Gans scattering to provide the major contribution to the opaque.[160]

In contrast, the inhomogeneity of synthetic networks is more difficult to be introduced (e.g., introducing particles, phase separation, designing new monomers). Therefore, polysaccharide-based networks with inhomogeneity benefit mechanical enhancement of the resulting DN hydrogels.

(5) The multistage "chain-pulling-out" fracture process of the polysaccharide-based networks provides a simple way to balance the mechanical properties between the natural rigid network and the synthetic flexible network. By such a fracture process, the prepared polysaccharide-based DN hydrogels rarely suffer from early macroscopic fracture. However, for fully synthetic DN hydrogels, the mechanical balance between the two networks needs to be finely adjusted.

(6) The polysaccharide-based network enhances the entanglement with the flexible network via physical interactions through the extensively existing chemical groups, such as carboxy, sulfonic acid, amino, amide, and hydroxy groups. These entanglements offer additional mechanical strength and energy-dissipation, which also helps the delocalization of the external stress.

(7) Polysaccharide-based networks endow the prepared DN hydrogels with the abilities of self-recovery and repeatable energy dissipation. For covalently cross-linked rigid networks, energy dissipation relies on the rupture of chemical bonds in the rigid network. However, for physically cross-linked polysaccharide-based networks, the molecular chains maintain integrity during deformation benefitted from the "chain-pulling-out" mechanism. The recoverable physical interactions and polysaccharide-based networks ensure the reusability and mechanical strength of the hydrogels after deformation. However, this is more difficult for the synthetic rigid networks, where the muscle training strategy[161−164] is developed to conquer this difficulty.

Furthermore, the reasons to explain the specific advantages of applying polysaccharides in the DN strategy can be given from the aspect of the application. Polysaccharides have diverse excellent physical, chemical, and biological properties that can be introduced to the hydrogels and embodied in subsequent applications. Meanwhile, polysaccharide-based DN hydrogels are typically appropriate for some applications, e.g., the 3D structure construction through the one-pot method and 3D printing. By using gelling polysaccharides, rigid polysaccharide networks with unique cross-linking zones can be spontaneously formed during the fabrication process without additional treatment. Obviously, this accessibility is not easy to achieve for synthetic networks.

The large polysaccharide family can meet the requirements of (i) rigid network, (ii) enhanced energy dissipation, (iii) simple and rapid network construction, (iv) recoverable cross-link, (v) tunable mechanical strength, (vi) in situ formation, (vii) similar physicochemical properties between batches (exopolysaccharides such as XG, GG, and Curdlan), (viii) cytocompatibility of the molecular chain and cross-linking type, (ix) biological activity (e.g., antibacteria, hemostasis, anti-inflammatory, cell growth, proliferation, migration, adhesion, and signaling), (x) biodegradability, (xi) various groups for modification, (xii) environmental protection, (xiii) low cost, (xiv) renewability, (xv) adsorption, and (xvi) antiswelling. Different application fields need different properties, which can be properly supported by these polysaccharide-based DN hydrogels.

(1) Strong and tough materials require a rigid network, enhanced energy dissipation, recoverable cross-linking, and tunable mechanical strength and focus on simple and rapid network construction and in situ formation. Polysaccharides can meet these requirements by forming junction zones via strong physical interactions (e.g., helices of GG and nanocrystals of CHT stabilized by ions and hydrogen bonds) in a simple way, which is harder for other materials.

(2) Circuits and strain sensors request the following: rigid network, recoverable cross-linking, tunable mechanical strength, and cytocompatibility between the molecular chain and cross-linking type. Besides the superior mechanical properties provided by the polysaccharide networks, polysaccharides are less toxic, bioactive, and biodegradable and can be promising materials as circuits and electrolytes.

(3) 3D printing requires simple and rapid network construction, in situ formation, and cytocompatibility of the molecular chain and cross-linking type. Polysaccharides at very low concentrations can simply construct rigid and effective networks with self-assembled elaborate structures through

https://doi.org/10.1021/acs.biomac.3c00765
Biomacromolecules XXXX, XXX, XXX−XXX

Table 2. Component, Self-Recovery Efficiency, Self-Healing Efficiency, and Virgin Mechanical Property of Polysaccharide-Based DN Hydrogel

Polysaccharide	Synthetic network	Self-recovery efficiency	Self-healing efficiency	Virgin mechanical property	Virgin mechanical property	Ref.
				Self-recovery Stress (MPa)/strain	Self-healing Stress (MPa)/strain	
$SA^{Ca^{2+}}$	$PAAm^{MBAA}$	$74\%^{D,80\circ C,24h}$		~0.135/600%		3
$SA^{Fe^{3+}}$	Poly(AAm-*co*-$AAc)^{Fe^{3+}}$	$64\%^{D,RT,4h}$	$(56\%^{S}, 17\%^{B})^{special\ method}$	~1.72/600%	3.24/1228%	87
$CMC^{Zn^{2+}}$	Poly(AAc-*co*-$NVP)^{Zn^{2+}}$	$42.5\%^{D,RT,0s}$	$(81\%^{S}, 91\%^{B})^{RT,24h}$	~0.7/650%	0.86/1019%	99
$CMC^{Fe^{3+}}$	PNAGA	$(84.9\%^{D}, 87.7\%^{M})^{RT,12h}$	$(89\%^{S}, \sim 78\%^{B})^{special\ method}$	~1.63/200%	~1.85/540%	71
QCE	PVA, $PAAc^{Fe^{3+}}$		$(\sim 83\%^{S}, 93.5\%^{B})^{RT,16h}$		1.13/465%	101
$CHT^{NaOH,\ NaCl}$	$PAAm^{MBAA}$	$95\%^{D,RT,4h}$		~1.67/200%		32
$CHT^{Na_2SO_4,Na_3cit}$	$PAAm^{MBAA}$	$(89.6\%^{D}, 96.6\%^{M})^{RT,4h}$		~3.3/200%		103
$HACC^{PAAc}$	$PAAc^{HACC}$	$85\%^{D,RT,6h}$	$(\sim 57\%^{S}, 59\%^{B})^{70\circ C,48h}$	~1.02/300%	3.31/870%	70
$CHT^{genipin}$DOPA $CHT^{Fe^{3+},genipin}$		$\sim 100\%^{D,RT,24h}$	Fast self-healing	~0.027/30%		33
Agar	$PAAm^{MBAA}$	$(65\%^{D}, 90\%^{M})^{100\circ C,10min}$		~0.17/900%		31
Agar	$PAAm^{SMA}$	$(40\%^{D}, 50\%^{M})^{RT,2min}$	$(40\%^{S}, 73.5\%^{B})^{RT,\ 24\ h}$	~0.17/900%	0.109/170%	109
Agar	Poly(AAm-*co*-$AAc)^{Fe^{3+}}$	$95\%^{D,RT,20min}$		~0.52/500%		76
GG^{Na+}	$PAAm^{SMA}$	$(79\%^{D}, 80\%^{M})^{37\circ C,1h}$	$(\sim 82\%^{S}, \sim 88\%^{B})^{37\circ C,Sh}$ able$^{90\circ C,20min}$	~0.085/500%	~0.11/~800%	115
κ-Car^{K^+}	$PAAm^{MBAA}$	$(98\%^{D}, 100\%^{M})^{90\circ C,20min}$		~0.145/500%	~0.78/~1800%	39
κ-Car^{K^+}	PNV	$(72.2\%^{D}, 42.6\%^{M})^{60\circ C,2min}$	$\sim 100\%^{85\circ C,Thermoplasticity}$	~0.195/500%	1.55 MPa/99%	35
$XG^{Ca^{2+}}$	$PAAm^{SMA}$	$93\%^{D,RT,300min}$	$(38\%^{S}, \sim 45\%^{B})^{70\circ C,48h}$	~0.86/300%	3.64/1575%	119
Curdlan	$PAAm^{SMA}$	$(97\%^{D}, 84\%^{M})^{95\circ C,4h}$	$(50\%^{S}, 52\%^{B})^{95\circ C,4h}$	~0.31/700%	0.805/2530%	120

extensive inter/intramolecular interactions. However, many synthetic networks lack this ability. In addition, diverse polysaccharide-based DN hydrogels can be fabricated by 3D printing because of the different cross-linking approaches of polysaccharides.

(4) Biomedical applications demand cytocompatibility of the molecular chain and cross-linking type, biodegradability, and biological activity, and notice the rigid network, recoverable cross-linking, tunable mechanical strength, in situ formation, various chemical groups for modification, and similar physicochemical properties between batches. Polysaccharides from natural species possess essential cytocompatibility. Meanwhile, some polysaccharides have unique bioactivities, such as HA (biodegradability, nonimmunogenicity, noninflammatory, viscoelastic characteristics, and bioactivity to affect cell adhesion, migration, and downstream cell signaling) and Curdlan (antitumor, anti-infective, anti-inflammatory, immunomodulating, and anti-HIV properties). Polysaccharide-based DN hydrogels for biomedical applications can be readily fabricated by introducing bioactive polysaccharides and their derivatives. Furthermore, such hydrogels can exhibit both bioactivity and toughness to conquer the low mechanical strengths of polysaccharide-based SN hydrogels and the lack of bioactivity in synthetic polymers. In addition, the in situ formed physically cross-linked polysaccharide-based networks also contribute to the injectability. Finally, exopolysaccharides (e.g., XG, GG, and Curdlan) obtained from fermentation present stable physical and chemical properties, thus contributing to the application as biomaterials, which can solve the deficiency that the physicochemical properties, of polysaccharides from plants and algae deviate largely from batch to batch.

(5) Adsorption materials request biodegradability, various groups for modification, environmental protection, renewability, and adsorption and antiswelling abilities. Polysaccharides with high adsorptive ability, ease of modification, abundance, renewability, cytocompatibility, generally low toxicity, and biodegradability are some of the most promising materials for environmental treatment. The two networks in a polysaccharide-based DN hydrogel can be finely adjusted for adsorption to achieve desirable properties.

This section summarizes the polysaccharides used in DN hydrogels and discusses their merits, presenting the inherent accessibility of these polysaccharides for the DN strategy and corresponding applications.

6. UNIQUE FEATURES ENDOWED BY POLYSACCHARIDES AND OTHER COMPONENTS

The components of the polysaccharide-based DN hydrogel are closely associated with the features of self-recovery, self-healing, nonswelling, and thermal plasticity. Self-recovery and self-healing are the two most attractive properties, where remarkable results are displayed in Table 2. Self-recovery efficiency is measured by energy dissipation (labeled with a superscript D) and Young's modulus (superscript M). Meanwhile, self-healing efficiency can be evaluated as energy dissipation (superscript D), tensile stress (superscript S), and elongation at break (superscript B). In addition, self-recovery efficiency is also labeled with the temperature and interval time as superscripts. The virgin mechanical property corresponds to the gel used for self-healing.

https://doi.org/10.1021/acs.biomac.3c00765
Biomacromolecules XXXX, XXX, XXX−XXX

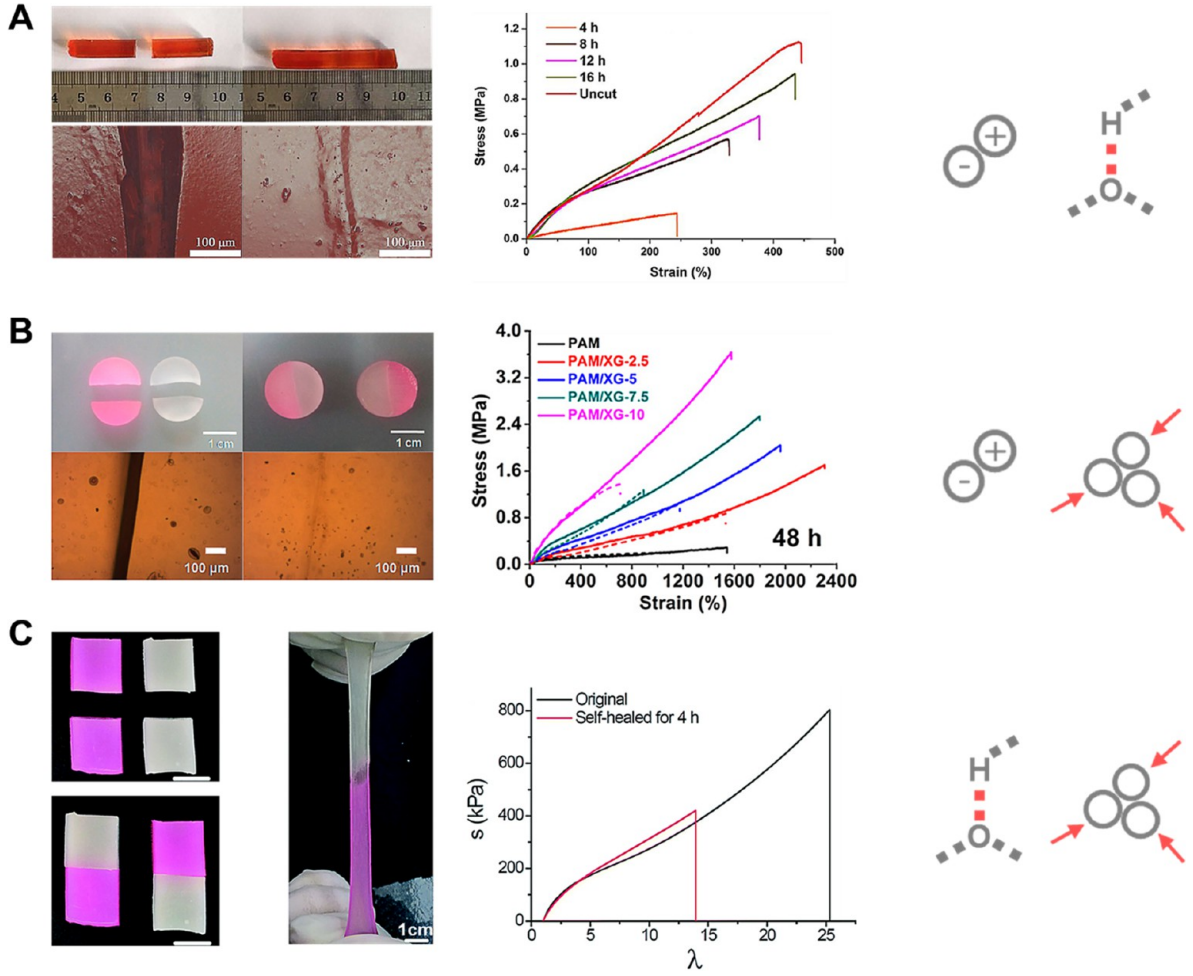

Figure 10. Self-healing polysaccharide-based DN hydrogels via diverse interactions: (A) PAAc-grafted QCE/PVA DN hydrogel via the ionic bond and hydrogen bond; (B) XG/poly(AAm-*co*-SMA) DN hydrogel via the ionic bond and hydrophobic interaction; (C) Curdlan/poly(AAm-*co*-SMA) DN hydrogel via hydrogen bond and hydrophobic interaction. Panel A is adapted with permission from ref 101. Copyright 2017 Elsevier. Panel B is adapted with permission from ref 119. Copyright 2016 ACS Publications. Panel C is adapted with permission from ref 120. Copyright 2020 Royal Society of Chemistry.

6.1. Self-Recovery. The enhanced mechanical strength of the DN hydrogel originates from the rupture of the rigid network, leading to a loss of mechanical strength during the second load process. Accordingly, efforts have been exerted to re-establish the broken rigid network and provide repeatable energy dissipation.[161−163] Compared with synthetic polymers, the molecular chains of physically cross-linked polysaccharide networks maintain integrity during deformation. Recoverable physical interactions endow polysaccharide-based DN hydrogels with self-recovery and self-healing.

DN hydrogels with a physically cross-linked rigid network can achieve high recovery efficiencies. Based on the ionic bonds between Fe^{3+} and catechol groups, an injectable CHT/DOPA-CHT DN hydrogel possesses a high self-recovery efficiency of ∼100% for dissipated energy at RT after 24 h ($\sim 100\%^{D,RT,24h}$).[33] Furthermore, the ionic bonds also contribute to the self-healing of the CHT/DOPA-CHT DN hydrogel. Moreover, cross-linked by hydrogen bonds, Yang et al.[32] have fabricated a CHT/PAAm DN hydrogel with a rigid network formed by CHT nanocrystals that possess the recovery efficiency of $90\%^{D,RT,4h}$. This DN hydrogel is even ∼2 times tougher than the first load after 10 successive loading−unloading tests and resting for 24 h. Recently, a GG/HPAAm DN hydrogel has been fabricated based on the hydrogen bond, ionic bond, and hydrophobic interaction. It possesses the self-recovery efficiencies of ($79\%^{D}$ and $80\%^{M}$)$^{37°C,1h}$ with self-healing, antifatigue, and cytocompatibility for cartilage repair.[115]

6.2. Self-Healing. In general, the self-healing of tough polysaccharide-based DN hydrogels requires physical interactions, such as hydrogen bonds, Van der Waals' force, salt-out effect, hydrophobic interaction, and ionic interaction.[165] High self-healing efficiency can be realized by the ionic and hydrogen bonds shown in the PAAc-grafted QCE/PVA DN hydrogel (Figure 10A). Moreover, hydrophobically cross-linked PAAm networks contribute to the self-healing of polysaccharide-based DN hydrogel. The PAAm network cross-linked by SMA through hydrophobic interaction is first improved as an efficient way to endow DN hydrogel with self-healing on agar/HPAAm DN hydrogel.[109] The obtained DN hydrogel exhibits self-healing efficiencies of $40\%^{S}$ and $73.5\%^{B}$ at RT for 24 h with a tensile strength of ∼ 0.109 MPa and a tensile strain of 170%. Afterward, Yuan et al.[119] have fabricated a dual physically cross-linked XG/HPAAm DN hydrogel (Figure 10B) with remarkable mechanical properties after self-healing. The self-healing efficiencies are $38\%^{S}$ and $\sim 45\%^{B}$ at 70

https://doi.org/10.1021/acs.biomac.3c00765
Biomacromolecules XXXX, XXX, XXX−XXX

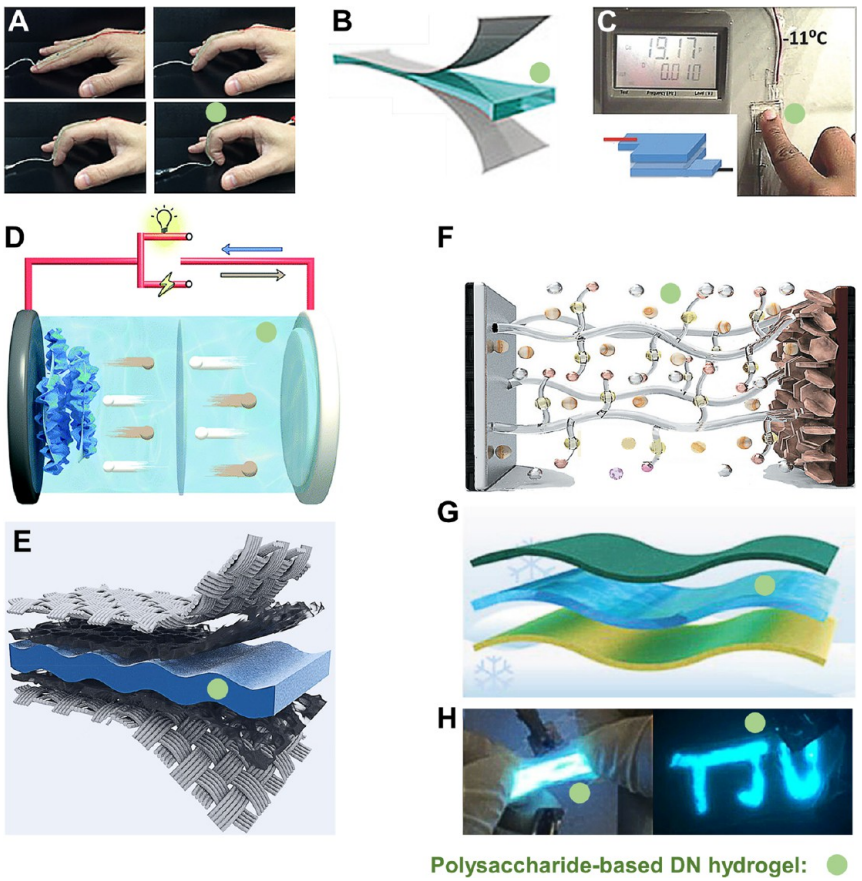

Figure 11. Polysaccharide-based DN hydrogels as flexible electrolytes: (A) the κ-CG/PAAm DN hydrogel as the strain sensor; (B) the agar/HPAAm DN hydrogel for supercapacitor; (C) the SA/PAAm DN hydrogel for pressure sensor worked at −11 °C; (D) a Zn-ion hybrid supercapacitor based on κ-CG/poly(AAm-*co*-AAc) DN hydrogel; (E) a low-temperature flexible supercapacitor by using the κ-CG/PAAm DN hydrogel electrolyte; (F) an aqueous Zn-MnO_2 battery involving cellulose nanofibrils; (G) a low-temperature zinc-ion battery based on the CCHT/PAAm DN hydrogel electrolyte and the Hofmeister effect of $Zn(ClO_4)_2$; and (H) an agar/PAAm DN hydrogel as the transparent electrolyte for the electroluminescent device. Panel A is reproduced with permission from ref 34. Copyright 2017 ACS Publications. Panel B is adapted with permission from ref 112. Copyright 2019 Wiley-VCH. Panel C is reproduced with permission from ref 179. Copyright 2018 Wiley-VCH. Panel D is reproduced with permission from ref 180. Copyright 2021 Royal Society of Chemistry. Panel E is reproduced with permission from ref 181. Copyright 2022 Elsevier. Panel F is reproduced with permission from ref 182. Copyright 2020 Wiley-VCH. Panel G is adapted with permission from ref 183. Copyright 2022 Wiley-VCH. Panel H is adapted with permission from ref 155. Copyright 2019 ACS Publications.

°C for 48 h when the initial mechanical properties are 3.64 MPa and 1575%. Ye et al.[120] have prepared a Curdlan/HPAAm DN hydrogel with self-healing efficiencies of (50%^{S}, 52%^{B})^{95oC,4h} with initial mechanical properties of 0.805 MPa and 2530% (Figure 10C).

The rigid network limits the mobility of the polymer chain of a healable flexible network, resulting in poor self-healing efficiency.[71] On this case, a softened rigid network is needed to re-establish the network structure at the damaged zone. For example, a fully physical-cross-linked DN hydrogel is prepared with a Fe^{3+} cross-linked CMC network and a hydrogen bond cross-linked PNAGA network.[71] To overcome the limitation of the rigid network on self-healing, Fe^{3+} is removed using ethylenediamine tetraacetic acid disodium salt (EDTA·2Na) to soften the CMC network. After the self-healing process, the CMC network is cross-linked again by immersing the DN hydrogel in the Fe^{3+} solution. Finally, the self-healing efficiencies reach 89%^{S} and ∼78%^{B} with initial mechanical properties of ∼1.85 MPa and 540%. Similarly, this method is applied to SA/Poly(AAm-*co*-AAc) DN hydrogel.[87]

The self-healing of a DN hydrogel with a healable rigid network is also dependent on whether the flexible network is cross-linked. According to research on a gelatin/PAAm DN hydrogel,[166] a poor self-healing property is shown if the PAAm network is cross-linked by 0.03 mol% MBAA. However, the PAAm network without the cross-linker endows this DN hydrogel with self-healing. A CHT/PAAm DN hydrogel without covalent cross-link also exhibits self-healing that is attributed to the molecular-chain motion and the topological entanglement.[167]

Apart from eternal physical interactions for self-healing, an exogenous remediation agent is applied to promote the self-healing efficiency of a polysaccharide-based DN hydrogel. The self-healing of the SA/guar gum DN hydrogel is enhanced using mesoporous silica nanoparticles to load glutaraldehyde and polydopamine.[91] Finally, the tensile strength and self-healing efficiency reached 7.0 MPa and 94.5%^{S}, respectively.

6.3. Nonswelling. Compared with the electrolyte polymers, many polysaccharide hydrogels have low swelling degrees. Therefore, polysaccharide networks can partly resist the swelling behavior of DN hydrogels. For polysaccharide-based DN hydrogels, the nonswelling performance is primarily endowed by the extensive ionic interactions between the two networks[70] and strong hydrogen bonds.[71] The swelling

https://doi.org/10.1021/acs.biomac.3c00765
Biomacromolecules XXXX, XXX, XXX−XXX

behavior of a HACC/PAAc DN hydrogel is tunable between swelling and shrinkage by changing the ratio of HACC and PAAc.[70] The electrostatic interactions between ammonium groups and carboxy groups are first partially shielded by NaCl. NaCl ions are then removed from the DN hydrogel during the dialysis process. As a result, ammonium groups and carboxy groups are close to each other to resist the swelling effect. Similarly, a SA/Poly(AAm-*co*-AAc) DN hydrogel cross-linked by Fe^{3+} can show the ability of swelling resistance through ionic bonds.[87] In addition, a supra-molecular PNAGA hydrogel is nonswelling in water due to the multiple hydrogen bonds.[168] Furthermore, a CMC/PNAGA DN hydrogel has exhibited swelling resistance in a water environment, which is attributed to the strong hydrogen bonds among PNAGA chains and the ionic interaction of the Fe^{3+} cross-linked CMC network.[71]

Swelling can also enhance the mechanical properties. Chen et al.[169] have discussed the correlation between the swelling behavior and the mechanical properties of an agar/PAAm hydrogel in detail. The hydrogen-bonded agar network and the covalently cross-linked PAAm network are nonswellable and highly swellable, respectively. Through exploring the relationship between the swelling behavior and mechanical properties, the final swollen agar/PAAm DN hydrogel even had a higher mechanical strength than the as-prepared hydrogel.

6.4. Other Features. Efforts are focused on realizing the tough adhesion of a polysaccharide-based DN hydrogel.[170−173] For example, catechol and 3,4-DOPA groups can endow hydrogels with strong and underwater adhesion[174] and have been applied to polysaccharide-based DN hydrogels, such as silk fibroin/HA,[175] CHT/PAAm,[105] and CS/PAAm[122] DN hydrogels. The polymer adhesion is affected by stiffness and surface roughness.[176] Recently, by utilizing this phenomenon, κ-CG/poly(*N*-acryloyl glycinamide-*co*-vinyl imidazole (VI)) (κ-CG/PNV) hydrogels have been fabricated and endowed with temperature-controlled adhesion.[35] BC has been applied to fabricate the BC/PVA DN hydrogel with super strong mechanical properties (tensile strength of 51 MPa and compression strength of 98 MPa), adhesive strength of 2.0 MPa, and wear resistant (three times more than cartilage).[95] Furthermore, inorganic materials are introduced to polysaccharide-based DN hydrogels to present unique properties, such as a SA/PAAm DN hydrogel with photoluminescent via Eu^{3+} and Tb^{3+} ions,[82] a SA/PAAm DN hydrogel with photoresponse through CNT,[86] and CHT/polyolefin DN hydrogel with a magnetocaloric effect based on an Fe_3O_4 nanoparticle.[104]

6.5. Challenges and Outlook. Despite the advances in introducing unique features to polysaccharide-based DN hydrogels, the multifunctionalization remains in its infancy. (1) Adhesion. Polysaccharide-based DN hydrogel with strong adhesion should be further developed. Meanwhile, under-water and controllable adhesion are highly needed for polysaccharide-based DN hydrogels as biomaterials. (2) Super strong DN hydrogel. The preparation of polysaccharide-based DN hydrogels as strong as natural tissues still needs to be overcome for researchers, where BC provides an avenue to greatly enhance the mechanical properties. (3) Stimulus-response. Polysaccharide-based DN hydrogels can be further hybridized with nanomaterials for additional functions, such as metal nanowires for conductivity, inorganic nanoparticles for optical properties, as well as cellulose nanocrystals for structural color and anisotropy. (4) Bionic structure. DN strategy provides an efficient way to combine bionic structure and mechanical strength. For example, DN hydrogels with aligned structures can be fabricated by stretching to simulate oriented natural tissues, such as muscle and the superficial zone of cartilage.

7. APPLICATIONS OF POLYSACCHARIDE-BASED DN HYDROGELS

7.1. Ionotronics. Polysaccharide-based DN hydrogels with ions can form ionotronics.[159,177] Liu et al.[34] have investigated the electrical properties of the κ-CG/PAAm DN hydrogel (Figure 11A). They evaluated the dependence of resistance on the applied strain, strain sensitivity, and conductive stability of the DN hydrogel. Furthermore, an adhesive CHT/PAAc DN hydrogel is fabricated as the strain sensor that is endowed with adhesive ability by catechol and pyrogallol groups functioned tannic acid.[105] Recently, a kind of tough, underwater adhesive, self-healing, and conductive DN hydrogel has been fabricated as the strain sensor by using dialdehyde carboxymethyl cellulose and CHT as the rigid network as well as PAA and Al^{3+} as the flexible network.[178] This strain sensor based on the underwater adhesive DN hydrogel can detect human movement in a watery environment.

Polysaccharide-based DN hydrogels containing ions have been used as the electrolytes to form supercapacitors, such as the HACC/PAAc DN hydrogel,[70] the Ag particle-tannic acid-CNC/PVA DN hydrogel,[184] and the agar/HPAAm DN hydrogel[112] (Figure 11B). As shown in Figure 11B, benefiting from the tough mechanical properties endowed by the DN strategy, the agar/HPAAm DN hydrogel and polypyrrole are used as the electrolyte and electrode, which presents almost no residual deformation left after being stretched to 500% strain for 30 times and to 100% for 1000 times. Moreover, the DN hydrogel containing salts can resist low temperatures. A SA/PAAm DN hydrogel containing 30 wt% $CaCl_2$ with a freezing point of −57 °C has been used to produce the antifreeze pressure sensor worked at −11 °C (Figure 11C).[179] Furthermore, in Figure 11D, a Zn-ion hybrid supercapacitor has been designed by using the K^+ cross-linked κ-CG rigid network and the MBAA cross-linked poly(AAm-*co*-AAc) network to form the DN hydrogel electrolyte.[180] This supercapacitor can possess toughness, a low self-discharge rate, high ionic conductivity, high and permanent capacity, and high energy density.

As shown in Figure 11E, a low-temperature flexible supercapacitor has been designed based on the κ-CG/PAAm DN hydrogel with a high concentration of LiCl.[181] At −40 °C, the κ-CG/PAAm electrolyte can present a conductivity of 1.9 S/m, high specific capacitance of 73.4 F/g, and permanent capacitance retention of 95.6% after 20000 cycles. Furthermore, it is noticed that the polysaccharide-based DN hydrogel can be used as the electrolyte in an aqueous Zn-MnO_2 battery (Figure 11F), where the electrolyte has been formed by cellulose nanofibrils cross-linked by hydrogen bond as the rigid network and poly(2-(methacryloyloxy)ethyl)diethy-(3-sulopropyl) cross-linked by MBAA as the flexible network.[182] This natural plant-based electrolyte can exhibit toughness and cytocompatibility. The fabricated solid-state Zn-MnO_2 battery presents high rate performance, e.g., a capacity of 275 mA h $g^{-1}_{MnO_2}$ at 1 C and a capacity of 74 mA h $g^{-1}_{MnO_2}$ at 30 C after 10 000 charging−discharging cycles.

Recently, the antifreezing ability endowed by the salt has been introduced to develop a high-performance zinc-ion

https://doi.org/10.1021/acs.biomac.3c00765
Biomacromolecules XXXX, XXX, XXX−XXX

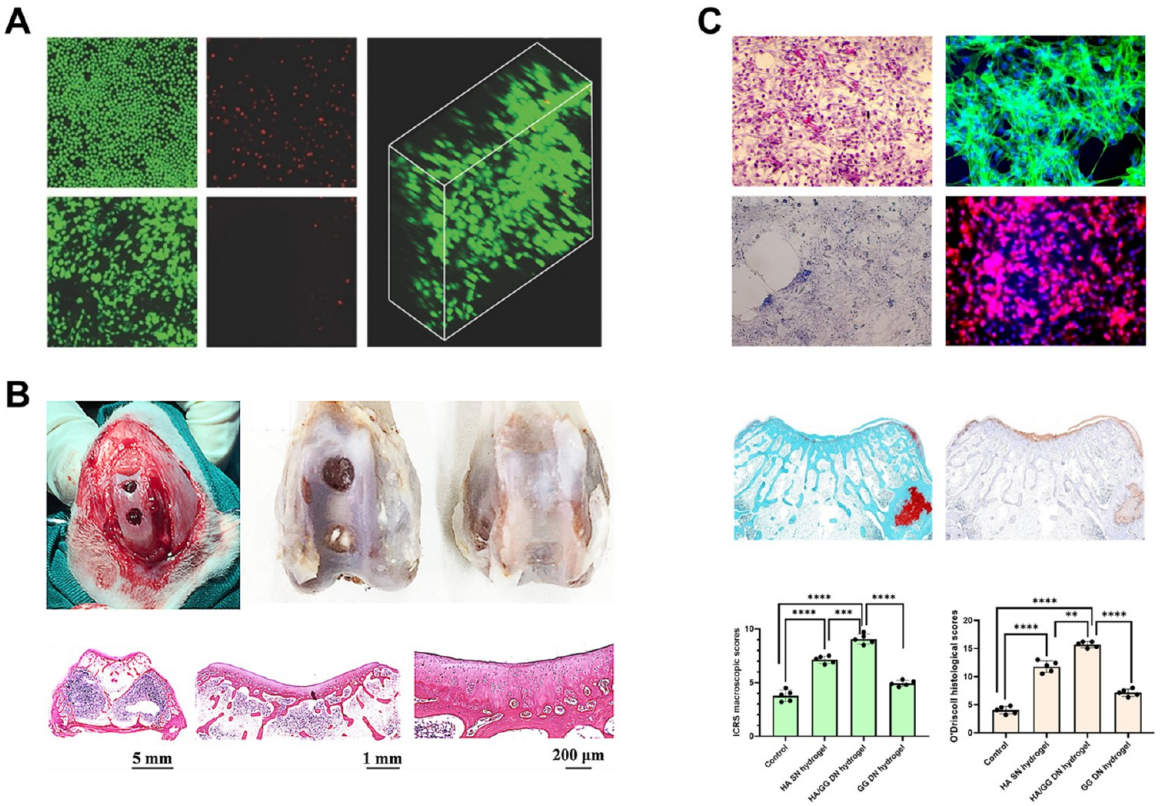

Figure 12. (A) Injectable DN hydrogel based on HA derivatives and a thermoresponsive engineered protein for cell encapsulation. (B) The polydopamine-CS/PAAm DN hydrogel was used for cartilage repair. (C) The HA-furan/GG DN hydrogel was used for cartilage repair. Panel A is adapted with permission from ref 93. Copyright 2017 Wiley-VCH. Panel B is adapted with permission from ref 122. Copyright 2018 ACS Publications. Panel C is adapted with permission from ref 188. Copyright 2022 Elsevier.

battery by using the CCHT/PAAm DN hydrogel electrolyte (Figure 11G).[183] The Hofmeister effect is applied where $Zn(ClO_4)_2$ with a low concentration can obviously decrease the freezing point because the chaotropic ClO_4^-, water, and polymer chains form ternary hydrogen bonds. At −30 °C, this hydrogel electrolyte can present a high ionic conductivity of 7.8 mS cm^{-1} and endow the Zn/polyaniline battery with a reversible capacity of 70 mA h g^{-1} under 5 A g^{-1} for 2500 cycles. Furthermore, besides sensing the thermal and mechanical stimulation, an agar/PAAm DN hydrogel with a high concentration of Li^+ has been fabricated as the tough and transparent electrolyte for fabricating an electroluminescent device.[155] This electroluminescent device is prepared by covering a dielectric emissive layer with two agar/PAAm DN hydrogel films. When the alternating voltage is applied, the emissive layer will be activated.

7.2. Cell Encapsulation and Tissue Engineering. A polysaccharide-based DN hydrogel combines the advantages of both natural resources and synthetic polymers.[79,185] On one hand, natural macromolecules and their derivatives are applied as hydrogels for biomaterials.[186] However, most polysaccharide-based SN hydrogels lack mechanical strength. On the other hand, the mechanical properties of synthetic hydrogels are tunable, stable, and tough but lacking biological activity.

The DN strategy contributes to the fabrication of injectable hydrogels with enhanced mechanical properties. As shown in Figure 12A, Wang et al.[93] have developed a kind of injectable DN hydrogel for cell delivery by using a dynamically and covalently cross-linked shear-thinning HA and a thermoresponsive engineered protein. The HA network is cross-linked by hydrazone bonds, and the protein network is formed by molecular aggregation at 37 °C. This gel can protect cells from the shear force during injection and resist the degradation of HA. Furthermore, Rodell et al.[187] have designed an injectable DN hydrogel based on HA derivatives to encapsulate cells and allow the maintenance of high cell viability. The rigid and flexible networks are cross-linked by the host−guest interaction and the covalent bond between methacrylated HA and dithiothreitol.

Articular cartilage comprises abundant type-II collagen and sulphated glycosaminoglycan (sGAG), which is poor in regeneration due to its avascular and aneural nature, and sparse chondrocytes.[36,189] Polysaccharide-based DN hydrogels with complex network structures can simulate ECM to promote cell proliferation,[36,79] as well as the migration and differentiation of stem cells. They can also provide a path for nutrients, oxygen, and cell excretion.[190] Meanwhile, the hydrogel with high mechanical strength, elasticity, and toughness can protect the normal cartilage around the defect from degeneration.[36] Furthermore, the tunable stiffness and dynamic cross-link of hydrogels contribute to cartilage repair.[191,192] The biological performance of scaffolds is associated with their physical properties, and tunable mechanical properties are indispensable for cartilage repair.[193] Furthermore, a study has shown that the phenotype of chondrocytes is also maintained in soft gels (∼350 Pa) formed by dynamic cross-links that are broken and reformed by cells during matrix remodeling and ECM deposition.[194]

Tough polysaccharide-based DN hydrogels have been applied in cartilage repair,[195] such as the HA-furan/GG,[188]

https://doi.org/10.1021/acs.biomac.3c00765
Biomacromolecules XXXX, XXX, XXX−XXX

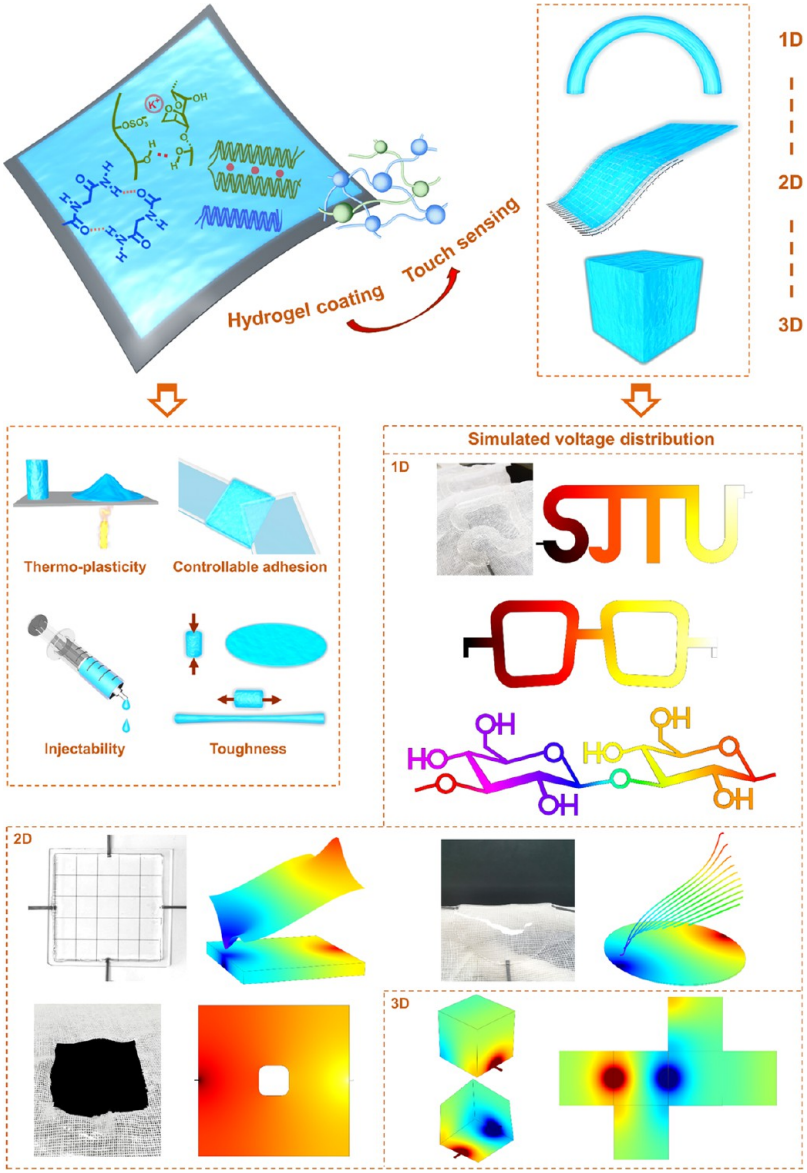

Figure 13. Injectable, tough, and thermoplastic supramolecular hydrogel coating based on the κ-CG/PNV DN hydrogel with controllable adhesion for touch sensing. Adapted with permission from ref 35. Copyright 2023 ACS Publications.

PDA-CS/PAAm (Figure 12B),[122] GG/HPAAm,[115] and CMCD/PAAm.[36] Recently, a HA-furan/GG DN hydrogel has been fabricated to support chondrocyte proliferation, new ECM deposition, and cartilage regeneration (Figure 12C).[188] The HA-furan/GG DN hydrogel provides stronger mechanical properties, a better ability to facilitate chondrocyte proliferation (higher gene expression levels of collagen II, SRY-related high mobility group box gene 9, and Aggrecan), a more efficient 3D microenvironment as the biomimetic ECM (higher DNA, total GAG, and total collagen contents), and a better cartilage-repair performance (better histological-staining results and higher International Cartilage Repair Society macroscopic and O'Driscoll histological scores) than HA-furan and GG SN hydrogels.

Recently, a polysaccharide-based DN hydrogel with temperature-dependent stiffening has been developed to combine injectability, degradation resistance, and bioactivity (named the BDNH hydrogel).[195] The adipic acid dihydrazide grafted CS and oxidized dextran were prepared as the flexible network cross-linked by Schiff base cross-linking between the amine and aldehyde groups. Then, HA conjugated poly(*N*-isopropylacrylamide) is fabricated as the rigid network to simulate the structure of the aggrecan aggregate and introduce temperature-dependent stiffening. The observed high cell viability, long-time cell proliferation, and cartilage specific matrix production endow the BDNH hydrogel with great potential for cartilage tissue engineering.

Artificial vascular conduits are fabricated based on a polysaccharide-based DN hydrogel.[92,196] Wang et al.[92] have fabricated a DN hydrogel bioink using Ca^{2+} cross-linked SA and microbial transglutaminase cross-linked gelatin. Then, hollow conduits are generated by microfluidic bioprinting to recreate vein- and artery-like tissues. Different kinds of vascular conduits are further seeded with four kinds of human cells, including vein and artery umbilical endothelial cells as well as vein and artery umbilical smooth muscle cells. The venous and arterial conduits imitate the properties of blood vessels including toughness and barrier behavior. Furthermore, these

https://doi.org/10.1021/acs.biomac.3c00765
Biomacromolecules XXXX, XXX, XXX−XXX

bioprinted conduits can be applied as models for studying diseases and drug testing in vitro. Additionally, these artificial blood vessels present the potential for in vivo vascular grafts.

7.3. Other Applications. A DN hydrogel combined with fabric is proven to have notable tough mechanical strength. An SA/PAAm DN hydrogel is reinforced with glass fabric that is covalently bonded to the hydrogel matrix.[88] This composite presents an elastic modulus of 35 MPa, a tensile stress of 2.40 MPa, and an impact resistance under low-speed impact for glass protection against impact. Besides glass fabric, BC is introduced as the rigid network to form the BC/PVA DN hydrogel with greater tensile and compression strengths (51 and 98 MPa) than cartilage (40 and 59 MPa).[95] Meanwhile, the interface between the BC/PVA DN hydrogel and metal achieves an adhesive strength of 2.0 MPa, exceeding that of the cartilage-bone interface (1.2 MPa). Most importantly, BC endows this hydrogel with wear resistance that is three times more than cartilage. In addition, mesoporous silica microrods have present great mechanical enhancement on Alg/PAAm DN hydrogels.[197,198]

Reversible interactions endow DN hydrogels with shape memory.[199] A κ-CG/PAAm DN hydrogel has the ability of moisture-induced shape memory, where DN hydrogel is dried under stretch and then shrinks back upon wetting.[200] An agar/poly(NAGA-*co*-*N*-benzylacrylamide) DN hydrogel shows the thermos-responsive shape memory.[201] The gel shape is programmed at 90 °C and fixed temporarily at a lower temperature before recovering to its original shape heated to 90 °C again.

The elimination of contaminants is important for the water resources. Therefore, SA/κ-CG DN hydrogel beads are developed to adsorb ciprofloxacin hydrochloride.[90] Similarly, an SA/CHT DN hydrogel is used for the heavy metal ion absorption of Pb^{2+}, Cu^{2+}, and Cd^{2+}.[89] Meanwhile, an antibacterial PAA-g-QCE/PVA hydrogel is fabricated against the attack of Gram-negative *E. coli* bacteria evaluated by the inhibition zone method and the antibacterial rate.[101]

Functional hydrogel coatings show promising application potential.[202] Recently, we proposed an approach to fabricate hydrogel coatings using an injectable, tough, and thermoplastic κ-CG/PNV DN hydrogel with temperature-controlled adhesion.[35] The PNV network is cross-linked by aggregated double helices via dual amide hydrogen bonds. Furthermore, robust slide rheostat-based touch sensing is applied for the κ-CG/PNV hydrogel coating to form 1D touch strips outputting linear and nonlinear relationships and 2D rigid, flexible, and specially shaped touch panels (Figure 13). The slide rheostat-based structure can significantly eliminate the water evaporation effect, and the baseline signal is close to zero. Moreover, this structure is robust under extreme conditions.

7.4. Challenges and Outlook. Despite the abundance of materials that have been used in diverse fields, significant issues still need to be studied. (1) Flexible electrical devices based on polysaccharide-based DN hydrogels can be designed with other elaborate structures, such as pressure, temperature, slip, and force vector sensors, triboelectric nanogenerators, and sensor arrays. (2) Deep insights into polysaccharide-based DN hydrogels as biomaterials remain lacking; for example, the effects of mechanical property, the rigidity of the polysaccharide network, cross-linking density and type, and network structure on cell attachment, migration, proliferation, and gene expression. (3) Polysaccharide-based DN hydrogel microspheres for use in cell encapsulation and drug delivery remain in their infancy. (4) Polysaccharide-based DN hydrogels can be hybridized with fabrics to combine the superior mechanical properties of synthetic polymers, as well as the ductility, cytocompatibility, bioactivity, conductivity, and adhesion of polysaccharide-based DN hydrogels.

8. CONCLUSION AND OUTLOOK

The DN strategy greatly improves the mechanical properties of hydrogels, making them comparable to naturally tough tissues, such as cartilage, tendon, and heart. DN hydrogels have extremely high mechanical characteristics, attributed to their reliable energy dissipation. Polysaccharide-based DN hydrogels combine the wide versatility and various chemical combinations of the DN strategy, outstanding properties of synthetic polymers, and advantages of renewable biological resources to offer great flexibility in design, making polysaccharide-based DN hydrogels some of the major parts of DN hydrogels. Due to the robustness of the DN strategy, polysaccharide-based DN hydrogels have the potential to be applied in almost all hydrogel fields as biocompatible, tough, and repairable materials, such as biomaterials, adsorption materials, shape-memory materials, actuators, flexible devices, and batteries. This review focuses on theories and experimental evidence about the strengthening mechanisms of DN hydrogels, the basic properties and gelling mechanism of applied polysaccharides, and the latest developments in polysaccharide-based DN hydrogels. This review elucidates the advantages of polysaccharides for DN hydrogels and the search for natural and synthetic materials with desirable properties, and covers major mechanical discussions of polysaccharide-based DN hydrogels. Polysaccharide-based DN hydrogels have made great achievements, but they still face certain challenges in the future as follows.

(1) Although a number of varieties of polysaccharides, including marine polysaccharides, microbial polysaccharides, plant polysaccharides, and animal polysaccharides, are utilized in the construction of a DN hydrogel, heteropolysaccharides, and plant polysaccharides are generally not structurally homogeneous and have indisciplinable molecular weights and a broad molecular weight distribution. These changeful characteristics often result in uncontrollable or inconstant physical and chemical properties of the resulting polysaccharide products. Taking into account the complex fine distinctions in chemical structures, molecular conformation, and unique multifunctionalities of polysaccharides alone with the accessibility of modification, there are still many good candidates in the polysaccharide family. Among them, the microorganism-derived polysaccharides produced by fermentation (bacterial polysaccharides) deserve more attention. One fundamental reason is that compared with heteropolysaccharides and plant polysaccharides, bacterial polysaccharides have potential advantages of reproducible physical and chemical properties (well-defined chemical structures with homogeneous repeating units, relatively high molecular weight and narrow molecular weight distribution with controllability, excellent modifiability, and processability). Other essential advantages of bacterial polysaccharides are a regular source of materials and being capable of production in large quantities regardless of the deterioration of eco-environments or climates. In addition, their preparation methods are much greener. Thus, further exploration of polysaccharides is necessary to meet the higher practical application requirements.

https://doi.org/10.1021/acs.biomac.3c00765
Biomacromolecules XXXX, XXX, XXX−XXX

(2) Mathematic and simulated models of polysaccharide-based networks. Little is known about the establishment of theoretical models to quantitatively calculate the mechanical properties of these hydrogels under a given composition and the contribution of different factors, such as sacrificed physical and chemical bonds, inhomogeneity degree, cross-linking density, concentration, entanglement, and network structure. Meanwhile, molecular simulations are reasonably necessary for polysaccharide-based DN hydrogels to (i) accelerate the simulation of a large and complex DN hydrogel model; (ii) develop new force fields to precisely analyze the contributions of the above factors; (iii) evaluate the mechanical properties of a particular composition before experiment; and (iv) design polysaccharide-based DN hydrogels depending on the required ability and application, such as analyses of ion and electron transport in energy storage and conversion. Efforts should also focus on explaining the mechanical behavior of polysaccharide-based DN hydrogels around the yield point.

(3) Fabrication. The fabrication method of the polysaccharide-based DN hydrogel can also be further studied. First, 3D printing is still a prospective method for designing tough DN hydrogels with custom and complex shapes. Moreover, the preparation of strong DN hydrogel microspheres by using microfluidic technology, the inverse emulsion method, and shear is in the early stages of research. The DN hydrogels can also be coated onto stiff substrates as hydrogel coatings to prepare materials with unique features such as extreme mechanical strength, bioactivity, and lubrication. Furthermore, the Hoffmeister effect has been proven efficient to greatly enhance the mechanical properties of hydrogels and DN hydrogels, which provides an efficient physical approach to fabricating tough polysaccharide-based DN hydrogels.

(4) Network structure. It is a future development trend to develop new polysaccharide-based DN hydrogels with novel networks, such as fully physical cross-linked networks and networks with unique cross-links. The new networks should endow the DN hydrogels with outstanding functionalities such as self-healing, fast self-recovery, recyclability, and biodegradability. Elaborate network structures are needed for the DN hydrogels as biomaterials to mimic the ECM, tissues, and organs such as dynamic bonds and programmable hierarchical polymer orientations. These structures need to endow the biocompatible and supportive scaffolds with high toughness and durability for cells to grow, proliferate, migrate, and differentiate.

(5) Mechanical strength. Many polysaccharide-based DN hydrogels with highlightable mechanical properties have been extensively studied, whereas the development of supertough DN hydrogels to prepare materials with comparable extreme mechanical properties as natural tissues remains a major challenge for researchers. Meanwhile, extreme applied environmental conditions of these DN hydrogels on mechanical properties need to be considered, such as the pH, temperature, and ionic strength. This issue may be eliminated by combining multiple enhancements to meet the intended application of the material such as three-network hydrogels. For biomedical usage, polysaccharide-based DN hydrogels with underwater adhesion and injectability as implant biomaterials remain lacking.

(6) Application. Studies on polysaccharide-based DN hydrogels applied in some attractive fields are still in their infancy, such as injectability and 3D printing, optical, electric, and magnetic tough materials, actuators, ionotronics, flexible electronic skins, and impact-resistance materials. Nevertheless, the inherent outstanding mechanical properties and cytocompatibilities brought by the polysaccharide-based DN concept provide an effective way to apply these hydrogels in many fields.

■ ASSOCIATED CONTENT

Supporting Information

The Supporting Information is available free of charge at https://pubs.acs.org/doi/10.1021/acs.biomac.3c00765.

Additional discussions on the fabrication and classification of polysaccharide-based DN hydrogels, including supplementary references(PDF)

■ AUTHOR INFORMATION

Corresponding Author

Hongbin Zhang − *Advanced Rheology Institute, Department of Polymer Science and Engineering, School of Chemistry and Chemical Engineering, Frontiers Science Center for Transformative Molecules, Shanghai Key Laboratory of Electrical Insulation and Thermal Aging, Shanghai Jiao Tong University, Shanghai 200240, China;* orcid.org/0000-0002-4419-4818; Email: hbzhang@sjtu.edu.cn

Authors

Pengguang Wang − *Advanced Rheology Institute, Department of Polymer Science and Engineering, School of Chemistry and Chemical Engineering, Frontiers Science Center for Transformative Molecules, Shanghai Key Laboratory of Electrical Insulation and Thermal Aging, Shanghai Jiao Tong University, Shanghai 200240, China;* orcid.org/0000-0003-3954-1325

Qingyu Liao − *Advanced Rheology Institute, Department of Polymer Science and Engineering, School of Chemistry and Chemical Engineering, Frontiers Science Center for Transformative Molecules, Shanghai Key Laboratory of Electrical Insulation and Thermal Aging, Shanghai Jiao Tong University, Shanghai 200240, China*

Complete contact information is available at: https://pubs.acs.org/10.1021/acs.biomac.3c00765

Author Contributions

Pengguang Wang: Investigation, Conceptualization, Writing original draft, Visualization. Qingyu Liao: Conceptualization, Review. Hongbin Zhang: Conceptualization, Visualization, Supervision, Review and Editing, Project administration, Funding acquisition.

Notes

The authors declare no competing financial interest.

■ ACKNOWLEDGMENTS

This work was supported by the National Natural Science Foundation of China (Grant No. 21774075).

■ ABBREVIATIONS

SA, alginate; BC, bacterial cellulose; CCHT, carboxymethylated chitosan; CHT, chitosan; CMC, carboxymethyl cellulose; CMCD, carboxymethylated Curdlan; CNC, cellulose nanocrystal; CEQC, carboxylethyl quaternized cellulose; CS, chondroitin sulfate; GG, gellan gum; HA, hyaluronic acid; HACC, 2-hydroxypropyltrimethyl ammonium chloride chitosan; HA-Cys-GMA, hyaluronic acid-cysteine-glycidyl meth-

https://doi.org/10.1021/acs.biomac.3c00765
Biomacromolecules XXXX, XXX, XXX−XXX

acrylate; KGM, konjac glucomannan; Odex, oxidized dextran; QCE, quaternized ammonium cellulose; XG, xanthan gum; κ-CG, κ-carrageenan; ELP-HYD, hydrazine modified protein; MBAA, *N*,*N*′-methylenebisacrylamide; NVP, *N*-vinyl-2-pyrrolidone; PAAc, poly(acrylic acid); PAAm, polyacrylamide; PAMPS, poly(2-acrylamido-2-methylpropanesulfonic acid); PDA, polydopamine; PEG, polyethylene glycol; PEGDA, polyethylene glycol diacrylate; PEGDE, poly(ethylene glycol diglycidyl ether); PNAGA, poly(*N*-acryloyl glycinamide); PNV, poly(*N*-acryloyl glycinamide-*co*-vinyl imidazole); PVA, polyvinyl alcohol; SMA, stearyl methacrylate; TPEG, tetra-PEG; VI, vinyl imidazole; 4-arm-PEG-NHS, four-armed poly(ethylene glycol) succinimidyl; 4-arm-PEG-NH_2, four-armed poly(ethylene glycol) amine; A-aGO, alginate-functionalized amino-graphene oxide; DLS, dynamic light scattering; DN, double-network; DOPA, 3,4-dihydroxiphenylalanine; EDL, electric double layer; GO, graphene oxide; HAP, hydroxyapatite; LysAAm, N_ε-acryloyl L-lysine; Na_3cit, sodium citrate; SANS, small-angle neutron scattering; SAXS, small-angle X-ray scattering

REFERENCES

(1) Zhao, X.; Chen, X.; Yuk, H.; Lin, S.; Liu, X.; Parada, G. Soft Materials by Design: Unconventional Polymer Networks Give Extreme Properties. *Chem. Rev.* **2021**, *121* (8), 4309−4372.

(2) Gong, J. P.; Katsuyama, Y.; Kurokawa, T.; Osada, Y. Double-Network Hydrogels with Extremely High Mechanical Strength. *Adv. Mater.* **2003**, *15* (14), 1155−1158.

(3) Sun, J.-Y.; Zhao, X.; Illeperuma, W. R. K.; Chaudhuri, O.; Oh, K. H.; Mooney, D. J.; Vlassak, J. J.; Suo, Z. Highly stretchable and tough hydrogels. *Nature* **2012**, *489* (7414), 133−136.

(4) Morris, V. J. Weak and Strong Polysaccharide Gels. In *Food Polymers, Gels and Colloids*; Dickinson, E., Ed.; Woodhead Publishing, 1991; pp 310−321.

(5) Goycoolea, F. M.; Richardson, R. K.; Morris, E. R.; Gidley, M. J. Stoichiometry and Conformation of Xanthan in Synergistic Gelation with Locust Bean Gum or Konjac Glucomannan: Evidence for Heterotypic Binding. *Macromolecules* **1995**, *28* (24), 8308−8320.

(6) Paradossi, G.; Chiessi, E.; Barbiroli, A.; Fessas, D. Xanthan and Glucomannan Mixtures: Synergistic Interactions and Gelation. *Biomacromolecules* **2002**, *3* (3), 498−504.

(7) Zhang, F.; Luan, T.; Kang, D.; Jin, Q.; Zhang, H.; Yadav, M. P. Viscosifying properties of corn fiber gum with various polysaccharides. *Food Hydrocolloid* **2015**, *43*, 218−227.

(8) Huang, W.; Shishehbor, M.; Guarín-Zapata, N.; Kirchhofer, N. D.; Li, J.; Cruz, L.; Wang, T.; Bhowmick, S.; Stauffer, D.; Manimunda, P.; Bozhilov, K. N.; Caldwell, R.; Zavattieri, P.; Kisailus, D. A natural impact-resistant bicontinuous composite nanoparticle coating. *Nat. Mater.* **2020**, *19* (11), 1236−1243.

(9) Li, C.; Rowland, M. J.; Shao, Y.; Cao, T.; Chen, C.; Jia, H.; Zhou, X.; Yang, Z.; Scherman, O. A.; Liu, D. Responsive Double Network Hydrogels of Interpenetrating DNA and CB[8] Host−Guest Supramolecular Systems. *Adv. Mater.* **2015**, *27* (21), 3298−3304.

(10) Cong, H.-P.; Wang, P.; Yu, S.-H. Stretchable and Self-Healing Graphene Oxide−Polymer Composite Hydrogels: A Dual-Network Design. *Chem. Mater.* **2013**, *25* (16), 3357−3362.

(11) Huang, P.; Chen, W.; Yan, L. An inorganic−organic double network hydrogel of graphene and polymer. *Nanoscale* **2013**, *5* (13), 6034−6039.

(12) Guan, Q.-F.; Han, Z.-M.; Yang, K.-P.; Yang, H.-B.; Ling, Z.-C.; Yin, C.-H.; Yu, S.-H. Sustainable Double-Network Structural Materials for Electromagnetic Shielding. *Nano Lett* **2021**, *21* (6), 2532−2537.

(13) Pan, K.; Peng, S.; Chu, Y.; Liang, K.; Wang, C. H.; Wu, S.; Xu, J. Highly sensitive, stretchable and durable strain sensors based on conductive double-network polymer hydrogels. *J. Polym. Sci.* **2020**, *58* (21), 3069−3081.

(14) Zhang, Y.; Chen, K.; Li, Y.; Lan, J.; Yan, B.; Shi, L.; Ran, R. High-Strength, Self-Healable, Temperature-Sensitive, MXene-Containing Composite Hydrogel as a Smart Compression Sensor. *ACS Appl. Mater. Interfaces* **2019**, *11* (50), 47350−47357.

(15) Li, Y.; Hu, X.; Cheng, W.; Shao, Z.; Xue, D.; Zhao, Y.; Lu, W. A novel high-toughness, organic/inorganic double-network fire-retardant gel for coal-seam with high ground temperature. *Fuel* **2020**, *263*, 116779.

(16) Zhang, F.; Wu, J.; Kang, D.; Zhang, H. Development of a complex hydrogel of hyaluronan and PVA embedded with silver nanoparticles and its facile studies on Escherichia coli. *J. Biomat. Sci-Polym. E.* **2013**, *24* (12), 1410−1425.

(17) Ran, J.; Jiang, P.; Liu, S.; Sun, G.; Yan, P.; Shen, X.; Tong, H. Constructing multi-component organic/inorganic composite bacterial cellulose-gelatin/hydroxyapatite double-network scaffold platform for stem cell-mediated bone tissue engineering. *Mat. Sci. Eng. C-Mater.* **2017**, *78*, 130−140.

(18) Aldana, A. A.; Houben, S.; Moroni, L.; Baker, M. B.; Pitet, L. M. Trends in Double Networks as Bioprintable and Injectable Hydrogel Scaffolds for Tissue Regeneration. *ACS Biomater. Sci. Eng.* **2021**, *7* (9), 4077−4101.

(19) Li, L.; Wu, P.; Yu, F.; Ma, J. Double network hydrogels for energy/environmental applications: challenges and opportunities. *J. Mater. Chem. A* **2022**, *10* (17), 9215−9247.

(20) Li, Z.; Lin, Z. Recent advances in polysaccharide-based hydrogels for synthesis and applications. *Aggregate* **2021**, *2* (2), No. e21.

(21) Williams, D. F. There is no such thing as a biocompatible material. *Biomaterials* **2014**, *35* (38), 10009−10014.

(22) Radhakrishnan, J.; Subramanian, A.; Krishnan, U. M.; Sethuraman, S. Injectable and 3D Bioprinted Polysaccharide Hydrogels: From Cartilage to Osteochondral Tissue Engineering. *Biomacromolecules* **2017**, *18* (1), 1−26.

(23) Haque, M. A.; Kurokawa, T.; Gong, J. P. Super tough double network hydrogels and their application as biomaterials. *Polymer* **2012**, *53* (9), 1805−1822.

(24) Gong, J. P. Why are double network hydrogels so tough? *Soft Matter* **2010**, *6* (12), 2583−2590.

(25) Chen, Q.; Chen, H.; Zhu, L.; Zheng, J. Fundamentals of double network hydrogels. *J. Mater. Chem. B* **2015**, *3* (18), 3654−3676.

(26) Nonoyama, T.; Gong, J. P. Double-network hydrogel and its potential biomedical application: A review. *P. I. Mech. Eng. H* **2015**, *229* (12), 853−863.

(27) Gu, Z.; Huang, K.; Luo, Y.; Zhang, L.; Kuang, T.; Chen, Z.; Liao, G. Double network hydrogel for tissue engineering. *WIREs Nanomed. Nanobi.* **2018**, *10* (6), No. e1520.

(28) Nonoyama, T.; Gong, J. P. Tough Double Network Hydrogel and Its Biomedical Applications. *Annu. Rev. Chem. Biomol.* **2021**, *12* (1), 393−410.

(29) Xu, X.; Jerca, V. V.; Hoogenboom, R. Bioinspired double network hydrogels: from covalent double network hydrogels via hybrid double network hydrogels to physical double network hydrogels. *Mater. Horiz.* **2021**, *8* (4), 1173−1188.

(30) Zhang, H.; Shi, L. W. E.; Zhou, J. Recent developments of polysaccharide-based double-network hydrogels. *J. Polym. Sci.* **2023**, *61* (1), 7−43.

(31) Chen, Q.; Zhu, L.; Zhao, C.; Wang, Q.; Zheng, J. A Robust, One-Pot Synthesis of Highly Mechanical and Recoverable Double Network Hydrogels Using Thermoreversible Sol-Gel Polysaccharide. *Adv. Mater.* **2013**, *25* (30), 4171−4176.

(32) Yang, Y.; Wang, X.; Yang, F.; Shen, H.; Wu, D. A Universal Soaking Strategy to Convert Composite Hydrogels into Extremely Tough and Rapidly Recoverable Double-Network Hydrogels. *Adv. Mater.* **2016**, *28* (33), 7178−7184.

(33) Azevedo, S.; Costa, A. M. S.; Andersen, A.; Choi, I. S.; Birkedal, H.; Mano, J. F. Bioinspired Ultratough Hydrogel with Fast Recovery, Self-Healing, Injectability and Cytocompatibility. *Adv. Mater.* **2017**, *29* (28), 1700759.

https://doi.org/10.1021/acs.biomac.3c00765
Biomacromolecules XXXX, XXX, XXX−XXX

(34) Liu, S.; Li, L. Ultrastretchable and Self-Healing Double-Network Hydrogel for 3D Printing and Strain Sensor. *ACS Appl. Mater. Interfaces* **2017**, *9* (31), 26429−26437.
(35) Wang, P.; Liao, Q.; Yuan, B.; Zhang, H. Injectable, Tough, and Thermoplastic Supramolecular Hydrogel Coatings with Controllable Adhesion for Touch Sensing. *ACS Appl. Mater. Interfaces* **2023**, *15* (27), 32945−32956.
(36) Wang, P.; Wu, M.; Li, R.; Cai, Z.; Zhang, H. Fabrication of a Double-Network Hydrogel Based on Carboxymethylated Curdlan/Polyacrylamide with Highly Mechanical Performance for Cartilage Repair. *ACS Appl. Polym. Mater.* **2021**, *3* (11), 5857−5869.
(37) Yang, C. H.; Wang, M. X.; Haider, H.; Yang, J. H.; Sun, J.-Y.; Chen, Y. M.; Zhou, J.; Suo, Z. Strengthening Alginate/Polyacrylamide Hydrogels Using Various Multivalent Cations. *ACS Appl. Mater. Interfaces* **2013**, *5* (21), 10418−10422.
(38) Zhang, M.; Ren, X.; Duan, L.; Gao, G. Joint double-network hydrogels with excellent mechanical performance. *Polymer* **2018**, *153*, 607−615.
(39) Liu, S.; Li, L. Recoverable and Self-Healing Double Network Hydrogel Based on κ-Carrageenan. *ACS Appl. Mater. Interfaces* **2016**, *8* (43), 29749−29758.
(40) Liu, S.; Zhang, H.; Yu, W. Simultaneously improved strength and toughness in κ-carrageenan/polyacrylamide double network hydrogel via synergistic interaction. *Carbohyd. Polym.* **2020**, *230*, 115596.
(41) Niu, R.; Qin, Z.; Ji, F.; Xu, M.; Tian, X.; Li, J.; Yao, F. Hybrid pectin-Fe^{3+}/polyacrylamide double network hydrogels with excellent strength, high stiffness, superior toughness and notch-insensitivity. *Soft Matter* **2017**, *13* (48), 9237−9245.
(42) Liang, S.; Wu, Z. L.; Hu, J.; Kurokawa, T.; Yu, Q. M.; Gong, J. P. Direct Observation on the Surface Fracture of Ultrathin Film Double-Network Hydrogels. *Macromolecules* **2011**, *44* (8), 3016−3020.
(43) Tominaga, T.; Tirumala, V. R.; Lin, E. K.; Gong, J. P.; Furukawa, H.; Osada, Y.; Wu, W.-l. The molecular origin of enhanced toughness in double-network hydrogels: A neutron scattering study. *Polymer* **2007**, *48* (26), 7449−7454.
(44) Fukao, K.; Nakajima, T.; Nonoyama, T.; Kurokawa, T.; Kawai, T.; Gong, J. P. Effect of Relative Strength of Two Networks on the Internal Fracture Process of Double Network Hydrogels As Revealed by in Situ Small-Angle X-ray Scattering. *Macromolecules* **2020**, *53* (4), 1154−1163.
(45) King, D. R.; Okumura, T.; Takahashi, R.; Kurokawa, T.; Gong, J. P. Macroscale Double Networks: Design Criteria for Optimizing Strength and Toughness. *ACS Appl. Mater. Interfaces* **2019**, *11* (38), 35343−35353.
(46) Tanaka, Y.; Kawauchi, Y.; Kurokawa, T.; Furukawa, H.; Okajima, T.; Gong, J. P. Localized Yielding Around Crack Tips of Double-Network Gels. *Macromol. Rapid Commun.* **2008**, *29* (18), 1514−1520.
(47) Yu, Q.; Tanaka, Y.; Furukawa, H.; Kurokawa, T.; Gong, J. Direct Observation of Damage Zone around Crack Tips in Double-Network Gels. *Macromolecules* **2009**, *42* (12), 3852−3855.
(48) Matsuda, T.; Nakajima, T.; Fukuda, Y.; Hong, W.; Sakai, T.; Kurokawa, T.; Chung, U.-i.; Gong, J. P. Yielding Criteria of Double Network Hydrogels. *Macromolecules* **2016**, *49* (5), 1865−1872.
(49) Jang, S. S.; Goddard, W. A.; Kalani, M. Y. S. Mechanical and Transport Properties of the Poly(ethylene oxide)−Poly(acrylic acid) Double Network Hydrogel from Molecular Dynamic Simulations. *J. Phys. Chem. B* **2007**, *111* (7), 1729−1737.
(50) Nakajima, T.; Kurokawa, T.; Furukawa, H.; Gong, J. P. Effect of the constituent networks of double-network gels on their mechanical properties and energy dissipation process. *Soft Matter* **2020**, *16* (37), 8618−8627.
(51) Edgecombe, S.; Linse, P. Monte Carlo simulation of two interpenetrating polymer networks: Structure, swelling, and mechanical properties. *Polymer* **2008**, *49* (7), 1981−1992.
(52) Higuchi, Y.; Saito, K.; Sakai, T.; Gong, J. P.; Kubo, M. Fracture Process of Double-Network Gels by Coarse-Grained Molecular Dynamics Simulation. *Macromolecules* **2018**, *51* (8), 3075−3087.
(53) Xin, H.; Saricilar, S. Z.; Brown, H. R.; Whitten, P. G.; Spinks, G. M. Effect of First Network Topology on the Toughness of Double Network Hydrogels. *Macromolecules* **2013**, *46* (16), 6613−6620.
(54) Arora, A.; Lin, T.-S.; Beech, H. K.; Mochigase, H.; Wang, R.; Olsen, B. D. Fracture of Polymer Networks Containing Topological Defects. *Macromolecules* **2020**, *53* (17), 7346−7355.
(55) Rivlin, R. S.; Thomas, A. G. Rupture of rubber. I. Characteristic energy for tearing. *J. Polym. Sci.* **1953**, *10* (3), 291−318.
(56) Nakajima, T.; Fukuda, Y.; Kurokawa, T.; Sakai, T.; Chung, U.-i.; Gong, J. P. Synthesis and Fracture Process Analysis of Double Network Hydrogels with a Well-Defined First Network. *ACS Macro Lett* **2013**, *2* (6), 518−521.
(57) Na, Y.; Kurokawa, T.; Katsuyama, Y.; Tsukeshiba, H.; Gong, J.; Osada, Y.; Okabe, S.; Karino, T.; Shibayama, M. Structural Characteristics of Double Network Gels with Extremely High Mechanical Strength. *Macromolecules* **2004**, *37* (14), 5370−5374.
(58) Zhao, Y.; Zhang, G.; Wu, C. Nonergodic Dynamics of a Novel Thermally Sensitive Hybrid Gel. *Macromolecules* **2001**, *34* (22), 7804−7808.
(59) Wu, C.; Zuo, J.; Chu, B. Laser light scattering studies of epoxy polymerization of 1,4-butanediol diglycidyl ether with cis-1,2-cyclohexanedicarboxylic anhydride. *Macromolecules* **1989**, *22* (2), 838−842.
(60) Ngai, T.; Wu, C. Effect of Cross-Linking on Dynamics of Semidilute Copolymer Solutions: Poly(methyl methacrylate-co-7-acryloyloxy-4-methylcoumarin) in Chloroform. *Macromolecules* **2003**, *36* (3), 848−854.
(61) Zhang, M.; Zhang, D.; Chen, H.; Zhang, Y.; Liu, Y.; Ren, B.; Zheng, J. A multiscale polymerization framework towards network structure and fracture of double-network hydrogels. *npj Comput. Mater.* **2021**, *7* (1), 39.
(62) Kawauchi, Y.; Tanaka, Y.; Furukawa, H.; Kurokawa, T.; Nakajima, T.; Osada, Y.; Gong, J. P. Brittle, ductile, paste-like behaviors and distinct necking of double network gels with enhanced heterogeneity. *J. Phys.: Conf. Ser.* **2009**, *184*, 012016.
(63) Nakajima, T.; Furukawa, H.; Tanaka, Y.; Kurokawa, T.; Gong, J. P. Effect of void structure on the toughness of double network hydrogels. *J. Polym. Sci. Pol. Phys.* **2011**, *49* (17), 1246−1254.
(64) Ahmed, S.; Nakajima, T.; Kurokawa, T.; Anamul Haque, M.; Gong, J. P. Brittle-ductile transition of double network hydrogels: Mechanical balance of two networks as the key factor. *Polymer* **2014**, *55* (3), 914−923.
(65) Tominaga, T.; Tirumala, V. R.; Lee, S.; Lin, E. K.; Gong, J. P.; Wu, W.-l. Thermodynamic Interactions in Double-Network Hydrogels. *J. Phys. Chem. B* **2008**, *112* (13), 3903−3909.
(66) Nakajima, T.; Furukawa, H.; Tanaka, Y.; Kurokawa, T.; Osada, Y.; Gong, J. P. True Chemical Structure of Double Network Hydrogels. *Macromolecules* **2009**, *42* (6), 2184−2189.
(67) Huang, M.; Furukawa, H.; Tanaka, Y.; Nakajima, T.; Osada, Y.; Gong, J. P. Importance of Entanglement between First and Second Components in High-Strength Double Network Gels. *Macromolecules* **2007**, *40* (18), 6658−6664.
(68) Tsukeshiba, H.; Huang, M.; Na, Y.-H.; Kurokawa, T.; Kuwabara, R.; Tanaka, Y.; Furukawa, H.; Osada, Y.; Gong, J. P. Effect of Polymer Entanglement on the Toughening of Double Network Hydrogels. *J. Phys. Chem. B* **2005**, *109* (34), 16304−16309.
(69) Shams Es-haghi, S.; Leonov, A. I.; Weiss, R. A. Deconstructing the Double-Network Hydrogels: The Importance of Grafted Chains for Achieving Toughness. *Macromolecules* **2014**, *47* (14), 4769−4777.
(70) Yuan, N.; Xu, L.; Xu, B.; Zhao, J.; Rong, J. Chitosan derivative-based self-healable hydrogels with enhanced mechanical properties by high-density dynamic ionic interactions. *Carbohyd. Polym.* **2018**, *193*, 259−267.
(71) Li, H.; Wang, H.; Zhang, D.; Xu, Z.; Liu, W. A highly tough and stiff supramolecular polymer double network hydrogel. *Polymer* **2018**, *153*, 193−200.

https://doi.org/10.1021/acs.biomac.3c00765
Biomacromolecules XXXX, XXX, XXX−XXX

(72) Nakajima, T.; Kurokawa, T.; Ahmed, S.; Wu, W.-l.; Gong, J. P. Characterization of internal fracture process of double network hydrogels under uniaxial elongation. *Soft Matter* **2013**, *9* (6), 1955−1966.
(73) Na, Y.-H.; Tanaka, Y.; Kawauchi, Y.; Furukawa, H.; Sumiyoshi, T.; Gong, J. P.; Osada, Y. Necking Phenomenon of Double-Network Gels. *Macromolecules* **2006**, *39* (14), 4641−4645.
(74) Es-haghi, S. S.; Leonov, A. I.; Weiss, R. A. On the Necking Phenomenon in Pseudo-Semi-Interpenetrating Double-Network Hydrogels. *Macromolecules* **2013**, *46* (15), 6203−6208.
(75) Wang, X.; Hong, W. Pseudo-elasticity of a double network gel. *Soft Matter* **2011**, *7* (18), 8576−8581.
(76) Chen, Q.; Yan, X.; Zhu, L.; Chen, H.; Jiang, B.; Wei, D.; Huang, L.; Yang, J.; Liu, B.; Zheng, J. Improvement of Mechanical Strength and Fatigue Resistance of Double Network Hydrogels by Ionic Coordination Interactions. *Chem. Mater.* **2016**, *28* (16), 5710−5720.
(77) Xin, H.; Brown, H. R.; Naficy, S.; Spinks, G. M. Mechanical recoverability and damage process of ionic-covalent PAAm-alginate hybrid hydrogels. *J. Polym. Sci. Pol. Phys.* **2016**, *54* (1), 53−63.
(78) Morris, E. R.; Nishinari, K.; Rinaudo, M. Gelation of gellan − A review. *Food Hydrocolloid* **2012**, *28* (2), 373−411.
(79) Xue, X.; Hu, Y.; Deng, Y.; Su, J. Recent Advances in Design of Functional Biocompatible Hydrogels for Bone Tissue Engineering. *Adv. Funct. Mater.* **2021**, *31* (19), 2009432.
(80) Kang, D.; Zhang, H.; Nitta, Y.; Fang, Y.; Nishinari, K. *Polysaccharides: Bioactivity and Biotechnology*; Springer: Cham, Switzerland, 2015.
(81) Fang, Y.; Zhang, H.; Nishinari, K. *Food hydrocolloids: Functionalities and applications*; Springer Nature, 2021.
(82) Wang, M. X.; Yang, C. H.; Liu, Z. Q.; Zhou, J.; Xu, F.; Suo, Z.; Yang, J. H.; Chen, Y. M. Tough Photoluminescent Hydrogels Doped with Lanthanide. *Macromol. Rapid Commun.* **2015**, *36* (5), 465−471.
(83) Zhang, X.; Sheng, N.; Wang, L.; Tan, Y.; Liu, C.; Xia, Y.; Nie, Z.; Sui, K. Supramolecular nanofibrillar hydrogels as highly stretchable, elastic and sensitive ionic sensors. *Mater. Horiz.* **2019**, *6* (2), 326−333.
(84) Liu, S.; Bastola, A. K.; Li, L. A 3D Printable and Mechanically Robust Hydrogel Based on Alginate and Graphene Oxide. *ACS Appl. Mater. Interfaces* **2017**, *9* (47), 41473−41481.
(85) Liu, Q.; Xia, C.; He, C.; Guo, W.; Wu, Z. P.; Li, Z.; Zhao, Q.; Xia, B. Y. Dual-Network Structured Hydrogel Electrolytes Engaged Solid-State Rechargeable Zn-Air/Iodide Hybrid Batteries. *Angew. Chem., Int. Ed.* **2022**, *61* (44), No. e202210567.
(86) Zhang, J.; Zeng, L.; Qiao, Z.; Wang, J.; Jiang, X.; Zhang, Y. S.; Yang, H. Functionalizing Double-Network Hydrogels for Applications in Remote Actuation and in Low-Temperature Strain Sensing. *ACS Appl. Mater. Interfaces* **2020**, *12* (27), 30247−30258.
(87) Li, X.; Wang, H.; Li, D.; Long, S.; Zhang, G.; Wu, Z. Dual Ionically Cross-linked Double-Network Hydrogels with High Strength, Toughness, Swelling Resistance, and Improved 3D Printing Processability. *ACS Appl. Mater. Interfaces* **2018**, *10* (37), 31198−31207.
(88) Xue, Q.; He, Y.; Zhang, X.; Zhang, X.; Cai, M.; Guo, C. F.; Yang, C. Strong Interfaces Enable Efficient Load Transfer for Strong, Tough, and Impact-Resistant Hydrogel Composites. *ACS Appl. Mater. Interfaces* **2022**, *14* (29), 33797−33805.
(89) Tang, S.; Yang, J.; Lin, L.; Peng, K.; Chen, Y.; Jin, S.; Yao, W. Construction of physically crosslinked chitosan/sodium alginate/calcium ion double-network hydrogel and its application to heavy metal ions removal. *Chem. Eng. J.* **2020**, *393*, 124728.
(90) Li, L.; Zhao, J.; Sun, Y.; Yu, F.; Ma, J. Ionically cross-linked sodium alginate/K-carrageenan double-network gel beads with low-swelling, enhanced mechanical properties, and excellent adsorption performance. *Chem. Eng. J.* **2019**, *372*, 1091−1103.
(91) Rao, Z.; Liu, S.; Wu, R.; Wang, G.; Sun, Z.; Bai, L.; Wang, W.; Chen, H.; Yang, H.; Wei, D.; Niu, Y. Fabrication of dual network self-healing alginate/guar gum hydrogels based on polydopamine-type microcapsules from mesoporous silica nanoparticles. *Int. J. Biol. Macromol.* **2019**, *129*, 916−926.
(92) Wang, D.; Maharjan, S.; Kuang, X.; Wang, Z.; Mille, L. S.; Tao, M.; Yu, P.; Cao, X.; Lian, L.; Lv, L.; He, J. J.; Tang, G.; Yuk, H.; Ozaki, C. K.; Zhao, X.; Zhang, Y. S. Microfluidic bioprinting of tough hydrogel-based vascular conduits for functional blood vessels. *Sci. Adv.* **2022**, *8* (43), No. eabq6900.
(93) Wang, H.; Zhu, D.; Paul, A.; Cai, L.; Enejder, A.; Yang, F.; Heilshorn, S. C. Covalently Adaptable Elastin-Like Protein-Hyaluronic Acid (ELP-HA) Hybrid Hydrogels with Secondary Thermoresponsive Crosslinking for Injectable Stem Cell Delivery. *Adv. Funct. Mater.* **2017**, *27* (28), 1605609.
(94) Weng, L.; Gouldstone, A.; Wu, Y.; Chen, W. Mechanically strong double network photocrosslinked hydrogels from N,N-dimethylacrylamide and glycidyl methacrylated hyaluronan. *Biomaterials* **2008**, *29* (14), 2153−2163.
(95) Zhao, J.; Tong, H.; Kirillova, A.; Koshut, W. J.; Malek, A.; Brigham, N. C.; Becker, M. L.; Gall, K.; Wiley, B. J. A Synthetic Hydrogel Composite with a Strength and Wear Resistance Greater than Cartilage. *Adv. Funct. Mater.* **2022**, *32* (41), 2205662.
(96) Nakayama, A.; Kakugo, A.; Gong, J. P.; Osada, Y.; Takai, M.; Erata, T.; Kawano, S. High Mechanical Strength Double-Network Hydrogel with Bacterial Cellulose. *Adv. Funct. Mater.* **2004**, *14* (11), 1124−1128.
(97) Sun, D.; Gao, Y.; Zhou, Y.; Yang, M.; Hu, J.; Lu, T.; Wang, T. Enhance Fracture Toughness and Fatigue Resistance of Hydrogels by Reversible Alignment of Nanofibers. *ACS Appl. Mater. Interfaces* **2022**, *14* (43), 49389−49397.
(98) Yang, J.; Han, C. Mechanically Viscoelastic Properties of Cellulose Nanocrystals Skeleton Reinforced Hierarchical Composite Hydrogels. *ACS Appl. Mater. Interfaces* **2016**, *8* (38), 25621−25630.
(99) Wu, Y.; Zeng, Y.; Chen, Y.; Li, C.; Qiu, R.; Liu, W. Photocurable 3D Printing of High Toughness and Self-Healing Hydrogels for Customized Wearable Flexible Sensors. *Adv. Funct. Mater.* **2021**, *31* (52), 2107202.
(100) Zhang, H.; Gan, X.; Song, Z.; Zhou, J. Amphoteric Cellulose-Based Double-Network Hydrogel Electrolyte Toward Ultra-Stable Zn Anode. *Angew. Chem., Int. Ed.* **2023**, *62* (13), No. e202217833.
(101) Wang, Y.; Wang, Z.; Wu, K.; Wu, J.; Meng, G.; Liu, Z.; Guo, X. Synthesis of cellulose-based double-network hydrogels demonstrating high strength, self-healing, and antibacterial properties. *Carbohyd. Polym.* **2017**, *168*, 112−120.
(102) Huang, J.; Frauenlob, M.; Shibata, Y.; Wang, L.; Nakajima, T.; Nonoyama, T.; Tsuda, M.; Tanaka, S.; Kurokawa, T.; Gong, J. P. Chitin-Based Double-Network Hydrogel as Potential Superficial Soft-Tissue-Repairing Materials. *Biomacromolecules* **2020**, *21* (10), 4220−4230.
(103) Yang, Y.; Wang, X.; Yang, F.; Wang, L.; Wu, D. Highly Elastic and Ultratough Hybrid Ionic−Covalent Hydrogels with Tunable Structures and Mechanics. *Adv. Mater.* **2018**, *30* (18), 1707071.
(104) Gang, F.; Yan, H.; Ma, C.; Jiang, L.; Gu, Y.; Liu, Z.; Zhao, L.; Wang, X.; Zhang, J.; Sun, X. Robust magnetic double-network hydrogels with self-healing, MR imaging, cytocompatibility and 3D printability. *Chem. Commun.* **2019**, *55* (66), 9801−9804.
(105) Cui, C.; Shao, C.; Meng, L.; Yang, J. High-Strength, Self-Adhesive, and Strain-Sensitive Chitosan/Poly(acrylic acid) Double-Network Nanocomposite Hydrogels Fabricated by Salt-Soaking Strategy for Flexible Sensors. *ACS Appl. Mater. Interfaces* **2019**, *11* (42), 39228−39237.
(106) Wang, L.; Zhang, X.; Yang, K.; Fu, Y. V.; Xu, T.; Li, S.; Zhang, D.; Wang, L.-N.; Lee, C.-S. A Novel Double-Crosslinking-Double-Network Design for Injectable Hydrogels with Enhanced Tissue Adhesion and Antibacterial Capability for Wound Treatment. *Adv. Funct. Mater.* **2020**, *30* (1), 1904156.
(107) Li, Z.; Yuan, B.; Dong, X.; Duan, L.; Tian, H.; He, C.; Chen, X. Injectable polysaccharide hybrid hydrogels as scaffolds for burn wound healing. *RSC Adv* **2015**, *5* (114), 94248−94256.
(108) Zhang, H.; Qadeer, A.; Chen, W. In Situ Gelable Interpenetrating Double Network Hydrogel Formulated from Binary

https://doi.org/10.1021/acs.biomac.3c00765
Biomacromolecules XXXX, XXX, XXX−XXX

Components: Thiolated Chitosan and Oxidized Dextran. *Biomacromolecules* **2011**, *12* (5), 1428−1437.
(109) Chen, Q.; Zhu, L.; Chen, H.; Yan, H.; Huang, L.; Yang, J.; Zheng, J. A Novel Design Strategy for Fully Physically Linked Double Network Hydrogels with Tough, Fatigue Resistant, and Self-Healing Properties. *Adv. Funct. Mater.* **2015**, *25* (10), 1598−1607.
(110) Bu, Y.; Shen, H.; Yang, F.; Yang, Y.; Wang, X.; Wu, D. Construction of Tough, in Situ Forming Double-Network Hydrogels with Good Biocompatibility. *ACS Appl. Mater. Interfaces* **2017**, *9* (3), 2205−2212.
(111) Li, X.; Yang, Q.; Zhao, Y.; Long, S.; Zheng, J. Dual physically crosslinked double network hydrogels with high toughness and self-healing properties. *Soft Matter* **2017**, *13* (5), 911−920.
(112) Wang, Y.; Chen, F.; Liu, Z.; Tang, Z.; Yang, Q.; Zhao, Y.; Du, S.; Chen, Q.; Zhi, C. A Highly Elastic and Reversibly Stretchable All-Polymer Supercapacitor. *Angew. Chem., Int. Ed.* **2019**, *58* (44), 15707−15711.
(113) Bakarich, S. E.; Pidcock, G. C.; Balding, P.; Stevens, L.; Calvert, P.; in het Panhuis, M. Recovery from applied strain in interpenetrating polymer network hydrogels with ionic and covalent cross-links. *Soft Matter* **2012**, *8* (39), 9985−9988.
(114) Liu, S.; Qiu, Y.; Yu, W.; Zhang, H. Highly Stretchable and Self-Healing Strain Sensor Based on Gellan Gum Hybrid Hydrogel for Human Motion Monitoring. *ACS Appl. Polym. Mater.* **2020**, *2* (3), 1325−1334.
(115) Wang, Y.; Yu, W.; Liu, S. Physically cross-linked gellan gum/hydrophobically associated polyacrylamide double network hydrogel for cartilage repair. *Eur. Polym. J.* **2022**, *167*, 111074.
(116) Lv, Y.; Pan, Z.; Song, C.; Chen, Y.; Qian, X. Locust bean gum/gellan gum double-network hydrogels with superior self-healing and pH-driven shape-memory properties. *Soft Matter* **2019**, *15* (30), 6171−6179.
(117) Shin, H.; Olsen, B. D.; Khademhosseini, A. The mechanical properties and cytotoxicity of cell-laden double-network hydrogels based on photocrosslinkable gelatin and gellan gum biomacromolecules. *Biomaterials* **2012**, *33* (11), 3143−3152.
(118) Deng, Y.; Huang, M.; Sun, D.; Hou, Y.; Li, Y.; Dong, T.; Wang, X.; Zhang, L.; Yang, W. Dual Physically Cross-Linked κ-Carrageenan-Based Double Network Hydrogels with Superior Self-Healing Performance for Biomedical Application. *ACS Appl. Mater. Interfaces* **2018**, *10* (43), 37544−37554.
(119) Yuan, N.; Xu, L.; Wang, H.; Fu, Y.; Zhang, Z.; Liu, L.; Wang, C.; Zhao, J.; Rong, J. Dual Physically Cross-Linked Double Network Hydrogels with High Mechanical Strength, Fatigue Resistance, Notch-Insensitivity, and Self-Healing Properties. *ACS Appl. Mater. Interfaces* **2016**, *8* (49), 34034−34044.
(120) Ye, L.; Lv, Q.; Sun, X.; Liang, Y.; Fang, P.; Yuan, X.; Li, M.; Zhang, X.; Shang, X.; Liang, H. Fully physically cross-linked double network hydrogels with strong mechanical properties, good recovery and self-healing properties. *Soft Matter* **2020**, *16* (7), 1840−1849.
(121) Wu, X.; Sun, H.; Qin, Z.; Che, P.; Yi, X.; Yu, Q.; Zhang, H.; Sun, X.; Yao, F.; Li, J. Fully physically crosslinked pectin-based hydrogel with high stretchability and toughness for biomedical application. *Int. J. Biol. Macromol.* **2020**, *149*, 707−716.
(122) Han, L.; Wang, M.; Li, P.; Gan, D.; Yan, L.; Xu, J.; Wang, K.; Fang, L.; Chan, C. W.; Zhang, H.; Yuan, H.; Lu, X. Mussel-Inspired Tissue-Adhesive Hydrogel Based on the Polydopamine-Chondroitin Sulfate Complex for Growth-Factor-Free Cartilage Regeneration. *ACS Appl. Mater. Interfaces* **2018**, *10* (33), 28015−28026.
(123) Zhu, J.; Guan, S.; Hu, Q.; Gao, G.; Xu, K.; Wang, P. Tough and pH-sensitive hydroxypropyl guar gum/polyacrylamide hybrid double-network hydrogel. *Chem. Eng. J.* **2016**, *306*, 953−960.
(124) Ching, S. H.; Bansal, N.; Bhandari, B. Alginate gel particles−A review of production techniques and physical properties. *Crit. Rev. Food Sci.* **2017**, *57* (6), 1133−1152.
(125) Lee, K. Y.; Mooney, D. J. Alginate: Properties and biomedical applications. *Prog. Polym. Sci.* **2012**, *37* (1), 106−126.
(126) Zhang, H.; Zhang, F.; Yuan, R. Chapter 13 - Applications of natural polymer-based hydrogels in the food industry. In *Hydrogels Based on Natural Polymers*; Chen, Y., Ed.; Elsevier, 2020; pp 357−410.
(127) Cao, L.; Lu, W.; Mata, A.; Nishinari, K.; Fang, Y. Egg-box model-based gelation of alginate and pectin: A review. *Carbohyd. Polym.* **2020**, *242*, 116389.
(128) Dodero, A.; Alberti, S.; Gaggero, G.; Ferretti, M.; Botter, R.; Vicini, S.; Castellano, M. An Up-to-Date Review on Alginate Nanoparticles and Nanofibers for Biomedical and Pharmaceutical Applications. *Adv. Mater. Interfaces* **2021**, *8* (22), 2100809.
(129) Zhu, F.; Yan, N.; Lu, X.; Xu, J.; Gu, H.; Liang, J.; Cheng, K.; Wang, X.; Ma, X.; Ma, N.; Zhao, X.; Chen, C.; Nie, G. Cell-Reprogramming-Inspired Dynamically Responsive Hydrogel Boosts the Induction of Pluripotency via Phase-Separated Biomolecular Condensates. *Adv. Mater.* **2023**, *35* (34), 2211609.
(130) Cai, Z.; Zhang, F.; Wei, Y.; Zhang, H. Freeze−Thaw-Induced Gelation of Hyaluronan: Physical Cryostructuration Correlated with Intermolecular Associations and Molecular Conformation. *Macromolecules* **2017**, *50* (17), 6647−6658.
(131) Wolf, K. J.; Kumar, S. Hyaluronic Acid: Incorporating the Bio into the Material. *ACS Biomater. Sci. Eng.* **2019**, *5* (8), 3753−3765.
(132) Chang, C.; Zhang, L. Cellulose-based hydrogels: Present status and application prospects. *Carbohyd. Polym.* **2011**, *84* (1), 40−53.
(133) Moon, R. J.; Martini, A.; Nairn, J.; Simonsen, J.; Youngblood, J. Cellulose nanomaterials review: structure, properties and nanocomposites. *Chem. Soc. Rev.* **2011**, *40* (7), 3941−3994.
(134) Ahmed, J.; Gultekinoglu, M.; Edirisinghe, M. Bacterial cellulose micro-nano fibres for wound healing applications. *Biotechnol. Adv.* **2020**, *41*, 107549.
(135) Shamshina, J. L.; Berton, P.; Rogers, R. D. Advances in Functional Chitin Materials: A Review. *ACS Sustainable Chem. Eng.* **2019**, *7* (7), 6444−6457.
(136) Abd El-Hack, M. E.; El-Saadony, M. T.; Shafi, M. E.; Zabermawi, N. M.; Arif, M.; Batiha, G. E.; Khafaga, A. F.; Abd El-Hakim, Y. M.; Al-Sagheer, A. A. Antimicrobial and antioxidant properties of chitosan and its derivatives and their applications: A review. *Int. J. Biol. Macromol.* **2020**, *164*, 2726−2744.
(137) Shen, X.; Shamshina, J. L.; Berton, P.; Gurau, G.; Rogers, R. D. Hydrogels based on cellulose and chitin: fabrication, properties, and applications. *Green Chem* **2016**, *18* (1), 53−75.
(138) H.P.S, A. K.; Saurabh, C. K.; A.S, A.; Nurul Fazita, M. R.; Syakir, M. I.; Davoudpour, Y.; Rafatullah, M.; Abdullah, C. K.; M. Haafiz, M. K.; Dungani, R. A review on chitosan-cellulose blends and nanocellulose reinforced chitosan biocomposites: Properties and their applications. *Carbohyd. Polym.* **2016**, *150*, 216−226.
(139) Xiao, L.; Xie, P.; Ma, J.; Shi, K.; Dai, Y.; Pang, M.; Luo, J.; Tan, Z.; Ma, Y.; Wang, X.; Rong, L.; He, L. A Bioinspired Injectable, Adhesive And Self-Healing Hydrogel with Dual Hybrid Network for Neural Regeneration After Spinal Cord Injury. *Adv. Mater.* **2023**, *35* (34), 2304896.
(140) Feng, D.; Bai, B.; Wang, H.; Suo, Y. Enhanced mechanical stability and sensitive swelling performance of chitosan/yeast hybrid hydrogel beads. *New J. Chem.* **2016**, *40* (4), 3350−3362.
(141) Zarrintaj, P.; Manouchehri, S.; Ahmadi, Z.; Saeb, M. R.; Urbanska, A. M.; Kaplan, D. L.; Mozafari, M. Agarose-based biomaterials for tissue engineering. *Carbohyd. Polym.* **2018**, *187*, 66−84.
(142) Habibi, H.; Khosravi-Darani, K. Effective variables on production and structure of xanthan gum and its food applications: A review. *Biocatal. Agric. Biotechnol.* **2017**, *10*, 130−140.
(143) Kumar, A.; Rao, K. M.; Han, S. S. Application of xanthan gum as polysaccharide in tissue engineering: A review. *Carbohyd. Polym.* **2018**, *180*, 128−144.
(144) Izawa, H.; Kaneko, Y.; Kadokawa, J.-i. Unique gel of xanthan gum with ionic liquid and its conversion into high performance hydrogel. *J. Mater. Chem.* **2009**, *19* (38), 6969−6972.

https://doi.org/10.1021/acs.biomac.3c00765
Biomacromolecules XXXX, XXX, XXX−XXX

(145) Bacelar, A. H.; Silva-Correia, J.; Oliveira, J. M.; Reis, R. L. Recent progress in gellan gum hydrogels provided by functionalization strategies. *J. Mater. Chem. B* **2016**, *4* (37), 6164−6174.
(146) Jafari, A.; Farahani, M.; Sedighi, M.; Rabiee, N.; Savoji, H. Carrageenans for tissue engineering and regenerative medicine applications: A review. *Carbohyd. Polym.* **2022**, *281*, 119045.
(147) Necas, J.; Bartosikova, L. Carrageenan: a review. *Vet. Med-Czech* **2013**, *58* (4), 187−205.
(148) Robal, M.; Brenner, T.; Matsukawa, S.; Ogawa, H.; Truus, K.; Rudolph, B.; Tuvikene, R. Monocationic salts of carrageenans: Preparation and physico-chemical properties. *Food Hydrocolloid* **2017**, *63*, 656−667.
(149) Evageliou, V. I.; Ryan, P. M.; Morris, E. R. Effect of monovalent cations on calcium-induced assemblies of kappa carrageenan. *Food Hydrocolloid* **2019**, *86*, 141−145.
(150) Cai, Z.; Zhang, H. Recent progress on Curdlan provided by functionalization strategies. *Food Hydrocolloid* **2017**, *68*, 128−135.
(151) Nishinari, K.; Zhang, H.; Funami, T. Chapter 29 - Curdlan. In *Handbook of Hydrocolloids*, Third edition; Phillips, G. O., Williams, P. A., Eds.; Woodhead Publishing, 2021; pp 887−921.
(152) Ganie, S. A.; Rather, L. J.; Li, Q. Review on Anti-cancer and Anti-microbial Applications of Curdlan Biomaterials. *J. Polym. Environ.* **2022**, *30* (4), 1284−1299.
(153) Verma, D. K.; Niamah, A. K.; Patel, A. R.; Thakur, M.; Singh Sandhu, K.; Chávez-González, M. L.; Shah, N.; Noe Aguilar, C. Chemistry and microbial sources of Curdlan with potential application and safety regulations as prebiotic in food and health. *Food Res. Int.* **2020**, *133*, 109136.
(154) Lafarge, C.; Cayot, N. Potential Use of Mixed Gels from Konjac Glucomannan and Native Starch for Encapsulation and Delivery of Aroma Compounds: A Review. *Starch - Stärke* **2018**, *70* (9−10), 1700159.
(155) Yang, B.; Yuan, W. Highly Stretchable and Transparent Double-Network Hydrogel Ionic Conductors as Flexible Thermal−Mechanical Dual Sensors and Electroluminescent Devices. *ACS Appl. Mater. Interfaces* **2019**, *11* (18), 16765−16775.
(156) Yang, D.; Yuan, Y.; Wang, L.; Wang, X.; Mu, R.; Pang, J.; Xiao, J.; Zheng, Y. A Review on Konjac Glucomannan Gels: Microstructure and Application. *Int. J. Mol. Sci.* **2017**, *18* (11), 2250.
(157) Nishinari, K.; Williams, P. A.; Phillips, G. O. Review of the physico-chemical characteristics and properties of konjac mannan. *Food Hydrocolloid* **1992**, *6* (2), 199−222.
(158) Ishwarya S, P.; R, S.; Nisha, P. Advances and prospects in the food applications of pectin hydrogels. *Crit. Rev. Food Sci.* **2022**, *62* (16), 4393−4417.
(159) Hu, R.; Yang, X.; Cui, W.; Leng, L.; Zhao, X.; Ji, G.; Zhao, J.; Zhu, Q.; Zheng, J. An Ultrahigh Stretchable and Recyclable Starch-Based Gel with Multiple Functions. *Adv. Mater.* **2023**, *35* (34), 2303632.
(160) Huber, E.; Frost, M. Light scattering by small particles. *Aqua* **1998**, *47* (2), 87−94.
(161) Matsuda, T.; Kawakami, R.; Namba, R.; Nakajima, T.; Gong, J. P. Mechanoresponsive self-growing hydrogels inspired by muscle training. *Science* **2019**, *363* (6426), 504−508.
(162) Matsuda, T.; Kawakami, R.; Nakajima, T.; Gong, J. P. Crack Tip Field of a Double-Network Gel: Visualization of Covalent Bond Scission through Mechanoradical Polymerization. *Macromolecules* **2020**, *53* (20), 8787−8795.
(163) Matsuda, T.; Kawakami, R.; Nakajima, T.; Hane, Y.; Gong, J. P. Revisiting the Origins of the Fracture Energy of Tough Double-Network Hydrogels with Quantitative Mechanochemical Characterization of the Damage Zone. *Macromolecules* **2021**, *54* (22), 10331−10339.
(164) Wei, G.; Kudo, Y.; Matsuda, T.; Wang, Z. J.; Mu, Q. F.; King, D. R.; Nakajima, T.; Gong, J. P. Sustainable mechanochemical growth of double-network hydrogels supported by vascular-like perfusion. *Mater. Horiz.* **2023**, *10* (9). DOI: 10.1039/D3MH01038D
(165) Taylor, D. L.; in het Panhuis, M. Self-Healing Hydrogels. *Adv. Mater.* **2016**, *28* (41), 9060−9093.
(166) Yan, X.; Chen, Q.; Zhu, L.; Chen, H.; Wei, D.; Chen, F.; Tang, Z.; Yang, J.; Zheng, J. High strength and self-healable gelatin/polyacrylamide double network hydrogels. *J. Mater. Chem. B* **2017**, *5* (37), 7683−7691.
(167) Dutta, A.; Maity, S.; Das, R. K. A Highly Stretchable, Tough, Self-Healing, and Thermoprocessable Polyacrylamide−Chitosan Supramolecular Hydrogel. *Macromol. Mater. Eng.* **2018**, *303* (12), 1800322.
(168) Dai, X.; Zhang, Y.; Gao, L.; Bai, T.; Wang, W.; Cui, Y.; Liu, W. A Mechanically Strong, Highly Stable, Thermoplastic, and Self-Healable Supramolecular Polymer Hydrogel. *Adv. Mater.* **2015**, *27* (23), 3566−3571.
(169) Chen, H.; Yang, F.; Hu, R.; Zhang, M.; Ren, B.; Gong, X.; Ma, J.; Jiang, B.; Chen, Q.; Zheng, J. A comparative study of the mechanical properties of hybrid double-network hydrogels in swollen and as-prepared states. *J. Mater. Chem. B* **2016**, *4* (35), 5814−5824.
(170) Ghobril, C.; Grinstaff, M. W. The chemistry and engineering of polymeric hydrogel adhesives for wound closure: a tutorial. *Chem. Soc. Rev.* **2015**, *44* (7), 1820−1835.
(171) Pourjavadi, A.; Tavakolizadeh, M.; Hosseini, S. H.; Rabiee, N.; Bagherzadeh, M. Highly stretchable, self-adhesive, and self-healable double network hydrogel based on alginate/polyacrylamide with tunable mechanical properties. *J. Polym. Sci.* **2020**, *58* (15), 2062−2073.
(172) Jafari, H.; Alimoradi, H.; Delporte, C.; Bernaerts, K. V.; Heidari, R.; Podstawczyk, D.; Niknezhad, S. V.; Shavandi, A. An injectable, self-healing, 3D printable, double network co-enzymatically crosslinked hydrogel using marine poly- and oligo-saccharides for wound healing application. *Appl. Mater. Today* **2022**, *29*, 101581.
(173) Karami, P.; Wyss, C. S.; Khoushabi, A.; Schmocker, A.; Broome, M.; Moser, C.; Bourban, P.-E.; Pioletti, D. P. Composite Double-Network Hydrogels To Improve Adhesion on Biological Surfaces. *ACS Appl. Mater. Interfaces* **2018**, *10* (45), 38692−38699.
(174) Maier, G. P.; Rapp, M. V.; Waite, J. H.; Israelachvili, J. N.; Butler, A. Adaptive synergy between catechol and lysine promotes wet adhesion by surface salt displacement. *Science* **2015**, *349* (6248), 628−632.
(175) Bai, S.; Zhang, X.; Lv, X.; Zhang, M.; Huang, X.; Shi, Y.; Lu, C.; Song, J.; Yang, H. Bioinspired Mineral−Organic Bone Adhesives for Stable Fracture Fixation and Accelerated Bone Regeneration. *Adv. Funct. Mater.* **2020**, *30* (5), 1908381.
(176) Raos, G.; Zappone, B. Polymer Adhesion: Seeking New Solutions for an Old Problem. *Macromolecules* **2021**, *54* (23), 10617−10644.
(177) Walker, B. W.; Portillo Lara, R.; Mogadam, E.; Hsiang Yu, C.; Kimball, W.; Annabi, N. Rational design of microfabricated electroconductive hydrogels for biomedical applications. *Prog. Polym. Sci.* **2019**, *92*, 135−157.
(178) Ling, Q.; Liu, W.; Liu, J.; Zhao, L.; Ren, Z.; Gu, H. Highly Sensitive and Robust Polysaccharide-Based Composite Hydrogel Sensor Integrated with Underwater Repeatable Self-Adhesion and Rapid Self-Healing for Human Motion Detection. *ACS Appl. Mater. Interfaces* **2022**, *14* (21), 24741−24754.
(179) Morelle, X. P.; Illeperuma, W. R.; Tian, K.; Bai, R.; Suo, Z.; Vlassak, J. J. Highly Stretchable and Tough Hydrogels below Water Freezing Temperature. *Adv. Mater.* **2018**, *30* (35), 1801541.
(180) Cui, H.; Mi, H.; Ji, C.; Guo, F.; Chen, Y.; Wu, D.; Qiu, J.; Xie, H. A durable MXene-based zinc ion hybrid supercapacitor with sulfated polysaccharide reinforced hydrogel/electrolyte. *J. Mater. Chem. A* **2021**, *9* (42), 23941−23954.
(181) Wu, S.; Lou, D.; Wang, H.; Jiang, D.; Fang, X.; Meng, J.; Sun, X.; Li, J. One-pot synthesis of anti-freezing carrageenan/polyacrylamide double-network hydrogel electrolyte for low-temperature flexible supercapacitors. *Chem. Eng. J.* **2022**, *435*, 135057.
(182) Mo, F.; Chen, Z.; Liang, G.; Wang, D.; Zhao, Y.; Li, H.; Dong, B.; Zhi, C. Zwitterionic Sulfobetaine Hydrogel Electrolyte Building Separated Positive/Negative Ion Migration Channels for Aqueous Zn-MnO2 Batteries with Superior Rate Capabilities. *Adv. Energy Mater.* **2020**, *10* (16), 2000035.

https://doi.org/10.1021/acs.biomac.3c00765
Biomacromolecules XXXX, XXX, XXX−XXX

(183) Huang, S.; Hou, L.; Li, T.; Jiao, Y.; Wu, P. Antifreezing Hydrogel Electrolyte with Ternary Hydrogen Bonding for High-Performance Zinc-Ion Batteries. *Adv. Mater.* **2022**, *34* (14), 2110140.
(184) Lin, F.; Wang, Z.; Shen, Y.; Tang, L.; Zhang, P.; Wang, Y.; Chen, Y.; Huang, B.; Lu, B. Natural skin-inspired versatile cellulose biomimetic hydrogels. *J. Mater. Chem. A* **2019**, *7* (46), 26442−26455.
(185) Khademhosseini, A.; Langer, R. A decade of progress in tissue engineering. *Nat. Protoc.* **2016**, *11* (10), 1775−1781.
(186) Zhao, Y.; Zhu, T.; Han, S.; Dong, Y.; Zhou, Y.; Qiao, Y.; Tian, Y.; Qiu, D.; Qu, X. Construction of Processable Ultrastiff Hydrogel for Periarticular Fracture Strutting and Healing. *Biomacromolecules* **2023**, *24* (5), 2075−2086.
(187) Rodell, C. B.; Dusaj, N. N.; Highley, C. B.; Burdick, J. A. Injectable and Cytocompatible Tough Double-Network Hydrogels through Tandem Supramolecular and Covalent Crosslinking. *Adv. Mater.* **2016**, *28* (38), 8419−8424.
(188) Cai, Z.; Tang, Y.; Wei, Y.; Wang, P.; Zhang, H. Double − network hydrogel based on exopolysaccharides as a biomimetic extracellular matrix to augment articular cartilage regeneration. *Acta Biomater* **2022**, *152*, 124−143.
(189) Gaharwar, A. K.; Singh, I.; Khademhosseini, A. Engineered biomaterials for in situ tissue regeneration. *Nat. Rev. Mater.* **2020**, *5* (9), 686−705.
(190) Li, X.; Ding, J.; Zhang, Z.; Yang, M.; Yu, J.; Wang, J.; Chang, F.; Chen, X. Kartogenin-Incorporated Thermogel Supports Stem Cells for Significant Cartilage Regeneration. *ACS Appl. Mater. Interfaces* **2016**, *8* (8), 5148−5159.
(191) Wang, L.-S.; Du, C.; Toh, W. S.; Wan, A. C. A.; Gao, S. J.; Kurisawa, M. Modulation of chondrocyte functions and stiffness-dependent cartilage repair using an injectable enzymatically cross-linked hydrogel with tunable mechanical properties. *Biomaterials* **2014**, *35* (7), 2207−2217.
(192) Aldana, A. A.; Morgan, F. L. C.; Houben, S.; Pitet, L. M.; Moroni, L.; Baker, M. B. Biomimetic double network hydrogels: Combining dynamic and static crosslinks to enable biofabrication and control cell-matrix interactions. *J. Polym. Sci.* **2021**, *59* (22), 2832−2843.
(193) Adkisson, H. D.; Martin, J. A.; Amendola, R. L.; Milliman, C.; Mauch, K. A.; Katwal, A. B.; Seyedin, M.; Amendola, A.; Streeter, P. R.; Buckwalter, J. A. The Potential of Human Allogeneic Juvenile Chondrocytes for Restoration of Articular Cartilage. *Am. J. Sport. Med.* **2010**, *38* (7), 1324−1333.
(194) Zhu, D.; Wang, H.; Trinh, P.; Heilshorn, S. C.; Yang, F. Elastin-like protein-hyaluronic acid (ELP-HA) hydrogels with decoupled mechanical and biochemical cues for cartilage regeneration. *Biomaterials* **2017**, *127*, 132−140.
(195) Thomas, J.; Chopra, V.; Rajput, S.; Guha, R.; Chattopadhyay, N.; Ghosh, D. Post-Implantation Stiffening by a Bioinspired, Double-Network, Self-Healing Hydrogel Facilitates Minimally Invasive Cell Delivery for Cartilage Regeneration. *Biomacromolecules* **2023**, *24* (7), 3313−3326.
(196) Andrique, L.; Recher, G.; Alessandri, K.; Pujol, N.; Feyeux, M.; Bon, P.; Cognet, L.; Nassoy, P.; Bikfalvi, A. A model of guided cell self-organization for rapid and spontaneous formation of functional vessels. *Sci. Adv.* **2019**, *5* (6), No. eaau6562.
(197) Choi, S.; Choi, Y. j.; Jang, M.-S.; Lee, J. H.; Jeong, J. H.; Kim, J. Supertough Hybrid Hydrogels Consisting of a Polymer Double-Network and Mesoporous Silica Microrods for Mechanically Stimulated On-Demand Drug Delivery. *Adv. Funct. Mater.* **2017**, *27* (42), 1703826.
(198) Choi, S.; Choi, Y.; Kim, J. Anisotropic Hybrid Hydrogels with Superior Mechanical Properties Reminiscent of Tendons or Ligaments. *Adv. Funct. Mater.* **2019**, *29* (38), 1904342.
(199) Löwenberg, C.; Balk, M.; Wischke, C.; Behl, M.; Lendlein, A. Shape-Memory Hydrogels: Evolution of Structural Principles To Enable Shape Switching of Hydrophilic Polymer Networks. *Acc. Chem. Res.* **2017**, *50* (4), 723−732.
(200) Lu, X.; Chan, C. Y.; Lee, K. I.; Ng, P. F.; Fei, B.; Xin, J. H.; Fu, J. Super-tough and thermo-healable hydrogel − promising for shape-memory absorbent fiber. *J. Mater. Chem. B* **2014**, *2* (43), 7631−7638.
(201) Feng, Z.; Zuo, H.; Gao, W.; Ning, N.; Tian, M.; Zhang, L. A Robust, Self-Healable, and Shape Memory Supramolecular Hydrogel by Multiple Hydrogen Bonding Interactions. *Macromol. Rapid Commun.* **2018**, *39* (20), 1800138.
(202) Liu, J.; Qu, S.; Suo, Z.; Yang, W. Functional hydrogel coatings. *Natl. Sci. Rev.* **2021**, *8* (2), nwaa254.

https://doi.org/10.1021/acs.biomac.3c00765
Biomacromolecules XXXX, XXX, XXX−XXX